YAP and β-catenin Co-operate to Drive Oncogenesis in Basal Breast Cancer

DISSERTATION
zur Erlangung des akademischen Grades

Doctor of Philosophy
(Ph.D.)

eingereicht an der

Lebenswissenschaftlichen Fakultät der Humboldt-Universität zu Berlin

von

Hazel Quinn, M.Sc.

Präsidentin/Präsident
der Humboldt-Universität zu Berlin

Prof. Dr.-Ing. Dr. Sabine Kunst

Dekanin/Dekan der Lebenswissenschaftlichen Fakultät
der Humboldt-Universität zu Berlin

Prof. Dr. Bernhard Grimm

Gutachter/innen

1. Prof. Dr. Thomas Sommer
2. Prof. Dr. Simone Reber
3. Prof. Dr. Walter Birchmeier

Tag der mündlichen Prüfung: 09.10.2020

This work was carried out from 03/2017 to 06/2020 under the supervision of Prof. Walter Birchmeier at the Max Delbrück Center for Molecular Medicine in Berlin.

TABLE OF CONTENTS

LIST OF ABBREVIATIONS

%	Percent
°C	Degrees Celsius
3D	Three-dimensional
AML	Acute Myeloid Leukaemia
ANOVA	Analysis of Variance
APC	Adenomatous polyposis coli
APC-Cy7	Allophycocyanin-Cyanin 7
ARM	Armadillo
BCL9	B-cell CLL/Lymphoma 9
BLBC	Basal-like Breast Cancer
BSA	Bovine Serum Albumin
CBP	CREB-Binding Protein
cDNA	Complementary DNA
chIP-seq	Chromatin-Immunoprecipitation Sequencing
CK	Cytokeratin
CK-1	Casein Kinase 1
CK14	Cytokeratin 14
CK8	Cytokeratin 8
Co-IP	Co-Immunoprecipitation
CSC	Cancer Stem Cell
CTCs	Circulating Tumour Cells
Ctrl	Control
DAPI	4', 6'-Diamidin-2-phenylindoldihydrochloride
DCIS	Ductal Carcinoma *In Situ*
DFS	Disease-Free Survival
DMSO	Dimethyl Sulfoxide
DNA	Deoxyribonucleic Acid
DPBS	Dulbecco's Phosphate-Buffered Saline

DVL	Dishevelled
E	Embryonic Day
e.g.	Example Given
ECM	Extracellular Matrix
EDTA	Ethylenediaminetetraacetic acid
EGF	Epidermal Growth Factor
EGFR	Epidermal Growth Factor Receptor
EMT	Epithelial to Mesenchymal Transition
ER	Oestrogen Receptor
ES	Embryonic Stem Cell
et al.	*et altera*
EYFP	Enhanced Yellow Florescent Protein
FACS	Florescent-associated cell sorting
FAK	Focal Adhesion Kinase
FBS	Foetal Bovine Serum
FZD	Frizzled
GFR	Growth Factor Reduced
GOBO	Gene expression-based Outcome for Breast cancer Online
GOF	Gain-Of-Function
GOF	Gain of Function
GPCR	G Protein Coupled Receptor
GPCR	G Protein Coupled Receptor
GSEA	Gene Set Enrichment Analysis
GSK-3β	Glycogen Synthase Kinase 3β
HCC	Hepatocellular Carcinoma
HER2	Human Epidermal Growth Factor Receptor 2
hESC	Human Embryonic Stem Cells
HGF	Hepatocyte Growth Factor
HMG-CoA	3-Hydroxy-3-Methylglutaryl Coenzyme A
i.e.	*id est:* that means
iPSC	Induced Pluripotent Stem Cell

KO	Knock-out
LaGeSo	Landesamt für Gesundheit und Soziales
LATS	Large tumour suppressor kinase 1
LEF1	Lymphoid Enhancer-binding Factor 1
LRP5/6	Low-density lipoprotein receptor-related protein 5
LTR	Long Terminal Repeat
MaSC	Mammary Stem Cell
MMTV	Mouse Mammary Tumour Virus
mRNA	Messenger Ribonucleic Acid
MST	Mammalian STE20-like protein kinase
NOD/SCID	Non-obese diabetic/severe combined immunodeficiency
NP-40	Tergitol-type NP-40
PAGE	Polyacrylamide Gel Electrophoresis
PBS	Phosphate-Buffered Saline
PDX	Patient Derived Xenograft
Pg	Progesterone
PI3K	Phosphoinositide 3-Kinase
PP	Post-Partum
PR	Progesterone Receptor
Prl	Prolactin
Procr	Protein C Receptor
PVDF	Polyvinylidene Fluoride
PyMT	Polyomavirus Middle T Antigen
Q	Quadrant
qPCR	Quantitative Polymerase Chain Reaction
R26	ROSA26
RBC	Red Blood Cell
RGF	Reduced Growth Factor
RHOA	Ras Homology family Member A
RNA	Ribonucleic acid
ROCK	Rho-associated protein kinase

RTK	Receptor Tyrosine Kinase
RT-qPCR	Reverse Transcription Quantitative Polymerase Chain Reaction
SDS	Sodium Dodecyl Sulfate
SEM	Standard Error of the Mean
SF	Scatter Factor
SH2	Src Homology 2
SIM	Simvastatin
SMA	Smooth muscle actin
STAT3	Signal Transducer and Activator of Transcription 3
TAZ/WWTR1	Transcriptional Co-Activator With PDZ-Binding Motif
TCF4	Transcription Factor 4
TECs	Tumour Epithelial Cells
TNBC	Triple Negative Breast Cancer
Tris	Tris-(hydroxymethyl) Aminoethane
U	Unit (enzymatic activity)
VEGFR	Vascular Endothelial Growth Factor Receptor
VP	Verteporfin
WAP	Whey Acidic Protein
Wg	Wingless
YAP	Yes Associated Protein
YFP	Yellow Florescent Protein

SUMMARY

In various cancer types, targeting cancer stem cells (CSCs) can serve as an effective approach for limiting therapy resistance and metastasis. While basal breast cancers encompass cells with CSC features, rational therapies remain poorly established. Here, I show that receptor tyrosine kinase (RTK) Met signalling promotes the activity of the Hippo component YAP in basal breast cancer. Further analysis revealed enhanced YAP activity within the CSC population. Utilising both genetic and pharmaceutical approaches, I show that interference of YAP activity delays tumour formation, prevents luminal to basal trans-differentiation and reduces CSC survival. Gene expression analysis of YAP knock-out mammary glands revealed a strong decrease in β-catenin target genes, suggesting that YAP is required for nuclear β-catenin activity. Mechanistically, I find that nuclear YAP interacts and overlaps with β-catenin and TEAD4 at common gene regulatory regions. Analysis of proteomic data from primary breast cancer patients identified significant upregulation of the YAP signature in basal compared to other breast cancers, suggesting that YAP activity is limited to basal breast cancers. Our data highlight the importance of YAP as a crucial tumour initiator and cancer stem cell regulator in basal breast cancer and demonstrates that its activity has prognostic value, when comparing basal with luminal breast cancers. This suggests that targeting the YAP/TEAD4/β-catenin complex through specific new drugs, which researchers in academia and industry are presently developing, is a potential therapeutic avenue for treating basal breast cancers in the future. This is the most important aspect of my thesis.

Zusammenfassung

Bei verschiedenen Krebs-Typen kann die molekulare Behandlung der Krebs-Stammzellen ein effektives Ziel sein, die Therapie-Resistenz und die Metastasierung der Tumore zu hemmen. Basaler Brustkrebs enthält Zellen mit Stammzell-Eigenschaften; hingegen sind rationale Therapien gegen diese Zellen nur wenige etabliert. Ich zeige in meiner Doktorarbeit, dass Rezeptor-Tyrosinkinase-Met-Signalvermittlung die Aktivität der Hippo-Komponente YAP im basalem Brustkrebs verstärkt. Weitere Analysen zeigten erhöhte YAP-Aktivität in den Krebsstammzell-Populationen. Durch Verwendung genetischer und pharmakologischer Methoden konnte ich zeigen, dass die Interferenz mit YAP die Tumor-Bildung verzögert und die luminal-basale Transdifferenzierung verhindert sowie das Krebsstammzell-Überleben reduziert. Gen-Expressions-Analysen von YAP-Knockout-Brustdrüsen zeigten eine starke Reduzierung der Expression der β-Catenin-Zielgene, was indiziert, dass YAP für nukleare β-Catenin-Aktivität essentiell ist. Ich habe weiter gefunden, dass nukleares YAP mit β-Catenin und TEAD4 interagiert und an gemeinsamen regulatorischen Gene-Regionen überlappt. Die Analyse von proteomischen Daten von primären Brustkarzinomen des Menschen zeigte eine signifikante Hoch-Regulation der YAP-Signatur in basalem im Vergleich zu andern Brustkarzinom-Typen, was suggeriert, dass YAP-Aktivität auf den basalen Brustkrebs limitiert ist. Unsere Daten beleuchten die Wichtigkeit von YAP als essentiellen Tumor-Initiator und Krebs-Stammzell-Regulator beim basalen Brustkrebs und zeigt, dass dessen Aktivität als Prognose-Faktor wichtig ist, wenn man basalen mit luminalem Brustkrebs vergleicht. Dies suggeriert, dass Behandlung des YAP/TEAD4/β-Catenin-Komplexes mit neuen, spezifischen Pharmaka, die die Wissenschaftler in Akademie- und Industrie-Instituten im Moment entwickeln, eine potentielle therapeutische Richtung darstellen, um basalen Brustkrebs in der Zukunft zu behandeln. Dies ist der wichtigste Aspekt meiner Doktorarbeit.

FIGURE INDEX

TABLE INDEX

1. INTRODUCTION

In my thesis, I have studied by genetic and pharmacological means basal (triple-negative) mammary gland cancer in a mouse model. In particular, I focused on the role and regulation of HIPPO-YAP signalling in tumour formation and cancer stem cells. Gene expression analysis confirmed higher expression of YAP in tumours of human patients with basal breast cancer, compared to tumours of patients with luminal breast cancer. In triple-negative breast cancer, high YAP correlated with a decrease of patient survival.

In the subsequent chapters, I highlight the differences between and the function of luminal and basal cells of the mammary gland. I explain the morphological changes the mammary gland undergoes during pregnancy with emphasis on its extensive plasticity. I introduce the WAP promoter for the conditional expression of oncogenes and cre recombinase. Thereafter, I introduce breast cancer, cancer stem cells, and the need to develop new rational therapies.

1.1. The Mammary Gland

1.1.1. Mammary gland structure and development

The mammary gland is a glandular exocrine structure that is required for milk production and the nourishment of mammalian offspring. This complex gland is composed of a multifactorial complex network consisting of the glandular epithelium's interaction with the extracellular matrix and stromal cells such as fat cells (adipocytes), inflammatory cells and fibroblasts. This niche is essential for the production of a dense extracellular matrix (ECM), which is required for both the structural and functional support of the ductal networks responsible for milk production and excretion[1,2]. Mammary ducts connect the milk producing lobules made up of groups of alveoli. Alveoli are lined with luminal milk-secreting cells, surrounded by basal/myoepithelial cells. During breast feeding, oxytocin stimulates the basal cells of the alveoli to contract leading to the excretion of milk (produced by luminal cells) into the lumen to the nipple[3–5].

Until puberty the ductal epithelium originating from the nipple is quiescent. During puberty, hormonal stimulation induces the epithelium to undergo branching morphogenesis and invade its way into the mammary fat pad. This invasion is orchestrated by an EMT-like mechanism, where the luminal epithelial cells located in the terminal end buds (surrounded by cap cells) rapidly proliferate at the leading edge of the

branches[6]. The virgin adult mammary gland consists of branching epithelial structures made up of a single layer of luminal epithelial cells surrounded by a single layer of basal/myoepithelial cells (Figure. 1.1). These two distinct mammary epithelial cell lineages can easily be distinguished from each other by their cytokeratin (CK) expression based on their differentiation status[7]. The luminal milk producing cells of the adult mammary gland express simple keratins (not stratified) such as CK8 and CK18. On the contrary, the basal/myoepithelial cells of the mammary gland express stratified keratins such as CK5 and CK14[8]. In order to carry out their functional role, the basal cells also express bundles of smooth muscle actin (α-SMA) in their cytoplasm, in addition to micro-filaments and myosin filaments which facilitate the contraction necessary for milk ejection[9]. Another marker that is often used to identify basal cells is p63, an essential molecule involved in cell adhesion and survival expressed in basal cells[10].

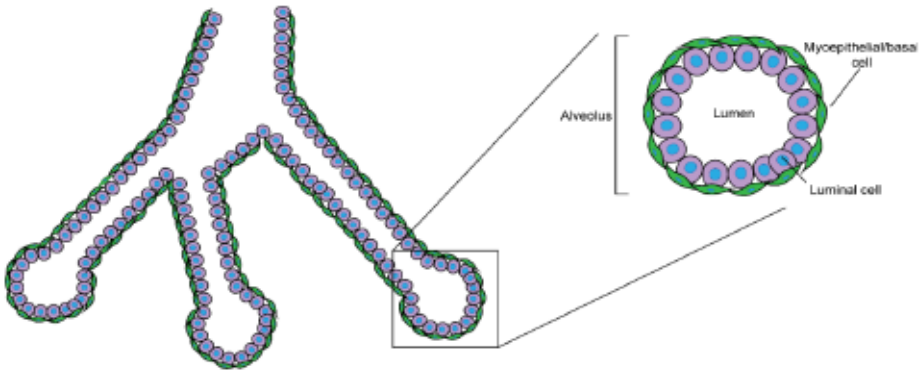

Figure 1.1: ***Mammary gland structure.*** Ductal tree (left) with alveoli consisting of luminal cells (purple) and myoepithelial/basal cells (green). Alveolus (right) depicting the empty lumen into which the milk is expelled.

Transplantation assays and lineage tracing studies in the mouse have led to the discovery of a hierarchy originating from a multipotent mammary stem cell (MaSC) branching into to both luminal and basal progenitor cells (Figure. 1.2). The first evidence for the existence of a MaSC came from the pioneering studies of mammary fat pad transplantation[11]. This technique assesses the repopulating potential of mammary epithelial cells by injecting these cells into the 'cleared' or 'de-epithelialized' mammary fat pad of recipient mice. It was shown that these transplanted cells have the ability to completely reconstitute the ductal tree and could be serially transplanted, suggesting the presence of mammary stem cells[12–14]. Many groups have identified various cell surface markers that can be used to distinguish and isolate the different epithelial cells of the mammary gland. In 2006, mammary stem cells were first isolated using the cell surface markers $CD29^{hi}$ $CD24^{med}$ and $CD49f^{hi}$ which had the ability to repopulate cleared mammary fat pads[15,16]. Following this, cell surface markers have been identified that

distinguish basal/myoepithelial and different luminal cell epithelial states; CD29^{hi} CD49f^{hi} CD24^{+} EpCAM$^{lo/med}$ cells are basal/myoepithelial cell enriched while CD49f$^{+/lo}$ CD29^{lo} CD24$^{+/hi}$ EpCAM^{hi} cells contain cells belonging to the luminal lineage. A number of additional markers have been identified and used to isolate different luminal cell epithelial states such as, c-kit, Sca-1 and CD61[17] (Figure 1.2). Most recently, it was shown that the Protein C Receptor (Procr), a Wnt target gene was a marker of multipotent mammary stem cells with the ability to repopulate both the luminal and basal epithelial cells of the mammary gland[18]. However, in 2019 single cell sequencing of the adult mammary gland identified 15 differentiation states of mammary epithelial cells consisting of 4 basal and 11 luminal, suggesting that the mammary gland is even more complex than originally thought[19].

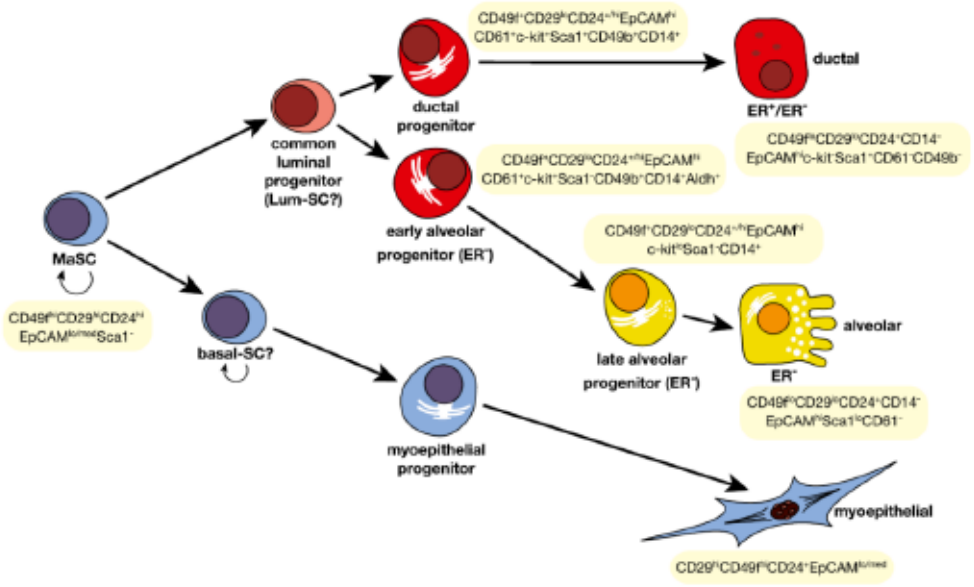

Figure 1.2: ***Mammary gland hierarchy.*** Cell surface markers of identified mammary epithelial cells in the mouse mammary gland, adapted from[17]. Left to right, mammary stem cell (MaSC) gives rise to both the luminal and basal cells of the mammary gland.

1.1.2. Mammary gland in pregnancy

Over a lifetime, the mammary gland undergoes dramatic and regular changes during puberty, the oestrous cycle, pregnancy (morphogenic branching), lactation and involution (Figure 1.3). In response to hormonal stimuli, the mammary gland undergoes massive structural remodelling by proliferation, differentiation and apoptosis through each of these stages[20–22]. Due to this plasticity, the mammary gland has been vastly used to elucidate the specification of cell fate, polarity and branching morphogenesis. During pregnancy, increasing levels of prolactin (Prl) and progesterone (Pg) leads to the

development of secretory lobuloalveoli and branching morphogenesis in preparation for lactation. Alveolar morphogenesis requires the epithelial cells of the ductal branches and alveoli to undergo massive proliferation to ensure efficient epithelial cell numbers and surface area for adequate milk production[23]. In mid-pregnancy, the mammary gland undergoes differentiation to initiate a secretory state[24]. During this phase, the alveoli form a single layer of polarized cells surrounding a lumen. A discontinuous layer of contractile basal/myoepithelial cells surround each alveolus, allowing the luminal cells to directly contact the basement membrane. This contact is required for the complete differentiation required for lobuloalveoli morphogenesis. In late pregnancy, the tight junctions of the alveoli close in preparation for lactation, i.e. activation of the secretory phase[23]. In addition to the vast expansion of the mammary epithelial cells, equal changes occur in other cells of the mammary gland, e.g. adipocytes and vascular cells. Adipocytes reduce their lipid content and are scattered throughout the gland[25]. Due to the high energy requirement of these massive tissue remodelling events and lactation, vascular cells also expand to supply the amino acids, sugars, etc[26]. Weaning of offspring induces the involution of the mammary gland. This is marked by the shedding of alveolar cells into the lumen. These cells undergo programmed cell death or apoptosis marked by detection of cleaved caspase-3. The master regulator of this process is Signal transducer and activator of transcription 3 (STAT3). STAT3 has also been shown to induce aberrant involution and is thought to induce neoplasia[27].

The Whey Acidic Protein (WAP) is a milk protein expressed specifically in the mammary gland during pregnancy in response to steroid and peptide hormonal cues[28]. WAP specificity in the mammary gland has been used to create inducible and tissue specific mouse models. WAP has been shown to be more specific for the mammary gland than the mouse mammary tumour virus (MMTV) long terminal repeat (LTR) promoter which has been shown to also be expressed in another glandular tissues such as the salivary gland[29–31]. Transgenes have been targeted into the WAP gene regulatory elements; upon pregnancy induction, these genes are readily expressed in the luminal epithelial cells. This approach has been used to study mammary gland development during pregnancy and tumorigenesis by placing transgenes under the control of the WAP promoter[32–34].

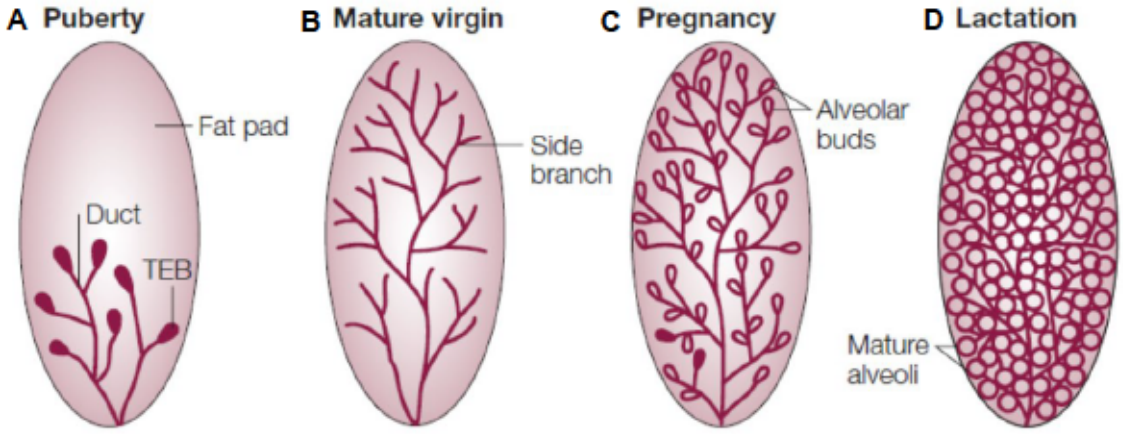

Figure 1.3: ***Mammary gland development during puberty, adulthood, pregnancy and lactation, adapted from***[240]***.*** **A.** The mammary ductal tree during puberty only fills half of the mammary fat pad. **B.** The adult virgin mammary gland with a fully developed ductal tree including side branches. **C.** During pregnancy the ductal tree expands with the development of alveolar buds. **D.** During lactation the mammary fat pad is completely filled with large milk producing mature alveoli.

1.2. Breast Cancer

Breast cancer is the most frequently diagnosed cancer in Europe, accounting for 15% of all cancer related cell deaths in females[35]. It is a cancer of the glandular epithelial cells in the mammary gland. Typically, breast cancer is classified as *in situ* or invasive depending on whether the tumour cells have broken through the basement membrane; that is made up of a fibrous, extracellular matrix that functions to separate cells from the underlying connective tissue[36]. Invasive tumours are considered to be more advanced and aggressive as they consist of diffuse cells, and harbour strong interactions with the microenvironment. This aids the metastasis of tumour cells to distant organs such as the lung, brain and bone[37].

In the advent of pre-diagnostic screening and neoadjuvant therapies, breast cancer 5-year survival rates have significantly increased due to early diagnosis. However, approximately 10-15% of breast cancer patients present to the clinic with a highly aggressive disease that has progressed into distant metastasis. These patients have poor prognoses and the prescribed therapy is usually only palliative. They receive chemotherapeutic agents such as tamoxifen that have a large range of off-target effects impeding the patient's quality of life. The heterogeneity of these late stage tumours makes them difficult to treat[38]. It is therefore required that additional prognostic markers are identified to improve mortality rates and increase the quality of palliative care for terminal patients with metastatic disease. To achieve this, it is essential to identify specific

signalling pathways and molecular mechanisms that influence the survival of tumour cells following therapeutic intervention.

1.2.1. Breast cancer classification

Breast cancer is a complex and heterogeneous disease comprised of a variety of cell types and extracellular components that generate numerous breast cancer subtypes with varied clinical outcome and response to therapy[39,40]. For about 20 years, breast cancers have been grouped based on their molecular subtypes in order to better predict patient prognosis and determine correct anti-cancer treatment strategies[41]. Several intrinsic molecular subtypes of breast cancers have been identified based on microarray gene expression analysis: Luminal A, Luminal B, Her2^{+}, Basal-like and Claudin-low (Figure 1.4).

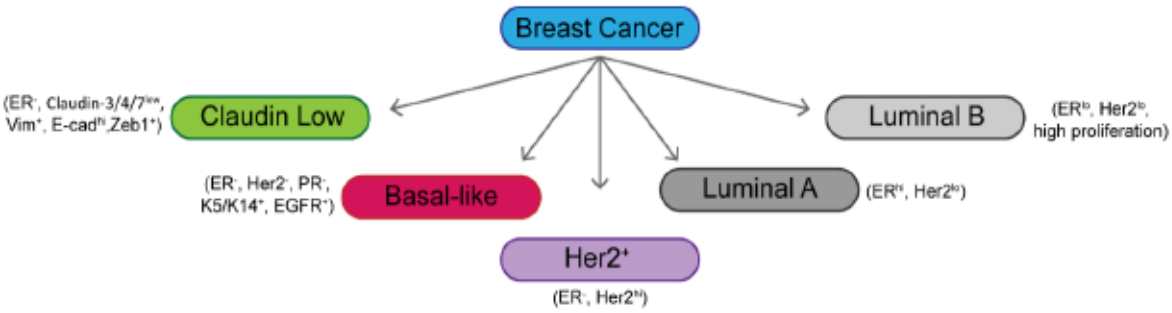

Figure 1.4: ***Breast cancer subtypes.***

These molecular subtypes have significantly different prognoses based on their predicted disease-free survival[42]. They are typically divided into different molecular subtypes based on the expression of the biomarkers Ki-67, estrogen receptor (ERα), progesterone receptor (PR) and the human epidermal growth factor receptor 2 (HER2). Luminal A breast cancers are the most common and have a low proliferative index (Ki-67), high expression of ERα and PR but not HER2. Patients diagnosed with Luminal A breast cancer have the best clinical outcome as these cancers generally respond well to hormone therapies[43]. Luminal B breast cancers have a similar molecular subtype to Luminal A. However, they have a high proliferative index (Ki-67) and can express the receptor HER2. Therefore, these tumours are more aggressive but respond well to hormonal therapy in combination with anti-HER2 therapy (Trastuzubmab)[44]. Patients that only express ERBB2/HER2, fall into the HER2-enriched subtype of breast cancer. These patients only respond to anti-HER2 therapy in combination with chemotherapy. Although

initial response to therapy is promising, these patients remain to have a low overall 5-year survival rate due to resistance generation[45]. Lastly, breast cancers presenting with no expression of the aforementioned hormone receptors are referred to as basal-like/triple-negative breast cancers (TNBC). These patients have a very poor prognosis due to the lack of targetable hormone receptors. As the only course of action for these patients is chemotherapy which has a number of toxic off-target effects, they typically have an extremely poor quality of life[41,46]. Within the TNBC subtype, a newly identified subtype accounting for 7-14% of invasive breast cancers known as Claudin-low has been described. Claudin-low breast cancers have low expression of luminal cell genes, epithelial cell-cell adhesion, tight junctions, E-cadherin and Claudins 2, 4 and 7. This molecular profile generates a strong epithelial to mesenchymal (EMT) and stem cell phenotype that significantly enhances the metastatic ability of these tumours[47,48] (Table 1.1)[49].

Molecular subtypes of Breast cancer			
Subtype	Immunohistochemistry	Prognosis	Notes
Luminal A	- Estrogen receptor positive - Progesterone receptor positive - HER-2 negative	Good	- Most common - Low grade - Low recurrence - Responsive to hormone therapy
Luminal B	- Estrogen receptor positive - Progesterone receptor positive - HER-2 positive or negative	Fair	- Higher grade - Higher recurrence than Lum A
HER-2 positive	- Estrogen receptor negative - Progesterone receptor negative - HER-2 positive	Poor	- May be amenable to anti-HER therapy - Resistance generation in most patients
Triple negative (basal)	- Estrogen receptor negative - Progesterone receptor negative - HER-2 negative	Poor	- Younger age at diagosis - No targeted therapy available - Aggressive with high rate of recurrence

Table 1.1: Breast cancer subtypes including molecular presentation (immunohistochemistry), prognosis and general notes associated with each subtype, adapted from[49].

Targeted therapies specifically block the activity of target molecules required for tumour cell growth and survival. It is clear that molecular subtyping of breast cancer has greatly improved the quality of life and overall survival of patients owing primarily to the development of target therapies. The first targeted therapy, in 1985, was a monoclonal antibody that binds and inhibits the HER2 receptor[50,51]. Since then, targeted therapies have come a long way with the development of tamoxifen against ER[52]. However, basal-like breast cancer (BLBC) has lagged behind the times with no targeted therapies available. It is clear more research is required to identify possible molecular therapeutic

targets in BLBC in order to improve both the patient's quality of life and overall 5-year survival.

1.2.2. Basal-like breast cancer

Basal-like breast cancer (BLBC) accounts for 15% of all breast cancers; they mainly affect young women and are often very aggressive with a high reoccurrence rate. Basal-like tumours have similar gene expression profiles to the normal basal/myoepithelial cells of the breast. For this reason they lack targetable receptors (that are present on luminal breast cancers) and are unresponsive to currently available targeted therapies. Upon clinical presentation, these tumours show a high mitotic index (high proliferation), strong lymphocyte infiltration and invasive phenotypes[53,54]. Although BLBCs are usually triple-negative, one study found that only around 75% of TNBC overlapped with a basal-like gene expression profile[55,56]. In order to correctly characterise BLBC and TNBC, the biomarker molecular expression pattern must be employed. Tumours positive for either CK5/6/14/17 and/or EGFR in addition to staining negative for ER, PR and HER2 are triple-negative BLBCs[57]. These features are responsible for the poor therapeutic response and high relapse rate.

Genetic mutations account for ~10% of breast cancers. The most well-studied basal-like breast cancers are familial and associated with BRCA1/2 mutations[58,59]. However, around 85% of all TNBC do not harbour hereditary BRCA mutations but somatic mutations in the tumour suppressor gene *TP53* in 80% of tumours[56,58]. Following this, *PIK3CA* is mutated in 9% of basal breast tumours. However, many components of this pathway are also amplified but not mutated in basal-like cancers such as *KRAS* (32%), *EGFR* (23%), *BRAF* (30%) and *PIK3CA* (49%). The receptor tyrosine kinase *MET* is amplified and a plausible target in basal-like tumours[56,60]. Based on these genetic data, it's likely that somatic mutations in *TP53* and the PI3K pathway are the most common drivers of basal breast cancers. Other pathways that contribute to disease but aren't necessarily initial drivers include components of the Wnt-β-catenin pathway[61]. Aberrant Wnt signalling is considered a characteristic of basal-like breast cancer and enhances metastasis likely through the activation of stem cell and mesenchymal like properties[61–63].

1.3. Cancer Stem Cells

Cancer stem cells (CSCs) or germ cells were proposed to be the origin of cancers around 150 years ago[64]. However, only recently with thanks to the advancement of stem

cell biology techniques we have been able to test this hypothesis. The first concrete evidence of the existence of CSCs came in 1994 when Lapidot and colleagues were able to isolate a subpopulation of acute myeloid leukaemia (AML) cells that when transplanted into NOD/SCID mice were able to initiate tumours resembling the primary tumour[65]. CSCs have the ability to self-renew (i.e. give rise to identical progeny) and differentiate leading to the repopulation and generation of a tumour that resembles the original. These properties are responsible for the longevity or even immortality of tumour cells, enabling them to constantly maintain the tumour mass by generating immense heterogeneity. With these properties, it is no wonder why CSCs contribute to metastasis, tumour relapse and resistance generation.

The first evidence for CSCs in solid tumours was from Al-Hajj et al., who used fluorescence activated cell sorting (FACS) to isolate different cell populations from human breast carcinomas based on the cell surface expression of CD24 and CD44. These populations were then transplanted into immuno-deficient mice. Only the $CD24^{-}$ $CD44^{+}$ population was readily competent to fully form tumours that resembled the primary specimen containing $CD24^{-}$ $CD44^{+}$ cells and $CD24^{+}$ $CD44^{+}$ cells. Serial transplantation of these tumours further confirmed the self-renewal capacity of $CD24^{-}$ $CD44^{+}$ cells[66]. These data support the hierarchy or CSC model, whereby fractioning tumour cells into CSC-enriched and CSC-depleted fractions show they have different tumour repopulating potentials.

Tumours are intrinsically heterogeneous comprising of cells with different differentiation status' and proliferative capacities as a result of vast genetic and epigenetic variation[67,68]. This observation has led to the proposal of multiple models to explain tumour heterogeneity; the stochastic and hierarchy/CSC model[69]. In the stochastic model, it is argued that tumours are homogenous and that any heterogeneity is a result of intrinsic (e.g., signalling pathways or transcriptional levels) or extrinsic influences (e.g., immune responses and the microenvironment). In this model, every cell in a given tumour has the ability to behave like a CSC as a result of intrinsic or extrinsic influences[70–72] (Figure 1.5, left). On the other hand, the CSC model argues that cellular hierarchy and/or heterogeneity is a result of a single CSC that has the ability to give rise to a fully heterogeneous tumour (Figure 1.5, right). This model is a caricature of normal development and repair in tissues such as the intestine and skin. CSCs are characterized by their ability to repopulate a fully heterogeneous tumour from a single cell. In this regard they have the ability to self-renew (the ability to give rise to descendants identical to themselves) and maintain the tumour as a whole[73,74]. CSCs are thought to contribute to metastasis which is responsible for over 90% of lethality in patients[75]. In order to

effectively terminate a tumour, one would have to specifically target CSCs to not only eradicate the primary tumour but also the metastatic lesions that arise from CSCs.

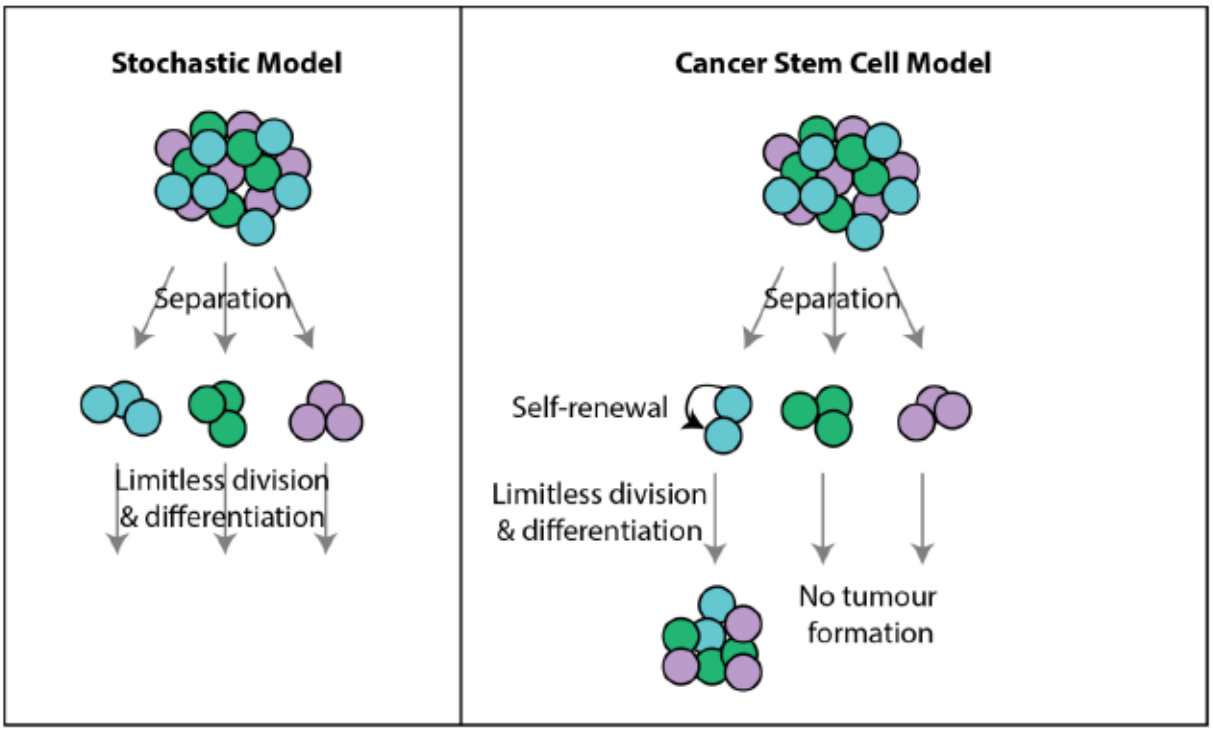

Figure 1.5: ***The cancer stem cell versus the stochastic model.*** Left, the stochastic model showing that in a heterogeneous tumour, each subtype can proliferate and differentiate without limits. Right, the CSC model showing that only a minute subset of tumour cells have the ability to self-renew, proliferate and differentiate without limits.

Metastasis, not the primary tumour, is the main cause of cancer mortality. Many studies have shown that CSCs correlate with metastasis. In glioblastoma and lung adenocarcinoma, the expression of the CSC marker CD133 correlates with poor clinical outcome[76,77]. Only about 0.01% of circulating tumour cells have the ability to develop macrometastases[78]. A recent study in human metastatic breast cancer found that the metastatic cells from low burden tissues have CSC, EMT, pro-survival and dormancy gene expression signatures. In contrast, high burden metastases express more luminal differentiated cells that resemble the primary tumour. Phenotypically, cells from low burden tissues had an extremely high tumour repopulating frequency when transplanted into immuno-deficient mice and could differentiate into luminal tumours[79]. To date, it remains unknown what specific cell type is responsible for metastasis. CSCs are thought to be responsible for this process as the CSC hypothesis states that only CSCs have the ability to initiate and sustain a fully heterogeneous tumour[80]. Several studies have provided evidence for the role of CSCs in breast cancer metastasis. One study showed that in early bone marrow metastasis, 71% of tumour cells expressed the CSC markers

$CD44^+$ $CD24^{-}$[81]. While another breast cancer study showed that pleural metastasis following neoadjuvant chemotherapy were enriched for the $CD44^+$ $CD24^-$ subpopulation suggesting both a link between CSCs with metastasis and chemoresistance[82].

Overall, CSCs are correlated with a decrease in patient survival[83]. This is likely due to their role in metastasis. Therefore, the probable key to improving patient survival following diagnosis is the identification of CSCs and the specific pathways that enable these cells to exhibit their function. Targeting these pathways will give rise to a new generation of anti-cancer therapeutics. In combination with traditional chemotherapeutics that target the majority of highly proliferative cells in a tumour, anti-CSC therapeutics will intercept the tumour at its core ultimately leading to its demise.

1.4. Signalling Pathways in Cancer

1.4.1. Wnt-β-catenin Signalling

Wnt signalling is an important pathway implicated in development, stem cell control and cancer. In 1980, Nüsslein and Wischaus identified the gene *wingless* (*wg*) as a segment polarity gene in Drosophila embryogenesis[84]. In 1982, Varmus and Nusse used the mouse mammary tumour virus (MMTV) to mutate oncogenes responsible for mammary gland tumours in mice. In doing so, they discovered the proto-oncogene *integration 1* (*int1*)[85]. In 1987, it was found that *wg* and *int1* were homologous genes, so the two names were amalgamated to Wnt1[86,87].

Wnt-β-catenin has two functions: in cell adhesion between cell surfaces and in signal transduction to the nucleus. Adherens junctions are cell-cell junctional structures composed of E-cadherin, α-catenin and β-catenin complexes that form homophillic, Ca^{2+}-dependent interactions that hold epithelial cells together. At adherens junctions, transmembrane E-cadherin with its C-terminal domain directly binds the ARM domain of β-catenin, which interacts with α-catenin that binds to actin filaments. Through this protein complex, adherens junctions can send signals to the actin cytoskeleton leading to the reorganisation of actin filaments[88–91].

In signal transduction, the Wnt-β-catenin pathway has been extensively studied and described in the context of development and disease. Wnt pathway activation can be canonical or non-canonical[92]. The canonical Wnt-β-catenin pathway is the most comprehensively studied. In this β-catenin dependent pathway, extracellular Wnt proteins

(which are glycoproteins secreted by neighbouring cells and tissues) bind to seven transmembrane receptors, Frizzled (FZD) and its co-receptors Low-density-lipoprotein receptor-related proteins 5/6 (LRP5/6)[93,94]. This binding induces the recruitment of cytoplasmic dishevelled (Dvl) that is activated by phosphorylation[92]. Active Dvl directly interacts with Axin inducing its translocation to the plasma membrane resulting in the formation of a Wnt signalosome[95]. Here the dissociation and inhibition of GSK-3β from Axin (in the destruction complex) results in GSK-3β no longer being able to phosphorylate β-catenin on its N-terminus usually responsible for its subsequent ubiquitination by β-TrCP and degradation by the proteasome[96]. As a result, stabilized β-catenin is free to associate with the transcription factors LEF1 or the TCF's and translocate to the nucleus, where they induce the transcription of a number of β-catenin target genes, e.g. *Axin2*, *Ccnd1* and *Snai1*[97,98] (Figure 1.6). The N-terminus of β-catenin recruits co-factors such as BCL9 and Pygo while the C-terminus binds p300/CBP. This transcriptional complex then leads to the transcription of Wnt target genes[99,100].

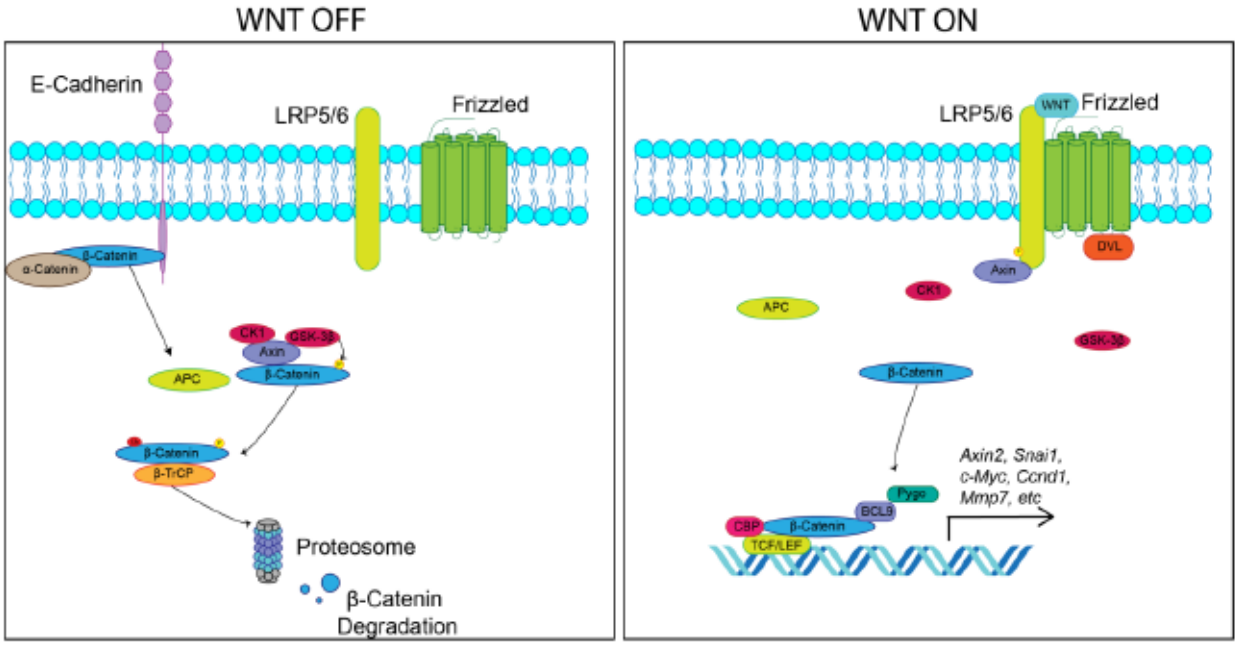

Figure 1.6: ***The canonical Wnt signalling pathway.*** Left, lack of Wnt ligands lead to the degradation of β-catenin by the destruction complex (Axin, Ck-1, Gsk-3β and APC). Right, in the presence of Wnt signals, Wnt binds to LRP/Frizzled receptors leading to the inactivation of the destruction complex. B-catenin therefore translocates to the nucleus where it binds with transcriptional co-activators such as TCF/LEF initiation the transcription of target genes.

β-catenin is a known proto-oncogene. It has been linked tumour initiation, growth and metastasis. Aberrant activation of β-catenin/Wnt through ligand over-expression, APC mutations and gain of function (GOF) β-catenin have all been shown to generate tumours in breast, skin, colon and liver[33,101–105]. APC mutations are the most common

mutation found in human colon cancers. APC is a tumour suppressor and negative regulator of β-catenin. It is part of the destruction complex that binds β-catenin molecules that have dissociated from adherens junctions resulting in β-catenin phosphorylation by CK1 and subsequently GSK-3β prior to proteosomal degradation[106].

In breast cancer, β-catenin is rarely mutated. However, in basal-like breast cancer β-catenin is highly expressed and active[107]. Nuclear and cytosolic localisation of β-catenin has been associated with basal cell markers, EMT and stem cell enrichment[61]. In agreement with these observations, mouse mammary tumours driven by aberrant β-catenin-Wnt activation (MMTV-Wnt1 and WAPcre; β-catenin^{GOF}) generate basal-like breast tumours with a stem cell-enriched population[33,108]. It is clear that β-catenin-Wnt signalling has important implications in tumorigenesis and stem cell phenotypes of basal-like mammary tumours that may yield a window to target CSCs in basal-like breast cancers.

1.4.2. HGF-Met Signalling

The HGF receptor tyrosine kinase Met is a proto-oncogene located on the cell surface of epithelial cells in the liver, breast, kidney and prostate[109,110]. The ligand responsible for Met activation was discovered as an inducer of scattering (scatter factor, SF) and motility (hepatocyte growth factor, HGF)[111–113]. The precursor of HGF is secreted by mesenchymal cells as a single-chain peptide that is cleaved by extracellular proteases at Arg494 and Val495. This bioactive mature form is made up of an α- and β-chain attached by disulphide bonds[114–116]. Once HGF binds the receptor, Met homodimerizes and becomes phosphorylated on active site tyrosines Y1234 and Y1235. Y1349 and Y1356 located at the carboxy-terminal tail subsequently become phosphorylated forming a Met unique dual SH2 recognition motif[117,118]. This phosphorylation cascade leads to activation of Src/focal adhesion kinase (FAK), phosphatidylinositol 3-kinase (PI3K), signal transducer and activator of transcription 3 (STAT-3) and RAS/MEK signalling pathways (Figure 1.7)[118–121].

The migratory or scattering phenotype induced by HGF-Met signalling has been implicated in embryonic development. This process, later termed epithelial to mesenchymal transition (EMT) is essential for the development of a three-dimensional body from the two-layer germinal disk. HGF-Met signalling has also been shown to be essential for later stages of development such as gastrulation, angiogenesis, nerve sprouting and bone remodelling. This has been demonstrated with targeted mutations or

genetic knock-out of HGF-Met in the mouse. Mouse embryos null for *Hgf* or *Met* die in utero due to mass defects during placental development[122,123]. HGF-Met signalling is therefore essential for development. This signalling pathway has also been implicated in the adult during wound healing and regeneration[124–126]. This is unsurprising due to the role of HGF-Met in EMT. EMT is an essential component of wound healing. In order for repair, epithelial cells located at the wound edge need to proliferate and migrate to fully regenerate/repair the tissue. In the adult liver, conditional knock-out of Met had no phenotypic effect under physiological conditions. However, upon liver injury these mice were hypersensitive to FAS-induced apoptosis while control mice acquired minor injuries[127].

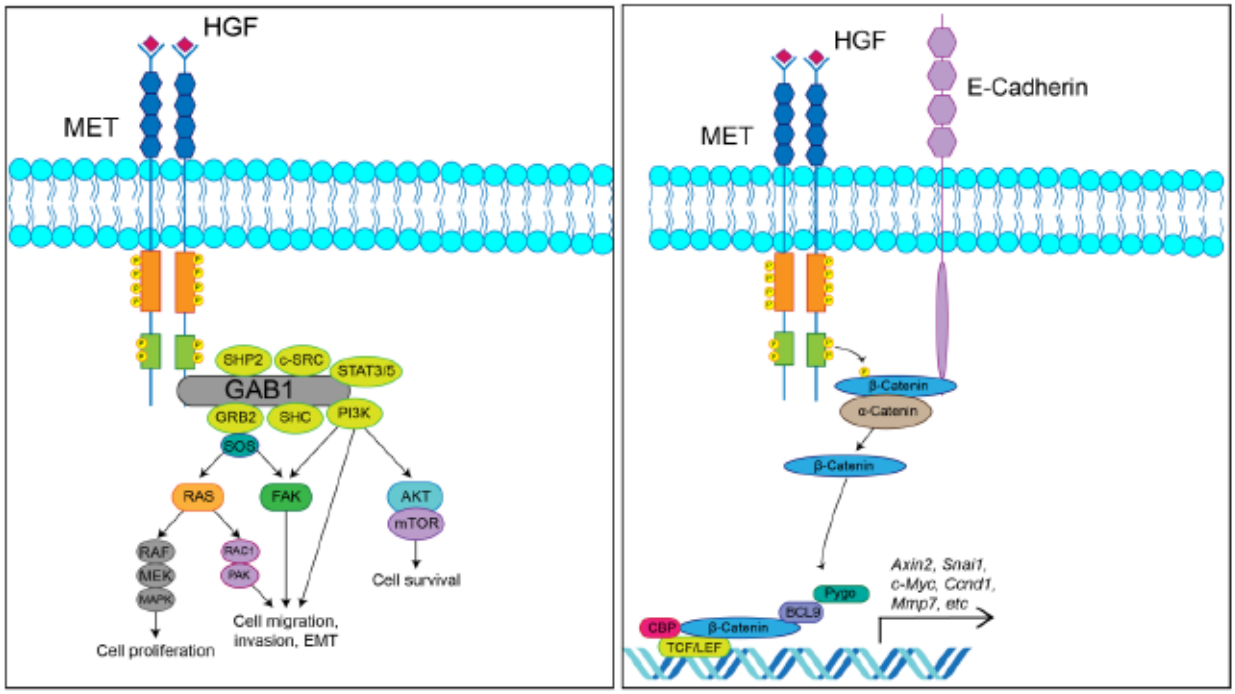

Figure 1.7: ***HGF-Met signalling.*** Left, classical HGF-Met signalling. Extracellular HGF binds the extracellular domain of the Met receptor leading to receptor homo-dimerization and phosphorylation of the intracellular domain. This forms a tandem SH2 motif that leads to the recruitment of adaptor proteins, GRB2 and SHC and the effector molecules PI3K, SRC, STAT3, SHP2 and STAT3 which lead to induction of cell proliferation, migration, invasion, survival and EMT. Right, HGF-Met induction of Wnt-β-catenin signalling. HGF binds the extracellular domain of the Met receptor. This leads to tyrosine phosphorylation of β-catenin, leading to its increased cytoplasmic and nuclear β-catenin. In the nucleus β-catenin induces gene transcription by interaction with TCF/LEF transcription factors.

It is a common phenomenon that pathways essential for embryonic development and tissue regeneration and repair are aberrantly altered in cancer. After all, cancer is essentially a developmental program gone astray. As for Wnt-β-catenin signalling, HGF-Met signalling has also been implicated in tumorigenesis and metastasis[128,129]. It has been found to be aberrantly activated in breast, liver, colon and pancreatic cancer. HGF-

Met is upstream of a number of cancer inducing/promoting signalling cascades including PI3K, RAS, STAT3 and β-catenin signalling resulting in the promotion of multiple tumorigenic effects such as angiogenesis, migration, invasion and metastasis[109]. Activation of the Met receptor facilitates anoikis resistance, survival of cells that have escaped the primary tumour and invaded into the blood stream[130]. Once these cells extravasate and colonize new tissues, HGF-Met continues its oncogenic role by interacting with the tumour microenvironment, inducing angiogenesis[131,132]. In support of this, cell lines expressing high levels of HGF-Met induce tumours and metastasis in nude mice[133].

In breast cancer, HGF-Met expression and activation is upregulated in about 70% and 48% of patients, respectively, and correlates with poor patient outcome[110,134]. While patients rarely (2–3%) generate sporadic *MET* mutations, activation of this receptor tyrosine kinase clearly has strong implications in tumorigenesis[135]. Gene and protein expression studies have shown that Met is an essential protein in basal breast cancer progression and metastasis[136]. In addition, HGF-Met activation in the mammary gland under the whey acidic protein (WAP) promoter controls the differentiation state of tumour cells and leads to the development of breast cancer with a gene signature similar to that of BLBC[33]. Therefore, HGF-Met signalling may likely be a plausible target for BLBCs.

1.4.3. Hippo-YAP Signalling

A critical signalling module that has been implicated in the maintenance, survival and expansion of stem cells is the Hippo pathway[137,138]. Two fundamental components of the Hippo pathway are Yes-associated protein (YAP) and transcriptional co-activator with PDZ-binding motif (TAZ) that both function as transcriptional co-activators. YAP activation is dependent on the upstream kinases of the Hippo pathway, Large tumour suppressor protein 1/2 (Lats1/2), mammalian STE20-like protein kinase 1/2 (Mst1/2) and the adaptor proteins Salvador homologue 1 (SAV1), MOB kinase activator 1A (MOB1A) and MOB1B[139]. In the absence of these signals, the Hippo pathway is inactive, resulting in the translocation of YAP into the nucleus where it binds its transcriptional activator TEAD 1-4 and elicits gene transcription. However, when active, these proteins promote LATS1/2-dependent phosphorylation of YAP/TAZ facilitating the binding of 14-3-3 leading to their cytoplasmic accumulation, ubiquitination and subsequent proteosomal degradation (Figure 1.8)[140].

HIPPO kinases can be regulated by a multitude of upstream factors including mechanical forces, Wnt signalling, metabolism, G protein coupled receptor (GPCR) and receptor signalling (HER2 and EGFR)[141–146]. In order to effectively time and execute the correct morphogenesis of limbs and organs during development, cells need to sense and interact with their surroundings. This is achieved by the cells ability to probe the ECM and microenvironment through adhesive proteins such as cell surface integrins[147]. In doing so, these cells develop an awareness of extracellular forces and can adjust their actomyosin contractility, reorganising their F-actin cytoskeleton, consequently altering their internal tension. This phenomenon is termed mechanotransduction and is an essential part of development, organ size, proliferation, self-renewal, wound healing and tumorigenesis[148]. Recently, YAP and TAZ activity have been demonstrated to be strongly regulated by the F-actin cytoskeleton's tension and conformation. YAP/TAZ has been shown to be activated in cells that have been plated onto stiff substrates due to activation of the Rho-associated protein kinase (ROCK) pathway and high non-muscle-myosin-II-driven cytoskeletal tension. Contrariwise, YAP/TAZ is sequestered in the cytoplasm when cells are plated onto soft substrates[141,149].

YAP and TAZ have been shown to play both positive and negative roles on Wnt signalling. At the level of canonical Wnt signalling, YAP/TAZ regulate Wnt signalling at the level of the β-catenin destruction complex. Azzolin, et al. have shown that YAP/TAZ interact with cytoplasmic β-catenin in the destruction complex. In the absence of Wnt signals, YAP and TAZ are sequestered in the cytoplasm by the destruction complex. However, upon Wnt stimulation YAP/TAZ are released from this complex and can freely translocate to the nucleus where they initiate their transcriptional activities with TEADs (1-4). It was further shown that YAP and TAZ are essential for the ubiquitin E3 ligase βTrCP to be recruited to the destruction complex. Therefore, in the absence of YAP/TAZ, β-catenin cannot be degraded resulting in increased nuclear β-catenin activity. In agreement with this, YAP/TAZ knock-out in embryonic stem cells compensates for loss of Wnt signalling with β-catenin being freely able to translocate to the nucleus[142]. At the level of non-canonical Wnt signalling, Hyun Woo, et al. have shown that Wnt ligand stimulation results in activation of YAP/TAZ through an alternative Wnt pathway acting through Wnt-FZD/ROR-$G\alpha_{12/13}$-Rho-Lats1/2-YAP/TAZ. In this model, Wnt5a/b or Wnt3a binds the FZD receptor activates the G-proteins $G\alpha_{12/13}$ that in turn activate Rho small GTPase activity to regulate the actin cytoskeleton, Lats1/2 inhibition and YAP/TAZ nuclear translocation[150]. It is clear that the HIPPO and Wnt pathways are tightly interlinked. There is much interest in identifying novel regulators of YAP/TAZ activity. Another pathway that was recently described is how the receptor tyrosine kinase EGFR activates YAP/TAZ activity in

hepatocellular carcinoma (HCC) cells. It was found that EGF stimulation of HCC cells induces YAP nuclear translocation[146]. Although elucidation of these upstream regulators is essential for identifying pathways that could be manipulated to induce wound healing and regeneration via YAP/TAZ activity, the manipulation of these pathways in the context of anti-cancer therapy will likely fail to the plasticity and multitude of these upstream pathways.

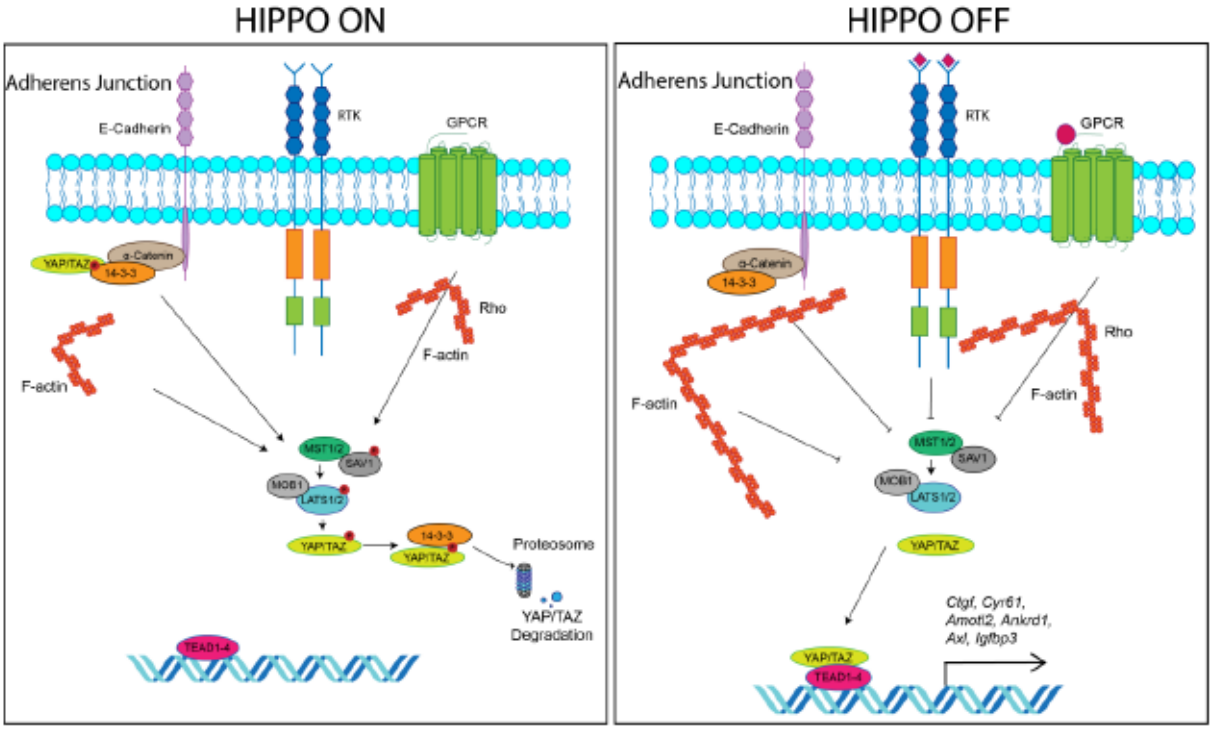

Figure 1.8: ***The HIPPO-YAP signalling pathway.*** Left, HIPPO pathway on. In the absence of upstream signals (cell-cell contact, actin reorganisation, RTK or GPCR activation), the central HIPPO kinases MST1/2 and LATS1/2 are phosphorylated and active, leading to the phosphorylation of YAP/TAZ, 14-3-3 binding and YAP/TAZ degradation by the proteasome. Right, HIPPO pathway off. In the presence of upstream signals, the core kinases MST1/2 and LATS1/2 are unphosphorylated and therefore rendered inactive. This results in the nuclear translocation of YAP/TAZ to the nucleus where they bind the transcriptional co-activator TEAD 1-4 leading to the transcription of target genes such as *Ctgf*, *Ankrd1* and *Igfbp3*.

YAP and TAZ are commonly activated in human malignancies. YAP and TAZ have been shown to promote tissue growth and proliferation through binding transcription factors such as TEADs and SMADs[151]. Aberrant activation of any of these programmes can initiate or contribute to the cancer programme. Aberrant activation of YAP has been shown to have a prominent effect on oncogenic signalling in many cancers, including breast cancer[152,153]. However, recent studies have suggested that YAP is beneficial or irrelevant in the context of breast cancer. One study suggests that YAP may function as a tumour suppressor, while the other suggests that YAP is not active in primary DCIS[154,155]. Clearly, there is much controversy in the field. Of note, these studies fail to investigate the

possible differential roles of YAP in luminal vs. basal breast cancers or in cell heterogeneity within tumours such as CSCs vs. more differentiated tumour cells.

2. AIMS OF THE THESIS

Breast cancer is the most frequently diagnosed cancer in women worldwide. In recent years, mortality rates have significantly decreased as a result of early detection and adjuvant therapies. However, the mortality rate of basal-like breast cancer patients has remained steady. Basal breast cancers are aggressive and don't respond well to adjuvant chemotherapeutics. Unlike luminal breast cancers that express targetable hormone receptors, basal breast cancers are poorly characterised and display a high cancer stem cell phenotype leading to resistance against chemotherapy. Indeed, identification of novel targetable molecular pathways is essential in the fight against this hostile disease. In the present study, I employ a mouse model of basal breast cancer, taking advantage of Wnt and Met signalling. Previously, we observed that combined Wnt and Met signalling hyper-drives the development of basal breast cancer with a high cancer stem cell phenotype. However, the molecular cooperation between these two pathways was unknown. I aimed to identify the culprit of Wnt-Met driven tumorigenesis using a proteomics based approach and use mouse genetics to study the importance of the identified protein in Wnt-Met driven tumorigenesis.

3. RESULTS

3.1. HGF-Met and Wnt-β-catenin signalling co-operate to drive basal-like mammary gland tumours

Studies have reported that basal-like tumours originate from the luminal compartment of the mammary gland[156]. Our laboratory has previously generated a mouse model of basal-like breast cancer that activates both Wnt and Met signalling under the control of the WAP (whey acidic protein) promoter[33]. WAP is expressed specifically in the mammary gland during and after pregnancy[157]. The Wnt-Met mouse model contains a WAP-driven cre recombinase and a gain-of-function β-catenin allele (β-Cat$^{\Delta ex3/wt}$) whereby the third exon of β-catenin (which is required for phosphorylation by GSK3 and subsequent ubiquitination and degradation by the proteasome) is flanked by two loxp sites[158]. In addition, HGF, the ligand responsible for activation of the Met receptor tyrosine kinase is also under the control of the WAP promoter, leading to overexpression of HGF and activation of the Met receptor[111,159]. Finally, these mice were crossed with an EYFP reporter, R26-stop-EYFP[160]. Upon cre-recombination, the stop cassette is removed allowing for constitutive expression of EYFP, thus allowing tracing of all Wnt-Met cells[33]

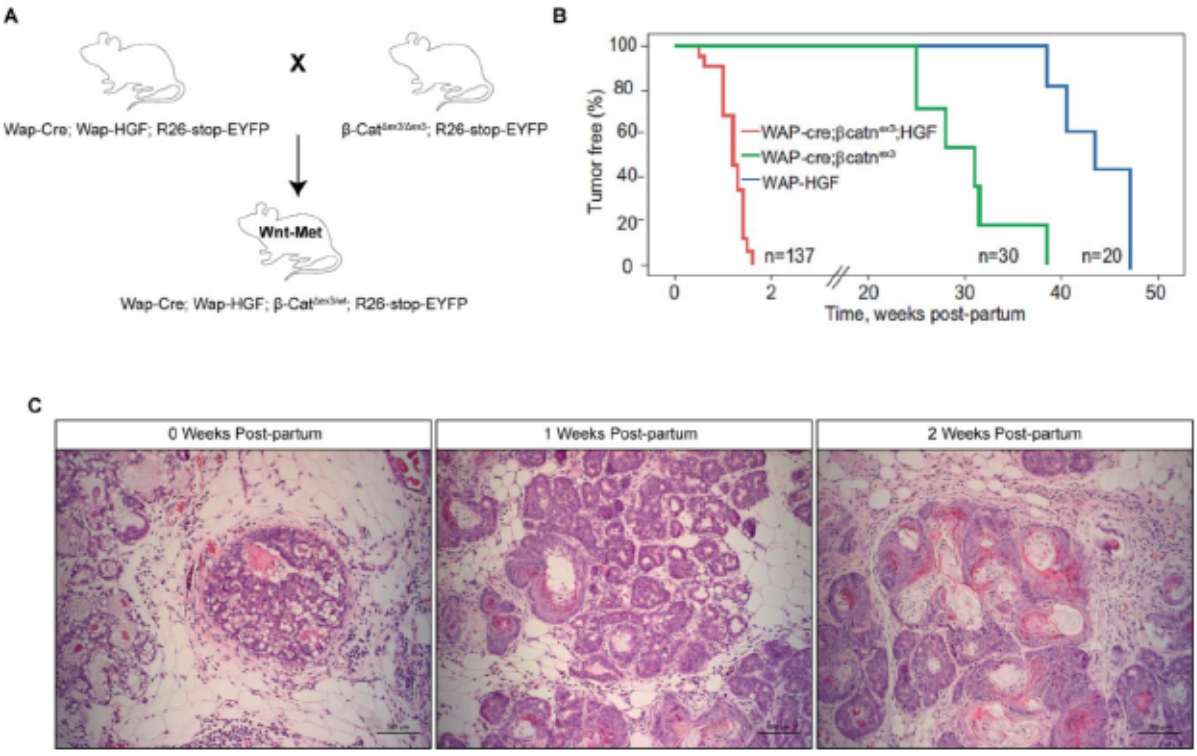

Figure 3.1: ***Wnt-Met signalling generates mammary gland tumours in mice***. **A.** Breeding scheme used to create Wnt-Met mice. **B.** Kaplan-Meier curve showing the percentage of tumour-free mice[33]. **C.** Haematoxylin and Eosin (H&E) staining of Wnt-Met tumours at 0, 1 and 2 weeks post-partum (PP), scale bar = 100μm.

(Figure 3.1A). Upon induction of the WAP promoter via pregnancy stimulation, Wnt-Met mice developed aggressive tumours in a little as two-weeks post-partum (PP), while the single mutants develop tumours in 30-40 weeks PP[33] (Figure 3.1B). At zero-weeks PP, Wnt-Met mammary glands appeared healthy, with loose stroma consisting primarily of adipoctyes and single layered acini with hollow lumen. At one-week PP, mammary glands were denser in epithelial cells with some filled acini but still exhibited healthy-looking loose adipocyte-enriched stroma. At later stages of tumorigenesis (for instance at two-weeks PP), the mammary gland stroma was almost completely adipocyte-free and filled with large amounts of fibroblasts[34], while the mammary acini were completely filled with dense tumour cells (Figure 3.1C).

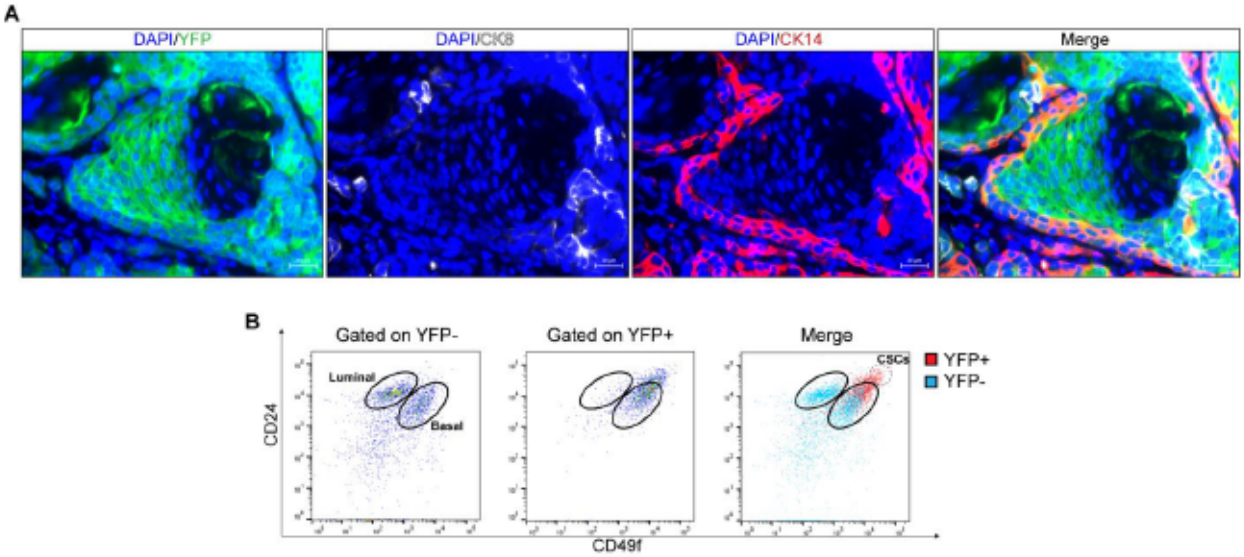

Figure 3.2: ***Wnt-Met signalling generates basal-like mammary gland tumours in mice.*** **A.** Immunofluorescence of Wnt-Met tumours two-weeks PP showing YFP (green), CK8 (white) and CK14 (red), scale bar 20µm. **B.** FACS plots of Wnt-Met tumours two-weeks PP showing YFP, CD24 and CD49f cells.

To show WAP-dependent transgene expression and that Wnt-Met tumours are basal-like, immunofluorescence was conducted. Cre-recombination was confirmed by strong expression of YFP (green). In addition, the basal-like phenotype was confirmed as a minimal number of cells stained positive for the luminal marker CK8 (white), while the basal marker CK14 (red) was highly expressed (Figure 3.2A). FACS for the cell surface markers CD24 and CD49f are widely used in the mammary gland field to isolate luminal, basal and stem-cell populations[73]. In the mouse, $CD24^{+}$ $CD49f^{+}$ cells represent the luminal cell population, while $CD24^{hi}$ $CD49f^{hi}$ cells represent the basal (stem cell-containing) population[16,161]. Therefore, in an effort to further characterise Wnt-Met tumours, FACS was performed on Wnt-Met tumour cells two-weeks PP. Untransformed

YFP$^-$ cells exhibited a clear separation of both the luminal (CD24$^+$ CD49f$^+$) and basal (CD24^{hi} CD49f^{hi}) populations. However, the YFP$^+$ (transformed) population primarily contained basal cells with a high shift towards the CD24^{hi} CD49f^{hi} population, indicating the generation of CSCs in Wnt-Met tumours (Figure 3.2B).

3. 2. RTK signalling drives tumorigenesis through YAP activation

3.2.1. HGF-Met regulates YAP and β-catenin activity in Wnt-Met mammary glands

The combination of β-catenin-Wnt and HGF-Met signalling significantly increases the development of mammary gland tumours in mice[33]. Previous reports have shown that receptor tyrosine kinase (RTK) signalling can activate YAP in hepatocytes[146]. Therefore, I speculated that HGF-Met signalling may regulate YAP activity in the mammary gland thereby increasing tumour development and growth. In collaboration with Philipp Mertins and Oliver Popp at the MDC, proteomic analysis of Wnt and Wnt-Met mammary glands at early stages of tumorigenesis promoted strong upregulation of the YAP signature[162], indicating that YAP is activated in double but not in single mutants (Figure 3.3A). Indeed, Wnt-Met double-mutant mammary glands contained 6-fold more YAP-positive nuclei, compared to single Wnt mutants (Figure 3.3B, C). This result was confirmed by Western blotting for active YAP (Figure 3.3D). In agreement with this, qPCR analysis revealed a significant increase in the YAP target genes *Ctgf*, *Cyr61*, *Igfbp3* and others in the mammary glands of Wnt-Met vs. Wnt alone mice (Figure 3.3E). Analysis of the phosphoproteome revealed a significant increase in YAP phosphorylation at S46 and T48, suggesting these sites for phosphorylation and nuclear activation (Figure.3. 3F).

In line with previous reports, I also investigated if HGF-Met signalling was also responsible for β-catenin nuclear translocation. Immunofluorescence microscopy revealed a ~20% increase of nuclear β-catenin in Wnt-Met cells vs. Wnt alone cells (Figure. 3.4A, B). Wnt target genes such as *Axin2*, *Lgr5* and others were increased in the mammary glands of Wnt-Met mice (Figure. 3.4C)[163,164]. Previously, we had conducted gene expression analysis on mammospheres generated from Wnt-Met tumours treated with the Met inhibitor PHA665752, which inhibits the kinase activity of the Met intracellular

domain. I analysed the expression of YAP (identified from[162]) and Wnt target genes. Remarkably, both YAP and Wnt target genes were significantly decreased in treated spheres (Figure. 3.5A). I confirmed this decrease by qPCR of the YAP target genes *Ctgf*, *Cyr61* and *Igfbp3* (Figure. 3.5B). Overall, these data show that HGF-Met signalling activates both YAP and β-catenin in the mammary gland.

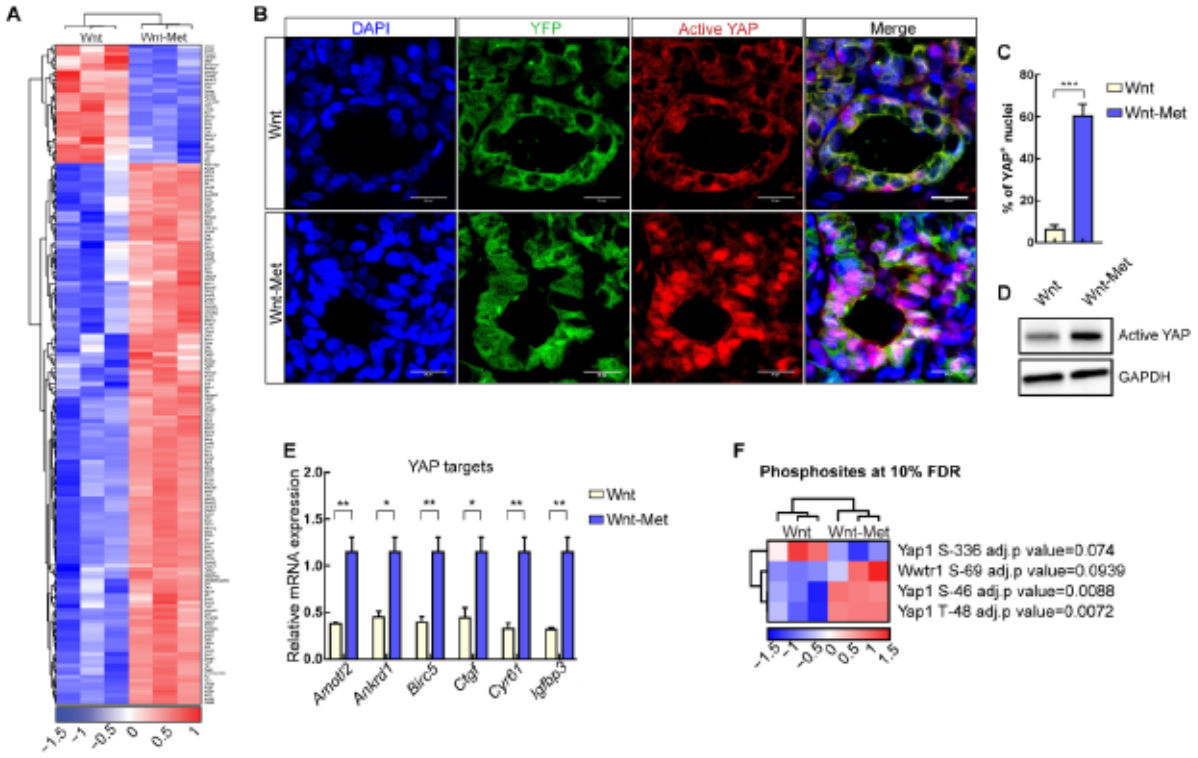

Figure 3.3: ***HGF-Met regulates YAP activity in Wnt-Met tumours***. **A.** Heatmap of proteomics analysis showing the YAP signature (based on Zanconato et al., 2016) in WAPicre; β-cat^{GOF}; ROSA26^{EYFP} (Wnt) in comparison to WAPicre; Wap-HGF; β-cat^{GOF} ; ROSA26^{EYFP} (Wnt-Met) mice at one-week PP. The YAP signature proteins shown were significant in a two-sample moderated t-test (adj. p-value ≤ 0.05; row-scaling was applied). Values are median-MAD-normalised across all proteins and row-scaled across all samples. **B.** Immunofluorescence of YFP (green) and active YAP (red) in WAPicre; β-cat^{GOF}; ROSA26^{EYFP} (Wnt) and WAPicre; Wap-HGF; β-cat^{GOF}; ROSA26^{EYFP} (Wnt-Met) mice at one-week PP, scale bar, 20μm. **C.** Quantification of YAP-positive nuclei (YAP+ nuclei/number of nuclei per field x100) in Wnt vs. Wnt-Met tissues. Data are mean ±SEM, n=3 biological replicates, ***p<0.001, by Student's t test. **D.** Western blot of active YAP in Wnt and Wnt-Met tissues at one-week PP. **E.** RT-qPCR of YAP target genes in Wnt and Wnt-Met tissues at one-week PP. Data are mean ±SEM, n=3 biological replicates, *p<0.05, **p<0.01, by Student's t-test. **F.** Heatmap of proteomics analysis showing YAP and TAZ (Wwtr1) phosphorylation sites that were significant in a two-sample moderated t-test (adj. p-value ≤ 0.1) revealing significant increase in YAP phosphorylation at S46 and T48 (row-scaling was applied). The heatmap shows median-MAD-normalised input data across all proteins and row-scaling across all samples as was clustered based on Euclidian distance.

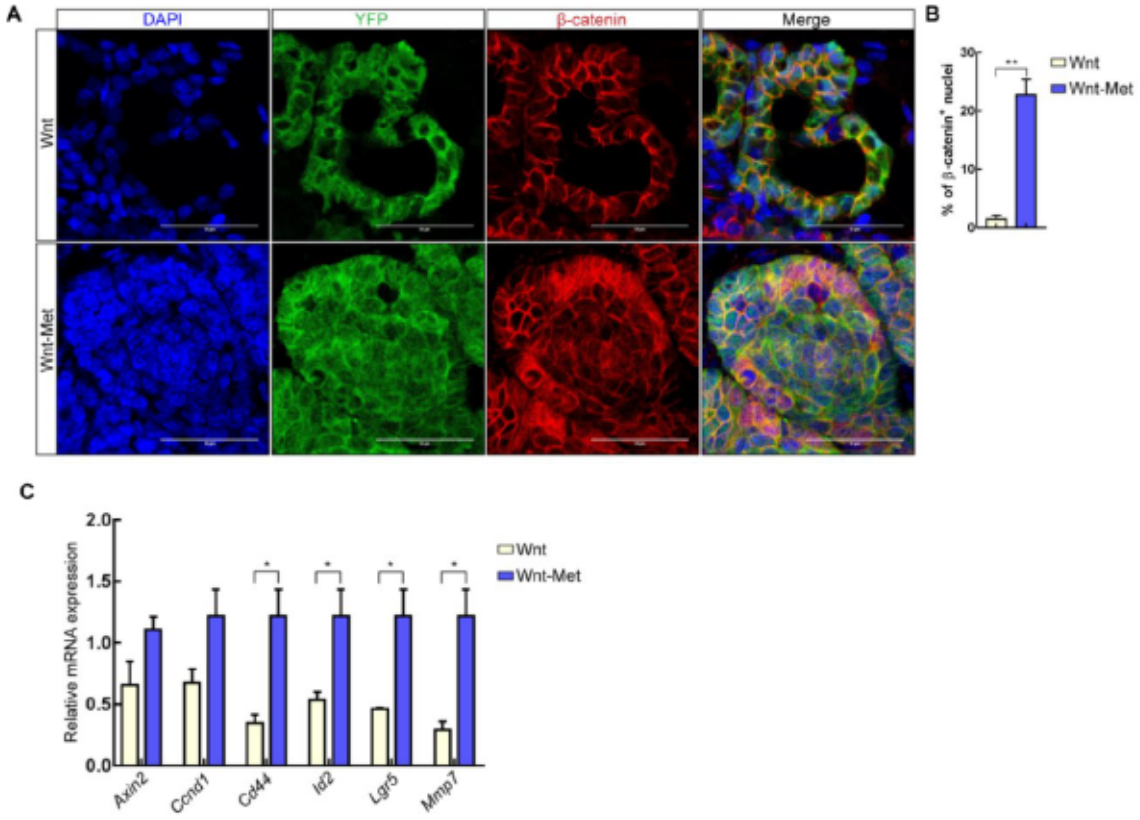

Figure 3.4: ***HGF-Met regulates β-catenin activity in Wnt-Met tumours.*** **A.** Immunofluorescence of YFP (green) and β-catenin (red) in WAPicre; β-cat^{GOF}; ROSA26^{EYFP} (Wnt) and WAPicre; WAP-HGF; β-cat^{GOF} ; ROSA26^{EYFP} (Wnt-Met) at one-week PP, scale bar, 20μm. **B.** Quantification of β-catenin-positive nuclei (β-catenin^{+} nuclei/number of nuclei per field x 100) in Wnt vs. Wnt-Met tissues. Data are mean ±SEM, n=3 biological replicates, **p<0.01, by Student's t test. **C.** RT-qPCR of YAP target genes in Wnt and Wnt-Met mammary glands. Data are mean ±SEM, n=3 biological replicates, *p<0.05.

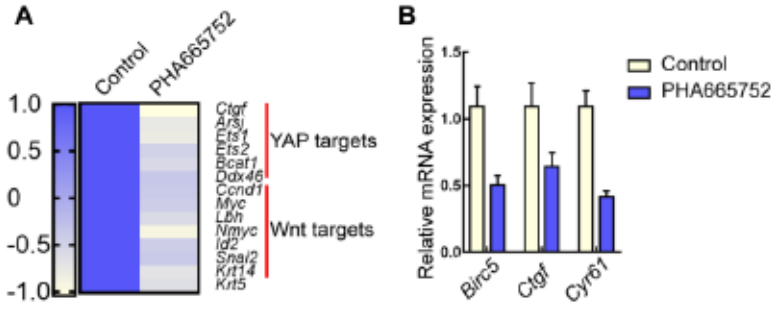

Figure 3.5: ***Met inhibition prevents YAP target gene expression.*** **A.** Heatmap of YAP and Wnt target genes of DMSO vehicle control and PHA665752-treated mammospheres. **B.** RT-qPCR of YAP target genes in DMSO vehicle control and PHA665752-treated Wnt-Met mammospheres.

3.2.2. MET regulates YAP and β-catenin target gene expression in human BT-549 cells

To investigate if the RTK MET regulated YAP and β-catenin in human cells, I next utilised the basal and triple-negative human breast cancer cell line BT-549. Knockdown of MET expression via siRNA resulted in a strong decrease in protein expression. Of note, siMET significantly decreased the levels of active YAP, as seen by Western blot (Figure 3.6A). In agreement with this and in line with the mouse data, MET knock-down also resulted in a significant decrease in the expression of YAP and Wnt target genes such as *IGFBP3*, *ANKRD1*, *CCND1* and *CLDN1*[162,165] (Figure 3.6B, C). These results show that HGF-MET signalling activates YAP in BT-549 cells.

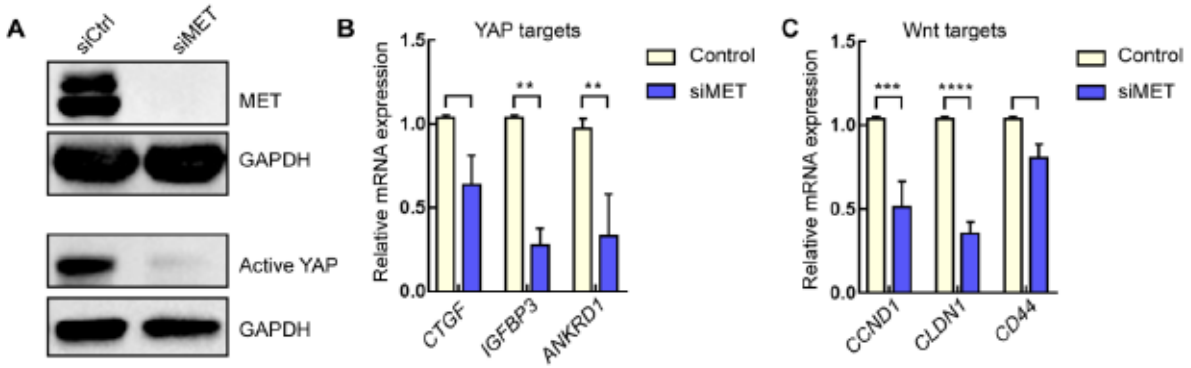

Figure 3.6: ***MET and HGF regulate YAP and β-catenin target gene expression in BT-549 cells.*** **A.** Western blot of BT-549 cells with siSramble or siMET, active YAP and GAPDH as a loading control. **B.** qPCR of YAP target genes upon siSramble and siMET knock-down, Data are mean ±SEM, n=3 biological replicates **p<0.006. **C.** qPCR of Wnt target genes upon siSramble and siMET knock-down, Data are mean ±SEM, n=3 biological replicates ***p<,0.0005 ****p<0.0001, n=3.

3.3. YAP activity in Wnt-Met tumours

3.3.1. YAP is active in Wnt-Met tumours

The Hippo transducer YAP has been implicated in tissue regeneration, stemness and resistance to anti-cancer therapies[166]. Recently, there have been conflicting reports regarding the role of YAP in breast cancer. Lee et al[155], have shown that YAP expression is exclusively cytoplasmic/inactive in DCIS. In agreement with this, Elster et al[154] suggested that YAP may function as a tumour suppressor in the context of breast cancer[154,155]. However, these reports focused primarily on studies in cell lines and failed to investigate the subtype-dependent roles of YAP in breast cancer. Therefore, I employed our Wnt-Met model to investigate if YAP is active in basal-like tumours. Immunohistochemistry staining for YAP revealed strong expression of active YAP in Wnt-Met tumours, which is unphosphorylated and nuclear (Figure. 3.7A). Total protein lysates

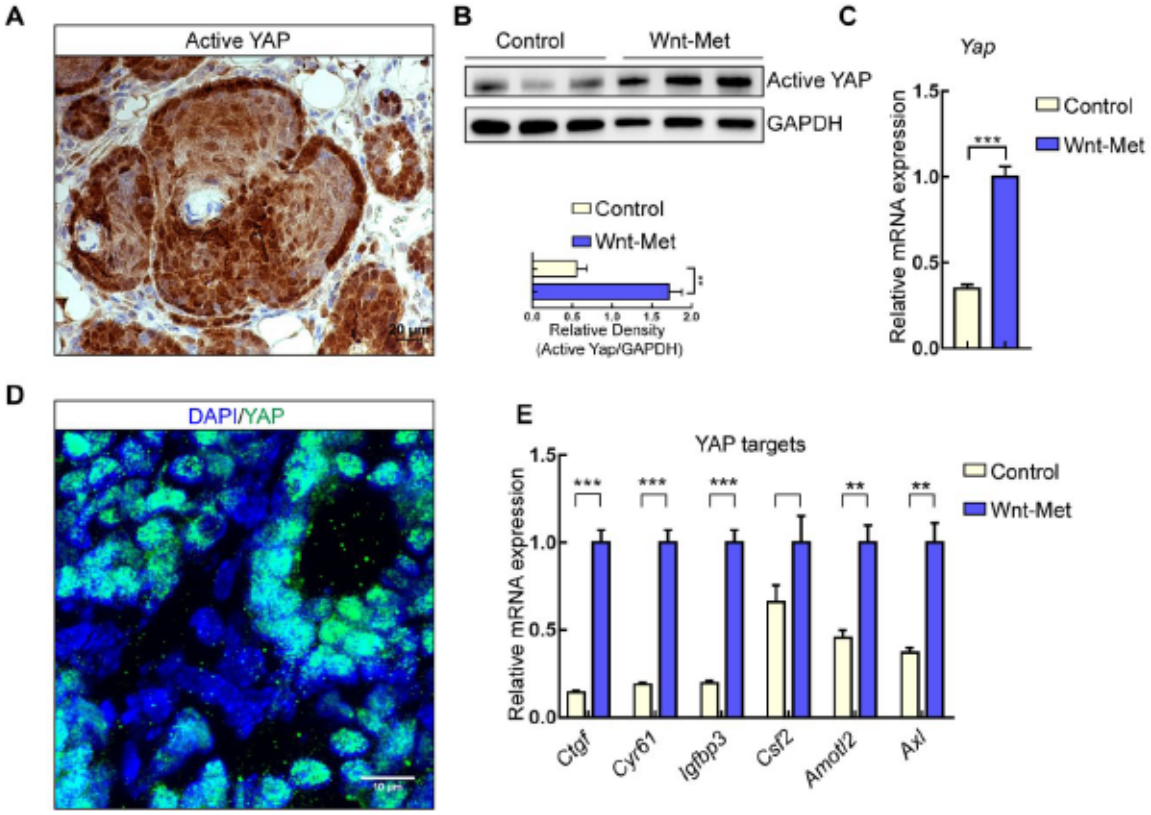

Figure 3.7: ***YAP is active in Wnt-Met tumours.*** **A.** Immunohistochemistry of active YAP in Wnt-Met tumours two-weeks PP, scale bar 20μm. **B.** Western blot analysis of Wapicre;YFP (Control) and Wnt-Met tumours at two-weeks PP showing active YAP expression, GAPDH was used as a loading control (upper). Quantification of active YAP expression using GAPDH as a loading control. **C.** qPCR analysis of *Yap* expression in Wapicre;YFP (Control) and. Wnt-Met mammary gland tissues two-weeks PP. **D.** Confocal image of active YAP (green) in Wnt-Met tumours two-weeks PP, scale bar 10μm. **E.** qPCR analysis of YAP target genes in Wapicre;YFP (Control) and Wnt-Met mammary gland tissues two-weeks PP. Data are mean ± SEM, n=3 biological replicates **p<0.01, ***p<0.001 by Student's t test.

of control mammary glands vs. Wnt-Met tumours also showed a significant elevation of active YAP, as shown by Western blot and qPCR respectively (Figure 3.7B, C). Furthermore, confocal microscopy of active YAP in Wnt-Met tumour sections showed strong nuclear staining of active YAP in Wnt-Met tumours further confirming YAP activity (Figure 3.7D). Finally, qPCR revealed elevated expression of the YAP target genes *Ctgf*, *Cyr61*, *Igfbp3* and others, confirming that YAP was functionally active in Wnt-Met tumours (Figure 3.7E).

3.3.2. YAP is active in the CSCs of Wnt-Met tumours

YAP is a crucial regulator of cell proliferation and stemness[167]. As mentioned previously, YAP has been shown to play an important role for many stem cell-associated properties, for example resistance to anoikis and tissue regeneration[152,168]. I therefore

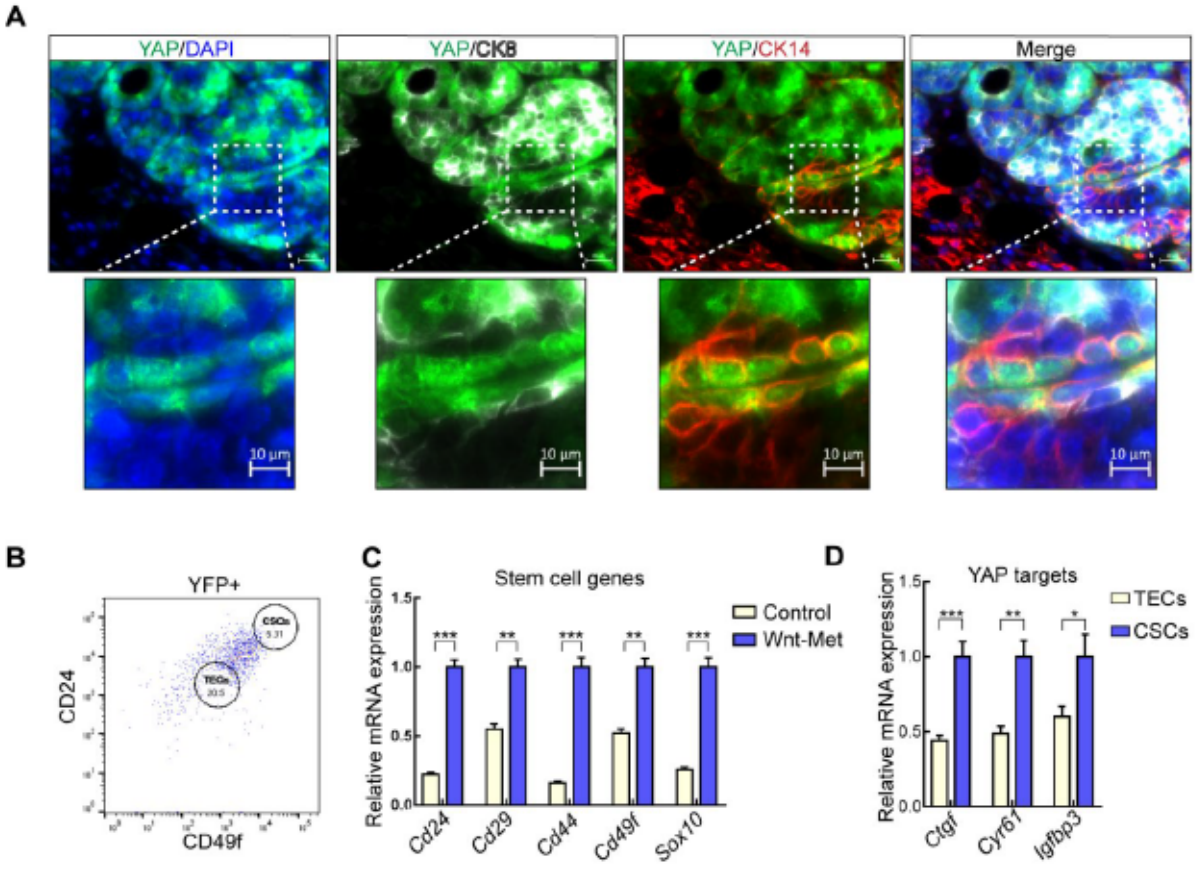

Figure 3.8: ***YAP is active in the CSCs of Wnt-Met tumours***. **A.** Immunofluorescence of YAP (green), K8 (white) and K14 (red) in Wnt-Met tumours two-weeks PP, scale bar 20 and 10µm. **B.** FACS of Wnt-Met tumours showing active the $CD24^{+}$ $CD49f^{+}$ (TEC) and $CD24^{hi}$ $CD49f^{hi}$ (CSC) populations. **C.** qPCR analysis of stem cell-associated genes in Wapicre;YFP (Control) and Wnt-Met tumours 2 weeks post-partum. **D.** qPCR analysis of YAP target genes in TECs vs. CSCs. Data are mean ± SEM, n=3 biological replicates *p<0.05, **p<0.01, ***p<0.001 by Student's t test.

postulated that YAP was active in the CSCs of Wnt-Met tumours. In the mammary gland, the basal cell compartment is known to harbour the stem cell population[161]. I investigated if YAP activity was restricted to the basal compartment of Wnt-Met tumours. Immunofluorescence analysis confirmed that YAP was nuclear in the CK14 (red) but not CK8 (white) cells of Wnt-Met tumours (Figure 3.8A). Making use of FACS-based isolation using the cell surface markers CD24 and CD49f described previously[33], I isolated CSC ($CD24^{hi}$ $CD49f^{hi}$) and the more differentiated tumour epithelial cells (TECs) ($CD24^{+}$ $CD49f^{+}$) (Figure 3.8B). qPCR of the stemness-associated genes *Cd29*, *Cd49f* and others[15,17] confirmed significantly elevated expression in control vs. Wnt-Met tissues (Figure 3.8C). In addition, the expression of YAP target genes was significantly higher in CSCs compared to TECs (Figure 3.8D). Overall, these results show that YAP is primarily active in the CSCs of Wnt-Met tumours, suggesting that YAP may be a potential target for anti-CSC therapy in breast cancer.

3. 4. Establishment of cell culture systems to study Wnt-Met stem-enriched cells

3.4.1. Stem cell-enriched spheres recapitulate Wnt-Met tumours

CSCs are responsible for minimal residual disease and eventual tumour relapse[169,170] and we have shown above that YAP is active in the CSCs of Wnt-Met tumours. In an effort to study the role of YAP in CSCs, I established a 3D stem cell-enriched culture system adapted from a previous publication[171]. Control mammary glands or Wnt-Met tumours were harvested two-weeks PP and digested into single cells. The single cell suspension was then seeded on 2D collagen I plates. Plates were incubated for 18hrs, enriching for epithelial cells. Epithelial cells were then seeded as single cells into a 50% reduced growth factor (RGF) Matrigel bubble supplemented with a stem-enriching medium[172] (Figure 3.9A). 5 days post-seeding, control spheres formed hollow lumen, while Wnt-Met-derived spheres formed primarily large disorganised, filled structures (Figure 3.9B). FACS for YFP showed that Wnt-Met spheres contained 1.4-fold (57% to 76%) more YFP-positive cells than controls (Figure 3.9C). Finally, I confirmed that the WAP promoter remained active in the spheres as seen by qRT-PCR of *Wap*, *Hgf* and the β-catenin target genes *Axin2*, *Lgr5* and *Procr* (Figure 3.9D).

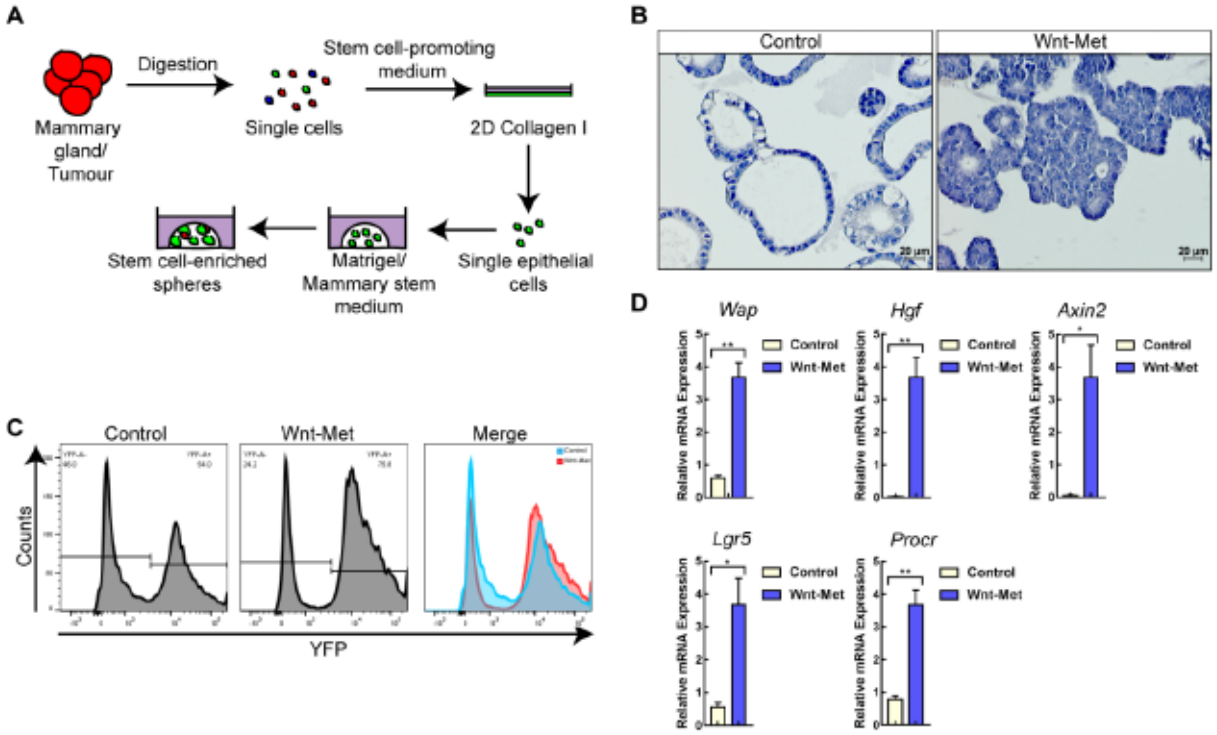

Figure 3.9: ***Establishment of a cell culture system to study CSCs.*** **A.** Schematic diagram showing the procedure for the generation of stem cell-enriched sphere cultures. **B.** H&E staining of spheres isolated from Wap-cre; YFP^{rosa26} (control) and Wnt-Met mammary glands, scale bar 20µm. **C.** FACS of YFP in Wap-cre; YFP^{rosa26} (control) and Wnt-Met single cells isolated from sphere cultures. **D.** qPCR analysis of Wnt-Met genes in Wap-cre; YFP^{rosa26} (control) and Wnt-Met sphere cultures. Data are mean ± SEM, n=3 biological replicates *p<0.05, **p<0.01, ***p<0.001 by Student's t test.

I next sought out to confirm that the stem cell-enriched cultures accurately recapitulated mammary gland tissues. Immunofluorescence of control vs. Wnt-Met spheres revealed that cultures derived from Wap-cre; R26-stop-EYFP mice were primarily composed of luminal CK8 positive YFP+ and YFP- cells (Figure 3.10A, upper panel). In contrast to this, Wnt-Met-derived cultures were almost entirely composed of basal CK14+, YFP+ cells with few luminal CK8+ cells, as observed *in vivo* (Figure 3.10A, lower panel). Since we aimed to use the stem cell-enriched spheres to study the CSCs of Wnt-Met tumours, we intended to test the sphere-forming ability of FACSorted CSCs compared to TECs. $CD24^{+}$ $CD49f^{+}$ TECs formed significantly fewer spheres when compared with $CD24^{hi}$ $CD49f^{hi}$ CSCs (Figure 3.10B, left). Lastly, I confirmed that Wnt-Met stem cell-enriched cultures exhibited high levels of nuclear β-catenin, representing the CSC-population (Figure 3.10C). These data show that stem cell-enriching conditions enrich for CSCs and mimic tumours.

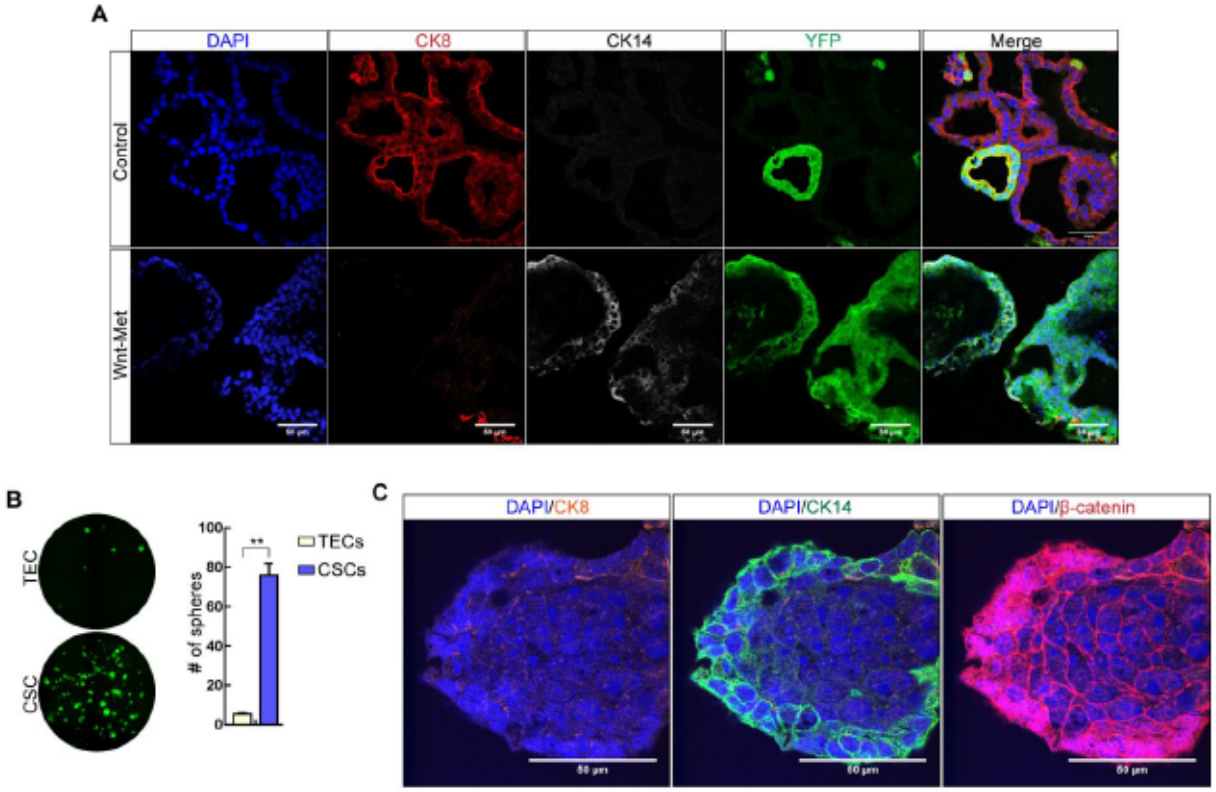

Figure 3.10: ***Wnt-Met stem cell-enriched spheres mimic in vivo tumours and contain CSCs***. **A.** Immunofluorescence of K8 (red), K14 (white) and YFP (green) in Wap-cre; YFP^{rosa26} (control) and Wnt-Met spheres, scale bar 50µm. **B.** Fluorescence microscopy of FACSorted TECs and CSCs after 7 days in culture. Data are mean ± SEM, n=3 biological replicates **p<0.01 by Student's t test. **C.** Confocal microscopy of Wnt-Met spheres for K8 (orange), C14 (green) and β-catenin (red), scale bar 50µm).

3.4.2. YAP is active in stem cell-enriched spheres

Immunofluorescence of YAP in Wnt-Met spheres confirmed strong expression of nuclear YAP (green) in stem cell-enriched Wnt-Met spheres (Figure 3.11A). Furthermore, active YAP (green) and the basal marker P63 (red) confirmed that YAP was specifically active in the basal cells of Wnt-Met spheres, as observed in tumours (Figure 3.11B). Finally, qPCR of YAP target genes revealed high YAP activity in Wnt-Met spheres compared to control (Figure 3.11C). Overall, stem cell-enriched cultures can be accurately used to mimic Wnt-Met tumours for further studies.

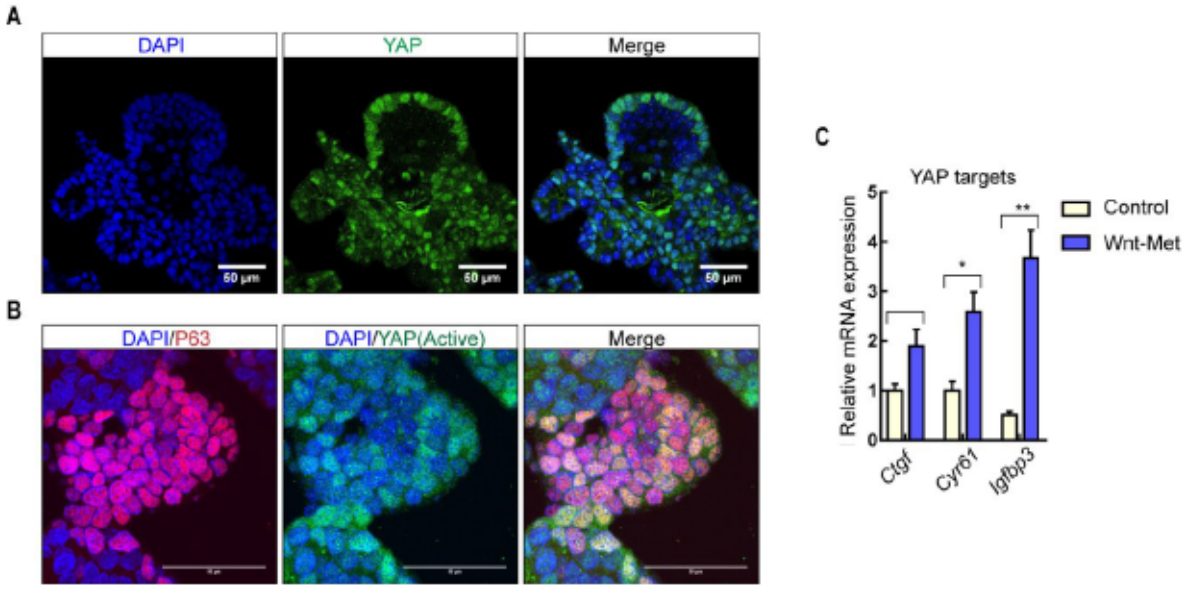

Figure 3.11: ***YAP is active in stem cell-enriched spheres.*** **A.** Immunofluorescence of YAP (green) in Wnt-Met spheres, scale bar 50µm. **B.** Confocal images of P63 (red) and active YAP (green) in Wnt-Met spheres, scale bar 50µm. **C.** qPCR analysis of YAP target genes in Wap-cre; YFP^{rosa26} (control) and Wnt-Met spheres. Data are mean ± SEM, n=3 biological replicates *p<0.05, **p<0.01 by Student's t test.

3. 5. The role of YAP in Wnt-Met tumours

3.5.1. Small molecule inhibition of YAP activity blocks growth and proliferation of stem cell-enriched spheres

As mentioned previously, YAP has been implicated in tumorigenesis. However, its role in breast cancer has been controversial[154,155]. I sought out to investigate the role of YAP in our Wnt-Met model of BLBC, using stem cell-enriched spheres. Many drugs screens have been conducted in an effort to identify inhibitors of YAP activity. To date there are two main small molecules that are widely used as YAP inhibitors. Verteporfin was shown to inhibit YAP interaction with its transcriptional activator, TEAD 1-4[173]. Statins were also found to inhibit YAP activity. Statins inhibit HMG-CoA reductase, leading to impaired geranylgeranylation of RHOA[144]. Ultimately, this leads to cytoplasmic retention and inactivation of YAP. Wnt-Met-derived spheres were grown from single cells for 5 days before being treated for 48 hrs with SIM or VP. The number of treated spheres were significantly decreased compared to control spheres and in addition, VP-treated spheres had a significantly reduced metabolic rate as measured using the CellTitreGlo[174] assay (Figure 3.12A, B). In addition, the proliferation rate of treated spheres was greatly retarded as marked by BrdU staining of VP-treated spheres and Ki-67 staining of SIM-

treated spheres (Figure 3.12C, D). Inhibition of YAP activity was confirmed by significant decrease in the expression of the YAP target genes *Amotl2*, *Ankrd1* and *Csf2*[162] in treated spheres (Figure. 3.12E). These results show that YAP is required for the growth, maintenance and proliferation of Wnt-Met-derived spheres.

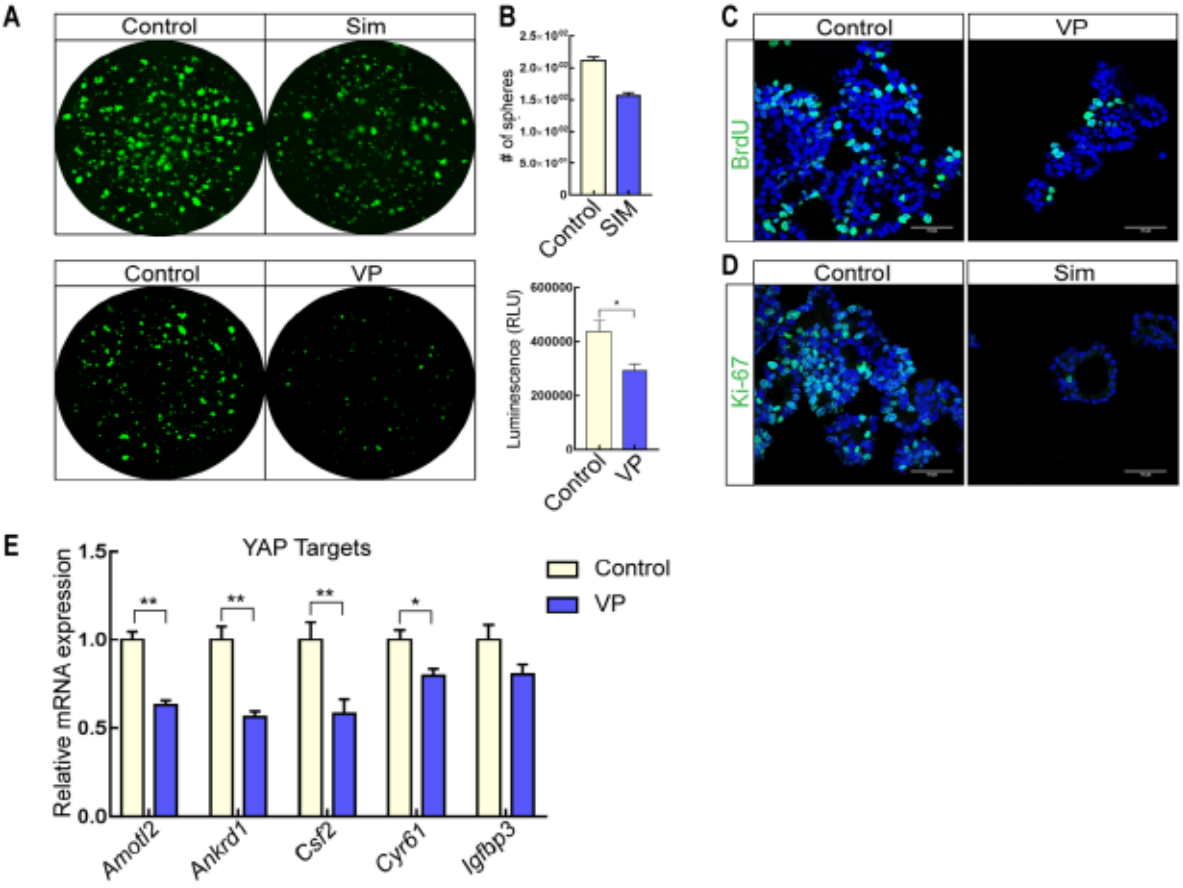

Figure 3.12: ***YAP controls growth and proliferation in stem cell-enriched spheres.*** **A.** Fluorescence microscopy of Wnt-Met spheres treated with DMSO vehicle control, SIM (2.5μM) and VP (2μM). **B.** Quantification of sphere number (top) and viability (bottom) of treated spheres **C, D.** Immunofluorescence images of the proliferation markers BrdU and Ki-67 in treated spheres. **E.** RT-qPCR analysis of YAP target genes upon DMSO vehicle control and VP treatment. Data are mean ± SEM, n=3 biological replicates *p<0.05, **p<0.01 by Student's t test.

3.5.2. YAP inhibition blocks the self-renewal of Wnt-Met stem cell-enriched spheres

Since Wnt-Met-derived spheres enrich for CSCs, I utilized this cell culture model to study the importance of YAP in Wnt-Met CSCs. FACS of VP-treated spheres for the CSC marker CD49f revealed a shift in the percentage of CD49f^{hi} cells (Figure 3.13A), indicating that YAP inhibition decreases the percentage of CSCs in Wnt-Met spheres. In

order to functionally test this, Wnt-Met stem cell-enriched cells were seeded as single cells and treated on day zero with VP or SIM. After 5 days, control spheres were large, ranging in size from 50-150µm, whereas treated cells completely failed to form spheres (Figure 3.13B).

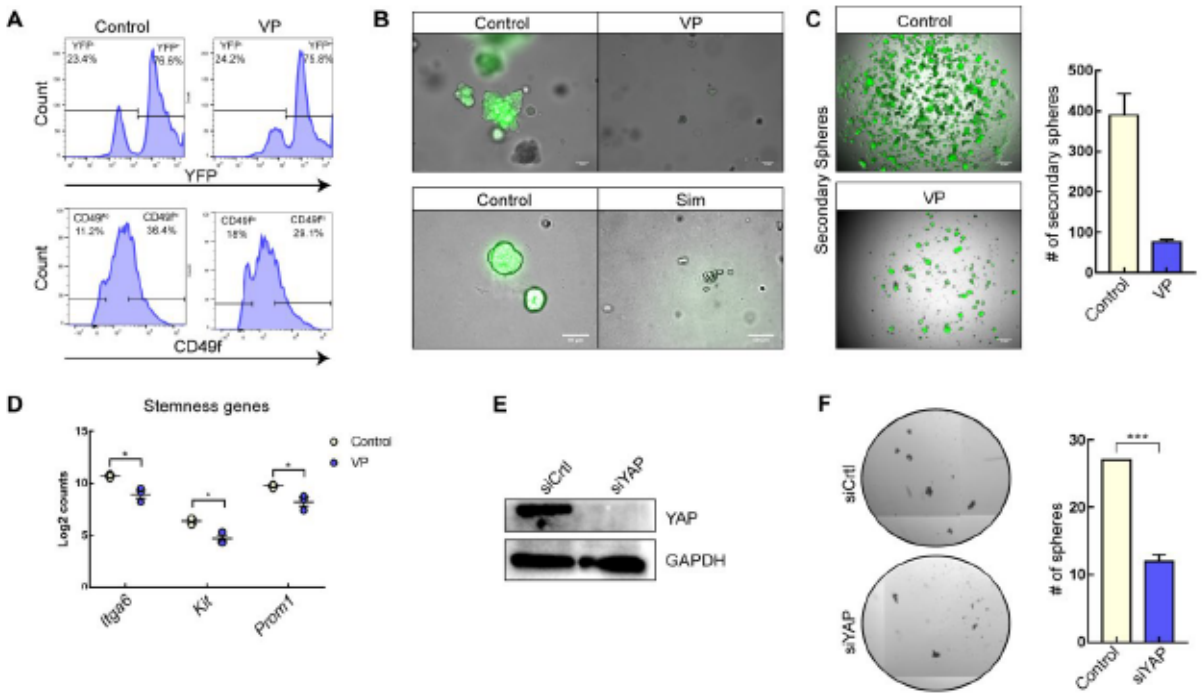

Figure 3.13: ***YAP inhibition blocks the initiation of Wnt-Met stem cell-enriched spheres*****. A.** FACS of DMSo vehicle control or VP-treated spheres showing YFP (top) and CD49f (bottom) expression. **B.** Bright-field and fluorescence microscopy of spheres treated from day zero with either DMSO vehicle control or VP (2µM) (top) and control or SIM (10µM) (bottom), scale bar 50µm. **C.** Bright-field and fluorescence images of secondary spheres generated from DMSO vehicle control and VP-treated spheres, quantification right, scale bar 500µm. **D.** Nanostring analysis of stem cell-associated genes in DMSO vehicle control and VP-treated spheres. Data are mean ± SEM, n=3 biological replicates *p<0.05 by Student's t test. **E.** Western blot of MDA-231 cells treated with siSramble or siYAP showing expression of YAP and GAPDH as a loading control. **F.** Bright-field images of spheres generated from MDA-231 cells treated with siScramble and siYAP. Data are mean ± SEM, n=3 biological replicates ***p<0.001 by Student's t test

A characteristic of CSCs is the ability to reproduce a full tumour from a single cell due to the self-renewal properties. A common method to study self-renewal is the generation of secondary spheres[172]. Wnt-Met stem cell-enriched spheres were allowed to grow for 5 days before being treated for 24 hrs with 1µM VP. Spheres were then collected and trypsinized to form single cells and reseeded. After 5 days, control spheres generated a dense population of 400 spheres per well, while VP-treated spheres merely produced <100 spheres per well indicating that YAP is important for the self-renewal of Wnt-Met CSCs (Figure 3.13C). An expression analysis for the stem cell-associated genes

Itga6, *Kit*[175] and *Prom1*[73] confirmed the inhibition of CSCs (Figure 3.13D). Finally, in order to study the effect of YAP in the CSCs of human basal-like breast cancer, I utilized the human tumour cell line MDA-MB-231 which has been reported to have high YAP activity[176]. siRNA knock-down of YAP in these cells significantly reduced the ability of these cells to form mammospheres, an assay widely used to show anoikis resistance of CSCs, a characteristic of CSCs[172,177] (Figure 3.13F). Overall, these results show that YAP is important for the maintenance and expansion of CSCs.

3.5.3. YAP inhibition delays tumour growth and proliferation *in vivo*

As I have established above the effect of YAP on the growth and proliferation of Wnt-Met stem cell-enriched spheres, I next wanted to confirm that YAP portrays the same effect in tumours. Wnt-Met mice were stimulated via pregnancy at 8-10 weeks old. From day zero PP, mice were treated daily with either vehicle control or 100mg/kg SIM via oral gavage. I observed a significant delay in tumour development and average tumour weight of SIM-treated mice compared to control (Figure 3.14A, B). Histological analyses of the mouse tumours revealed loose stroma in addition to smaller more hollow acini in SIM-

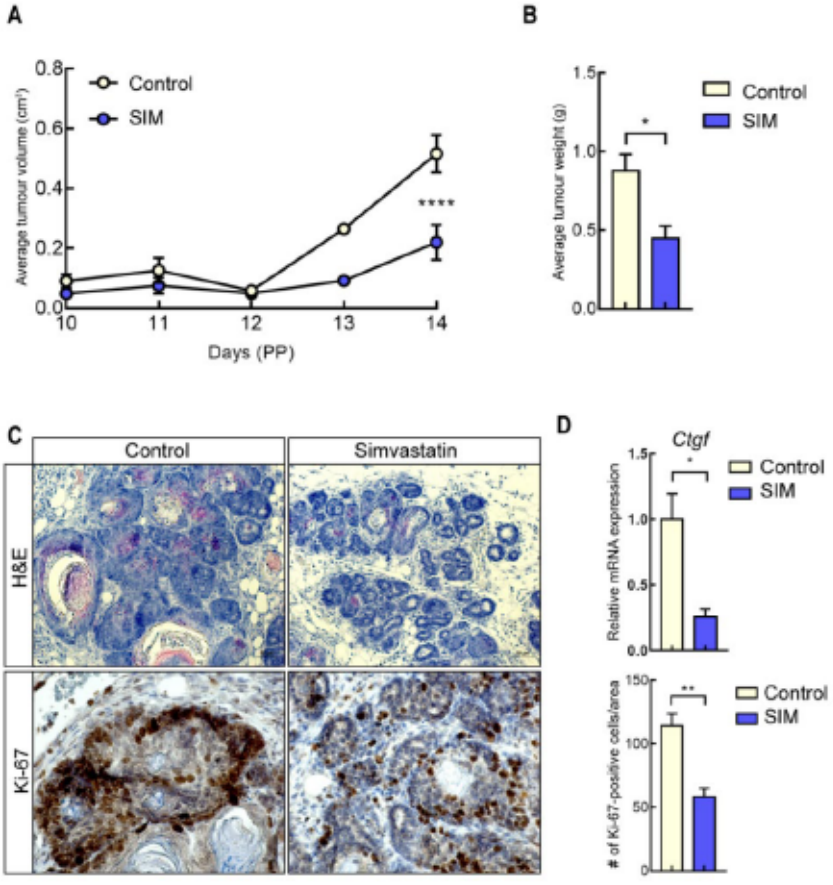

Figure 3.14: ***YAP inhibition delays Wnt-Met tumour formation.*** **A.** Tumour growth curve of Wnt-Met mice treated with either vehicle control or SIM (100mg/kg) daily from day zero post-partum. Data are mean ±SEM, n=3 biological replicates, ****p<0.0001, Two-way ANOVA, Sidak's multiple comparisons test. **B.** Average tumour weight of vehicle control and SIM-treated mice. Data are mean ±SEM, n=3 biological replicates, *p<0.05 by Student's t test. **C.** H&E staining of vehicle control and SIM-treated tumours, scale bar 50μm (top). Immunostaining of Ki-67 in Wnt-Met tumours treated with either vehicle control or SIM, scale bar 20μm (bottom), quantification on the right. Data are mean ±SEM, n=3 biological replicates, **p<0.01 by Student's t test. **D.** qPCR analysis of the YAP target gene *Ctgf* in vehicle control and SIM-treated Wnt-Met tumours. Data are mean ±SEM, n=3 biological replicates, *p<0.05 by Student's t test

treated tumours. In addition, the proliferation of the treated tumours was significantly decreased, suggesting that treated tumours were at an earlier stage of tumorigenesis due to their slower proliferation rate (Figure 3.14C). qPCR analysis confirmed YAP inhibition, as I observed a marked decreased in the expression of the YAP target gene *Ctgf* (Figure 3.14D). These data confirm that YAP inhibition delays the growth and proliferation of Wnt-Met tumours

3.5.4. YAP knock-out delays Wnt-Met tumour formation

Since I found that YAP is highly activated in Wnt-Met basal breast cancer, I next examined its functional role by genetic means. I crossed floxed YAP alleles[178] into Wnt-Met mice. Upon stimulation via pregnancy, homozygous YAP ablation in Wnt-Met mice (denoted Wnt-Met-YAP^{KO}) produced an increase in the number of tumour-free mice from 11 days in controls (Wnt-Met-heterozygous YAP ablation) to 17days (Figure 3.15A). The average tumour weight of Wnt-Met-YAP^{KO} mammary glands was also significantly decreased (Figure 3.15B). I confirmed *YAP* ablation by qPCR (Figure 3.15C). Remarkably, H&E staining and immunohistochemistry of Wnt-Met-YAP^{KO} mammary glands revealed large alveoli, which were largely YAP-free and exhibited healthy one-layered acini with a significant decrease in proliferation, as seen by Ki-67 staining (Figure 3.15D, lower panel, marked by red arrowheads, quantification in Figure 3.15E). In contrast, Wnt-Met-YAP^{Ctrl} mammary glands showed large tumorous areas, which were strongly YAP-stained, and large empty alveoli could not be discerned (Figure 3.15D, upper panel). Fluorescent images of YFP confirmed successful cre-recombination, i. e., YFP-positive cells were found in single-layered acini in Wnt-Met-YAP^{KO} glands, in contrast to filled tumours in the controls (Figure 3.16A). FACS revealed a 5.5-fold decrease in the content of CD49f^{hi} CD24^{hi} CSCs in Wnt-Met-YAP^{KO} mammary glands when compared with controls (Figure 3.16B). Taken together, these data demonstrate that YAP is crucial for the generation of CSCs and tumour initiation in Wnt-Met tumours.

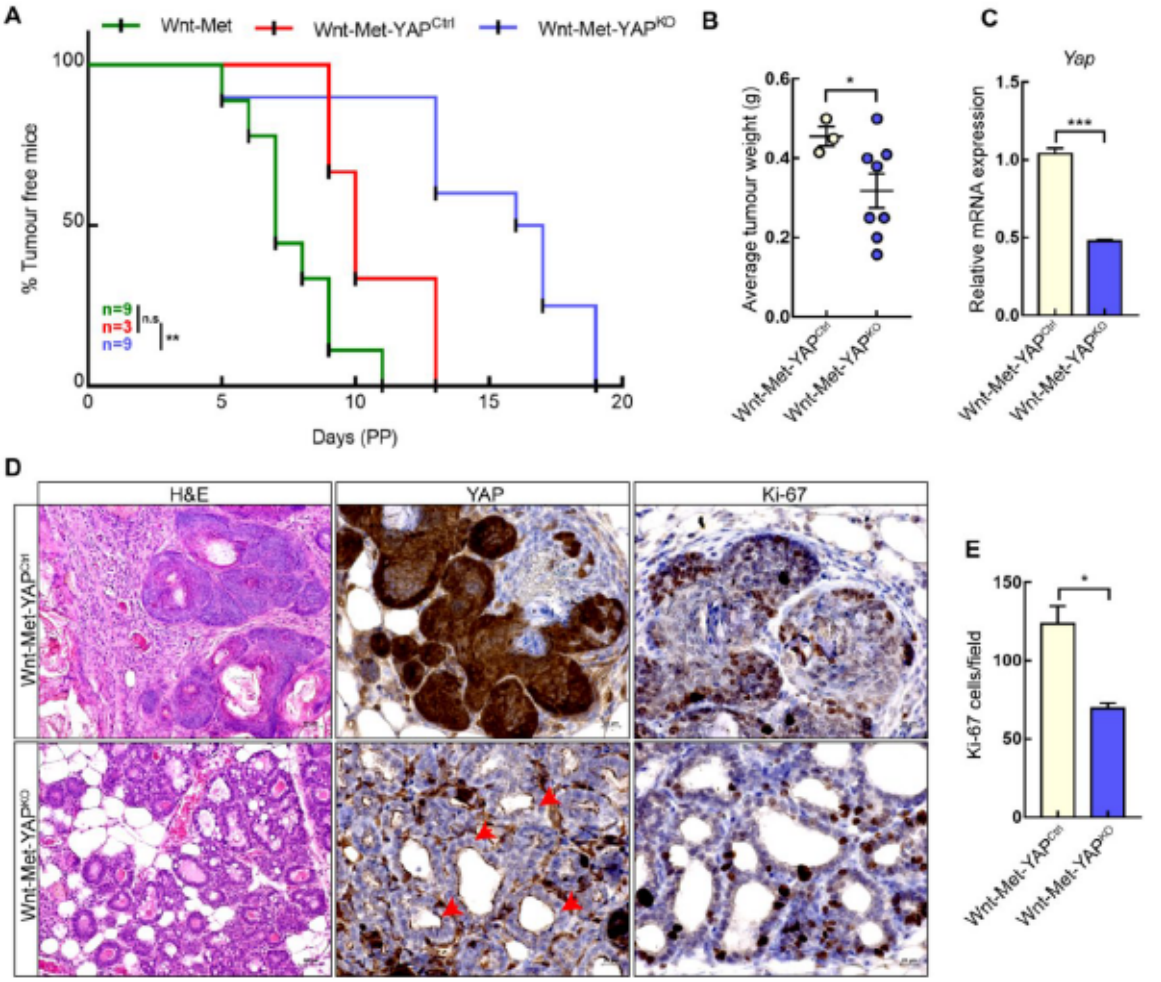

Figure 3.15: ***Genetic ablation of YAP delays Wnt-Met tumour formation.*** **A.** Graph showing tumour-free mice in Wnt-Met, Wnt-Met-YAP$^{Ctrl(HET)}$ and Wnt-Met-YAP^{KO} **p<0.001, by Gehan-Breslow-Wilcoxon test. **B.** Average tumour weight of Wnt-Met-YAP$^{Ctrl(HET)}$ and Wnt-Met-YAP^{KO} mice. Data are mean ±SEM, *p<0.05, by Student's t-test. **C.** RT-qPCR of *Yap* mRNA expression in Wnt-Met-YAP$^{Ctrl(HET)}$ and Wnt-Met-YAP^{KO} tumours. Data are mean ±SEM, n=3 biological replicates, ***p<0.001, by Student's t test. **D.** Comparison of Wnt-Met-YAP$^{Ctrl(HET)}$ (upper pictures) and Wnt-Met-YAP^{KO} (lower pictures) mammary glands at 2.4 weeks PP. H&E staining (left panel), immunohistochemistry of YAP (middle panel) and Ki-67 (right panel), red arrowheads mark single cell-layered healthy YAP-free epithelia, scale bar, 50µm and 20µm. **E.** Quantification of Ki-67-positive cells. Data are mean ±SEM, n=3 biological replicates, *p<0.05, by Student's t test.

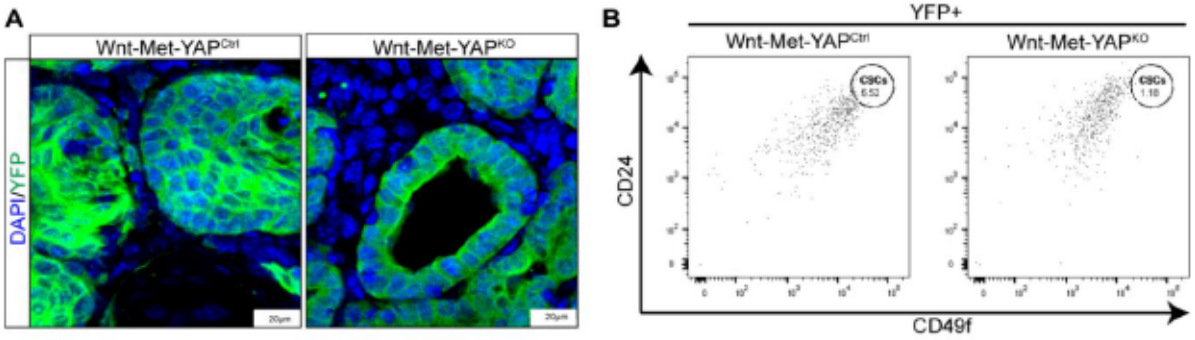

Figure 3.16: ***Genetic ablation of YAP depletes CD24^{hi} CD49f^{hi} cells.*** **A.** Confocal microscopy of YFP (green) in Wnt-Met-YAP$^{Ctrl(HET)}$ and Wnt-Met-YAP^{KO} mammary glands at 2.4 weeks PP, scale bar, 20µm. **B.** FACS plot showing CSCs in Wnt-Met-YAP$^{Ctrl(HET)}$ and Wnt-Met-YAP^{KO} mammary glands.

3.5.5. YAP inhibition prevents the luminal–basal switch and nuclear accumulation of β-catenin and YAP

Met signalling induces the trans-differentiation of luminal mammary gland cells into basal cells[33,179]. To examine whether Met-induced trans-differentiation also depends on YAP, I examined Wnt-Met-YAP^{Ctrl} and Wnt-Met-YAP^{KO} mammary glands for the expression of the luminal cell maker CK8 and the basal cell marker P63. I observed strong expression of P63 in control glands, which exhibited a minimal expression of CK8 (Figure 3.17A, B, left panels). Strikingly in contrast, Wnt-Met-YAP^{KO} mammary glands showed negligible P63-positive cells but a high number of CK8-positive cells (Figure. 3.17A, B, right panel). RT-qPCR of the luminal marker *Krt8* and the basal marker *Dnp63* confirmed an increase in luminal cells and a decrease in basal cells in Wnt-Met-YAP^{KO} mammary glands (Figure 3.17C). As confirmation, in Wnt-Met tumours I found a strong expression of CK14 and a low expression of CK8, a pattern which was reversed in SIM-treated tumours (Figure 3.17D). Overall, these data provide genetic and pharmacological evidence that YAP is required for the acquisition of basal characteristics in Wnt-Met

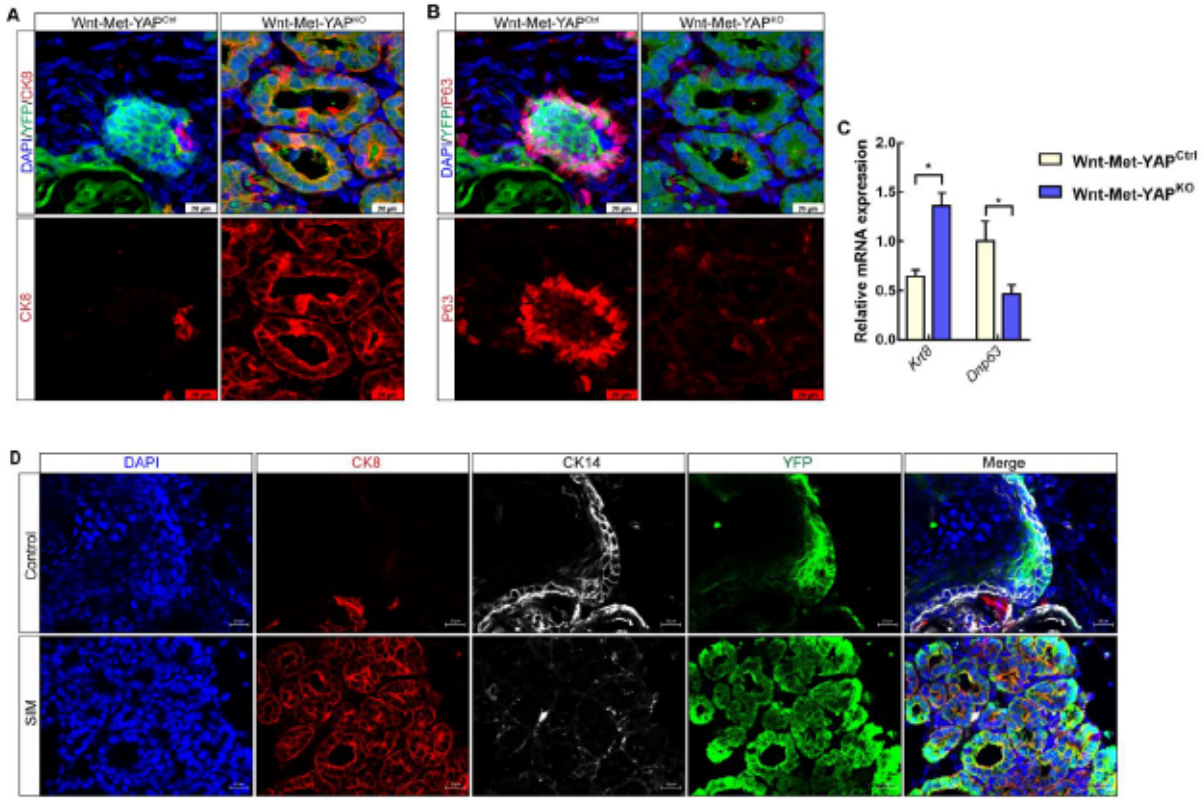

Figure 3.17: ***YAP inhibition prevents the luminal to basal switch.*** **A.** Confocal microscopy of YFP (green) and CK8 (red) in Wnt-Met-YAP$^{Ctrl(HET)}$ and Wnt-Met-YAP^{KO} mammary glands at 2.4 weeks PP, scale bar, 20µm. **B.** Confocal microscopy of YFP (green) and P63 (red) in Wnt-Met-YAP$^{Ctrl(HET)}$ and Wnt-Met-YAP^{KO} mammary glands at 2.4 weeks PP, scale bar, 20µm. **C.** RT-qPCR analysis of *Krt8* and *Dnp63* in Wnt-Met-YAP$^{Ctrl(HET)}$ and Wnt-Met-YAP^{KO} mammary glands. Data are mean ±SEM, n=3 biological replicates, *p<0.05, by Student's t test. **D.** Confocal microscopy of DMSO vehicle control and SIM-treated Wnt-Met tumours for YAP (green) and β-catenin (red), scale bar 50µm.

tumours.

3.6. YAP activity upon β-catenin inhibition

3.6.1. ICG-001 treatment enhances YAP activity and senescence-associated genes in Wnt-Met spheres

To understand if β-catenin transcriptional activity is required for the nuclear function of YAP, I treated Wnt-Met spheres with the Wnt-β-catenin inhibitor ICG-001 that inhibits the nuclear interaction of β-catenin with CBP preventing the transcription of β-catenin-CBP target genes[180]. Phenotypically, treated spheres exhibited reduced viability and self-renewal ability indicating impairment of CSC properties (Figure 3.18A, B). Gene Set Enrichment Analysis (GSEA) identified a downregulation in genes associated with DNA damage repair and cell cycle control (Figure 3.19A). Strongly downregulated genes included *Skp2*, *Ccna2*, *Ccne2* and *Cdc25c* all involved in cell cycle progression[181–183] (Figure 3.19B). By contrast, genes associated with senescence were significantly upregulated, such as *Cdkn2b*/p15 and the p53 targets *Gadd45a* and Cdkn1a/p21[184,185] (Figure 3.19C). Gene expression analysis revealed expression changes in genes associated with Wnt, apoptosis, the cell cycle and DNA damage repair (Figure 3.20A). A strong upregulation of the YAP target genes *Areg*, *Ankrd1*, *Ctgf* and *Cavin2* was

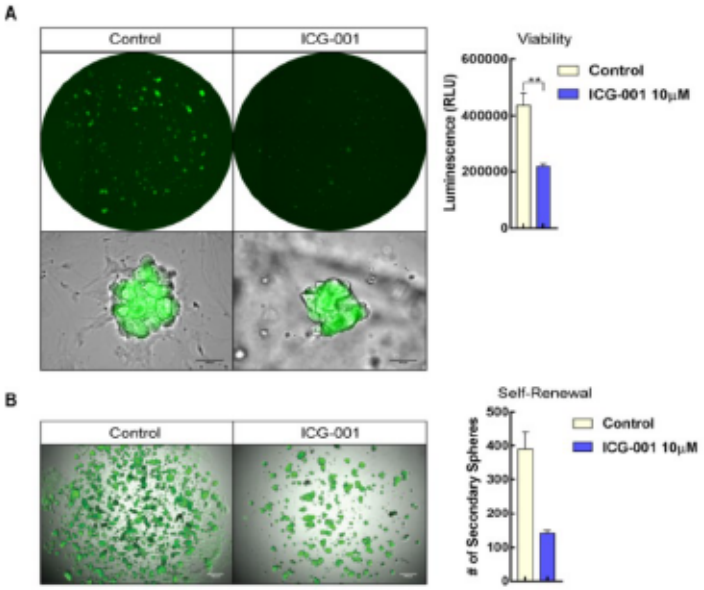

Figure 3.18: ***ICG-001-treatment reduces viability and self-renewal for CSCs.*** **A.** Bright-field and fluorescence images of Wnt-Met spheres in DMSO vehicle control and ICG-001-treated CSCs (10μm) for 48 hours, right, CellTitreGlo viability **p<0.005. **B.** Bright-field and fluorescence images of secondary spheres generated from Wnt-Met spheres in DMSO vehicle control and ICG-001-treated (10μm) CSCs for 48 hours, quantification on the right.

observed in ICG-001-treated spheres (Figure 3.20B). In agreement with the upregulation of YAP target genes, nuclear YAP was elevated 3-fold in the treated spheres (Figure 3.20C). Based on these data, I hypothesized that YAP activity may mediate survival of Wnt-Met spheres upon ICG-001-treatment. In agreement with this, co-inhibition of both YAP and β-catenin led to an enhanced decrease in the self-renewal of Wnt-Met spheres (Figure 3.21A). These data show that although CBP/β-catenin inhibition significantly reduces sphere viability and CSC properties, and that an upregulation of YAP activity and a senescence/dormancy programme may lead to cell survival and anti-CSC therapy resistance.

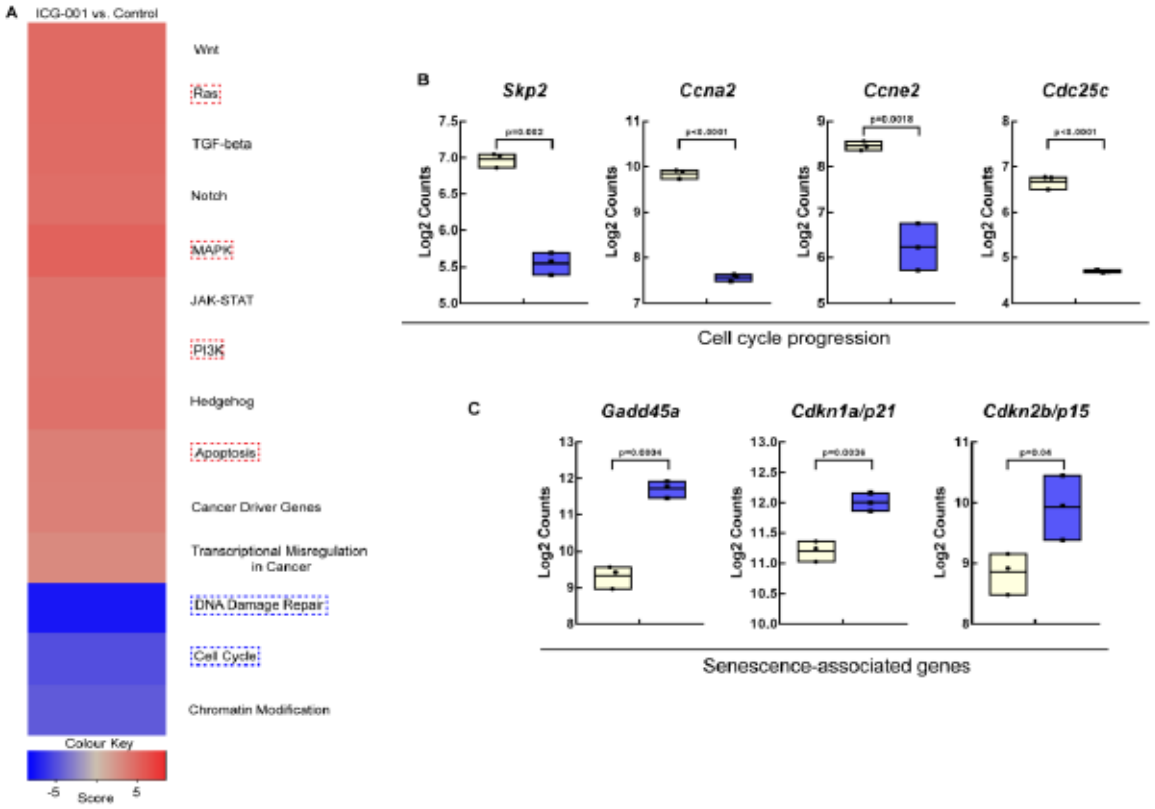

Figure 3.19: ***ICG-001-treatment induces a senescence gene expression profile.*** **A.** Gene Set Enrichment Analysis of gene expression changes in DMSO vehicle control and ICG-001-treated (10μM) spheres. **B.** Log2 counts of genes associated with cell cycle progression (DMSO vehicle control – yellow, ICG-001-treated (10μM) - blue). **C.** Log2 counts of genes associated with senescence (DMSO vehicle control – yellow, ICG-001-treated (10μM) - blue). Data are mean ±SEM, n=3 biological replicates, by Student's t test.

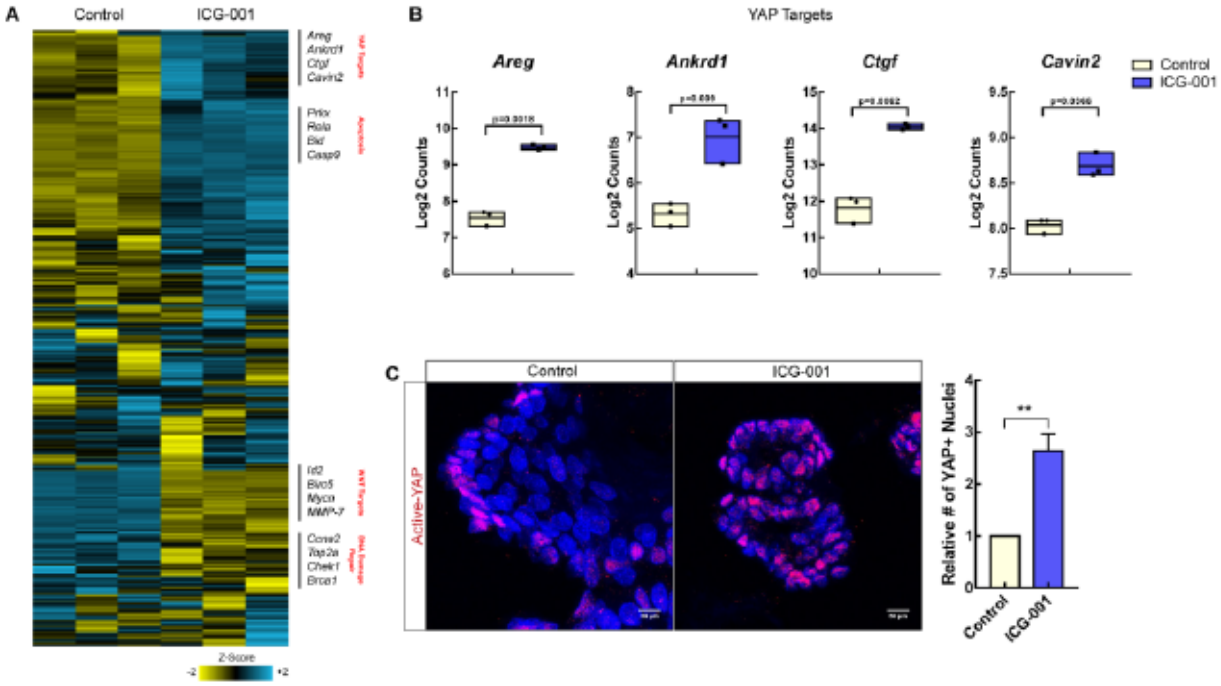

Figure 3.20: ***ICG-001-treatment enhances YAP activity.*** **A.** NanoString heatmap showing differential gene expression of Wnt-Met spheres treated with either DMSO vehicle control or ICG-001 (10μm) for 48 hours. **B.** Log2 counts of YAP target gene mRNA transcripts. Data are mean ±SEM, n=3 biological replicates, p-value calculated by Student's t test. **C.** Confocal microscopy for YAP expression in DMSO vehicle control and ICG-001-treated spheres, quantification on the right. Data are mean ±SEM, n=3 biological replicates, **p<0.01.

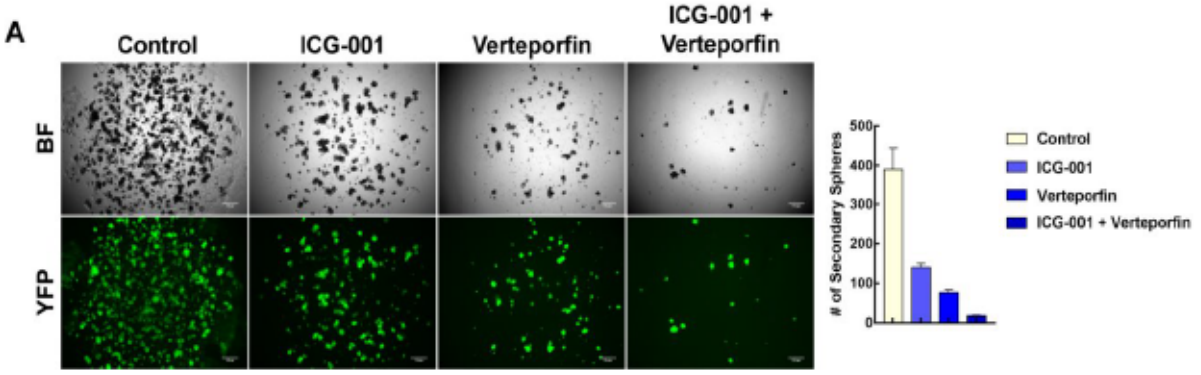

Figure 3.21: ***Combination YAP-TEAD and β-catenin-CBP inhibition prevents CSC self-renewal.*** **A.** Bright-field (upper) and fluorescence images (lower) of secondary spheres generated from Wnt-Met primary spheres treated with DMSO vehicle control, ICG-001 (10μM), VP (1μM) and combination for 24 hrs, scale bar 500μm, quantification on the right.

3. 7. YAP regulates β-catenin activity

3.7.1. YAP controls β-catenin nuclear activity

I next investigated if YAP is required for the transcriptional activity of β-catenin. NanoString gene expression analysis[186] of control and Wnt-Met-YAP^{KO} mammary glands was performed. A strong decrease in YAP and β-catenin activity in Wnt-Met-YAP^{KO} mammary glands was found (Figure 3.22A): target genes such as *Ctgf* and *Igfpb3* (YAP targets) and *Axin2* and *BMP4* (β-catenin targets) were downregulated in Wnt-Met-YAP^{KO} tissues, indicating that YAP is required for the nuclear activity of β-catenin (Figure 3.22B, C). Next I examined if YAP regulates the nuclear translocation of β-catenin. Quantification of β-catenin-positive nuclei showed an 11-fold decrease in Wnt-Met-YAP^{KO} mammary glands compared to controls (Figure 3.23A). Furthermore, pharmacological inhibition of YAP completely inhibited β-catenin nuclear translocation (Figure 3.23B). These data show that YAP is required for the nuclear translocation and activity of β-catenin.

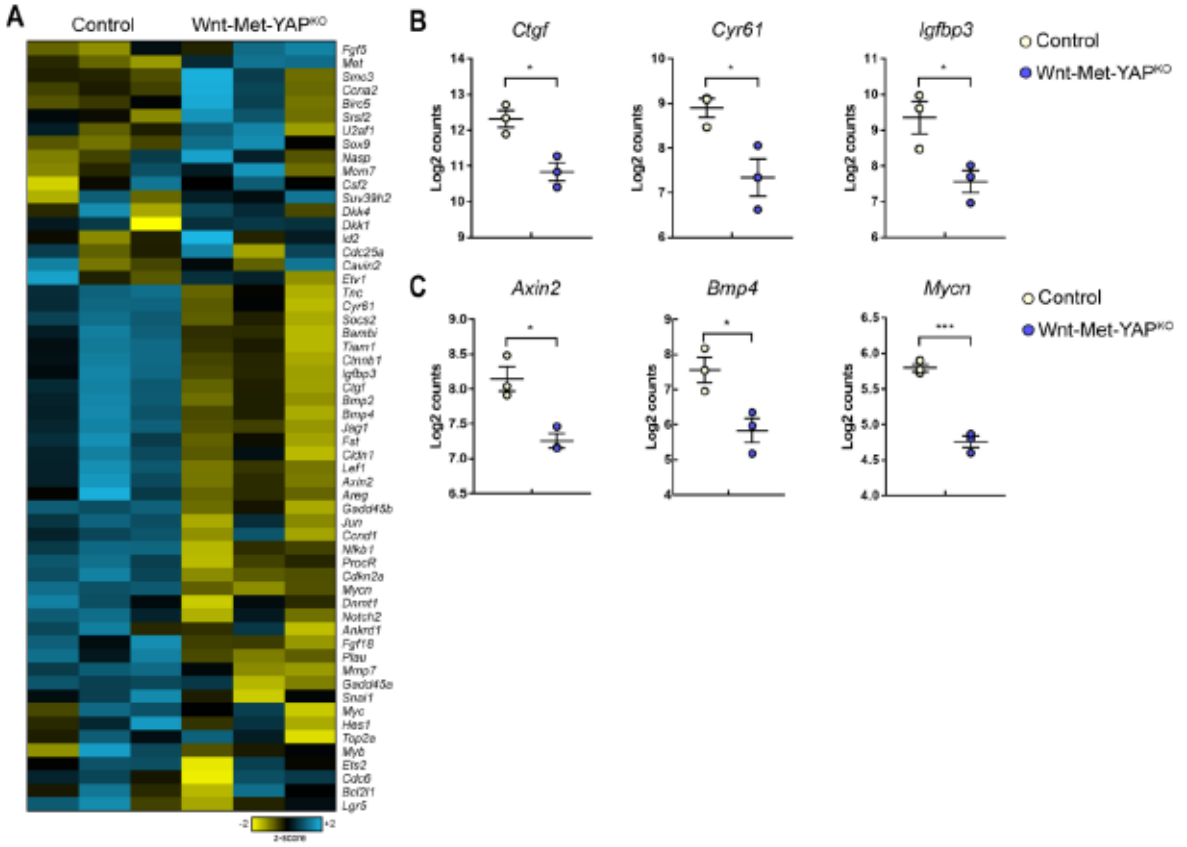

Figure 3.22: ***YAP regulates Wnt target gene transcription.*** **A.** Heatmap showing differential gene expression of YAP and β-catenin target genes in Wnt-Met-YAP$^{Ctrl(HET)}$ (Control) and Wnt-Met-YAP^{KO} mice. **B.** Log2 counts of the YAP target genes *Ctgf*, *Cyr61* and *Igfbp3*. **C.** Log2 counts of the β-catenin target genes *Axin2*, *Bmp4* and *Mycn*. Data are mean ±SEM, n=3 biological replicates, *p<0.05, ***p<0.001, by Student's t test.

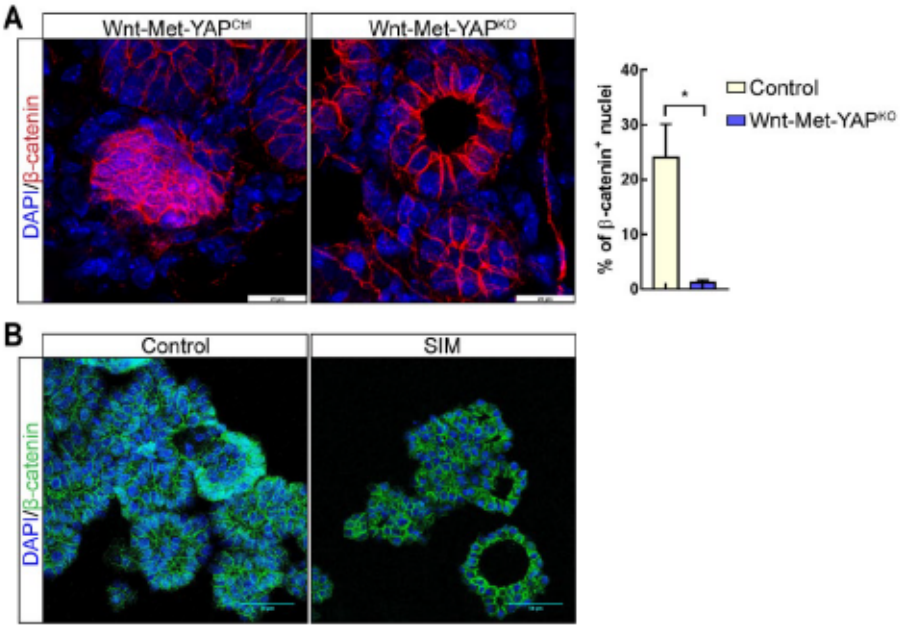

Figure 3.23: ***YAP regulates β-catenin nuclear translocation.*** **A.** Confocal microscopy of β-catenin (red) in Wnt-Met-YAP$^{Ctrl(HET)}$ (Control) and Wnt-Met-YAP^{KO} mice. Quantification of nuclear β-catenin on the right. Data are mean ±SEM, n=3 biological replicates, *p<0.05, by Student's t test. **B.** Confocal microscopy of β-catenin (green) in DMSO vehicle control and SIM-treated stem cell-enriched spheres, scale bar, 50μm

3.7.2. YAP and β-catenin interact

YAP has been reported to be required for the development of β-catenin-driven tumours[187]. I hypothesized that since YAP inhibition results in a decrease in the expression of a number of β-catenin target genes, YAP may in fact form a transcriptional complex with β-catenin in the nucleus to control the expression of a number of common target genes. First, I investigated if nuclear YAP and β-catenin are co-expressed in the nucleus of Wnt-Met tumours. Immunofluorescence of YAP and β-catenin in Wnt-Met stem cell-enriched spheres and tumours showed that YAP strongly co-localized in the nucleus with β-catenin, indicating that both YAP and Wnt are both important transcription factors in the CSCs in Wnt-Met tumours (Figure 3.24A). YAP and β-catenin have been shown to directly interact within the β-catenin destruction complex of the cytoplasm, where Wnt activation results in the release of β-catenin and YAP into the nucleus[142]. However, no study has concisely shown the nuclear interaction of these transcriptional regulators in mammary gland cancer. I confirmed the interaction of nuclear YAP and β-catenin by co-immunoprecipitation of active YAP, which is exclusively nuclear in Wnt-Met stem cell-enriched spheres. This revealed strong co-immunoprecipitation of β-catenin^{GOF} and TEAD4 (Figure 3.24B).

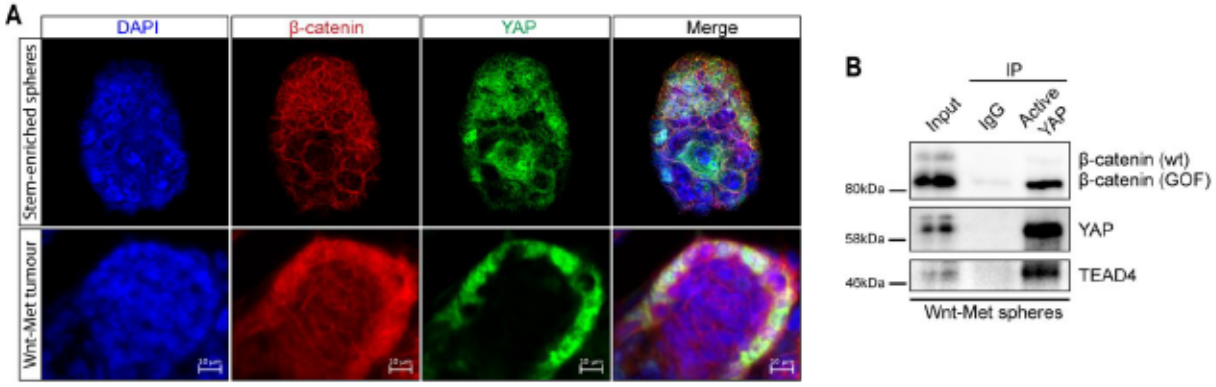

Figure 3.24: ***YAP, β-catenin and TEAD4 interact in the nucleus.*** **A.** Confocal microscopy of stem cell-enriched spheres and Wnt-Met tumours for β-catenin (red) and YAP (green), scale bar 10µm. **B.** Co-immunoprecipitation of active YAP and β-catenin in Wnt-Met spheres showing interaction of both with TEAD4, n=3.

3.7.3. β-catenin and TEAD4 co-localise at common gene promoters and enhancers

YAP has been reported to be required for the development of β-catenin driven tumours[187]. I hypothesized that since YAP inhibition results in a decrease in the expression of a number Wnt target genes, YAP/TEAD may bind with β-catenin to regulatory regions of common target genes to control gene expression in cancer stem cells. To test our hypothesis, in collaboration with Clemens Messerschmidt of the BIH, TEAD4 and CTNNB1 (β-catenin) chIP-seq data from hESC H1 cells were downloaded from chIP-Atlas[188]. We identified a distal enhancer of *AXIN2* and a strong enhancer of *NUAK2* (a newly identified YAP target gene[189]) containing overlapping β-catenin, TEAD4 and YAP1 chIP-seq peaks (Figure 3.25A, B). Overall, these data show that TEAD4, β-catenin and YAP1 can co-locate at gene promoters and enhancers of both Wnt and YAP target genes.

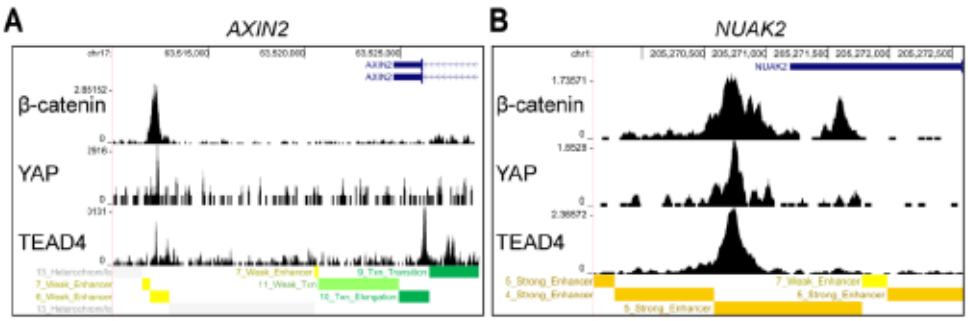

Figure 3.25: ***YAP, β-catenin and TEAD4 bind common gene regulatory regions.*** **A.** ChIP-seq tracks for YAP, β-catenin and TEAD4 showing overlapping signals at an *AXIN2* enhancer region. **B.** ChIP-seq tracks for YAP, β-catenin and TEAD4 showing overlapping signals at a strong *NUAK2* enhancer region.

3. 8. YAP in human breast cancer

3. 8. 1. YAP is active in human BLBC

To validate the clinical relevance of our data, in collaboration with Philipp Mertins and Oliver Popp of the MDC, we analysed YAP activity in different breast cancer subtypes. The analysis of human primary patient data[190] revealed high expression of the YAP signature[162] in basal breast cancer, in contrast to other subgroups of breast cancers (Figure 3.26A). Confocal analysis of active YAP in six basal breast cancer PDX models[191] showed cells with strong nuclear YAP (Figure 3.27A). I confirmed elevated YAP activity by qPCR of YAP target genes, *CTGF*, *IGFBP3* and *ANKRD1*[162] in spheres of human basal breast cancer cell lines BT549, MDA231 and SUM1315, compared to luminal breast cancer cell lines MCF7, BT474 and T47D (Figure 3.27B).

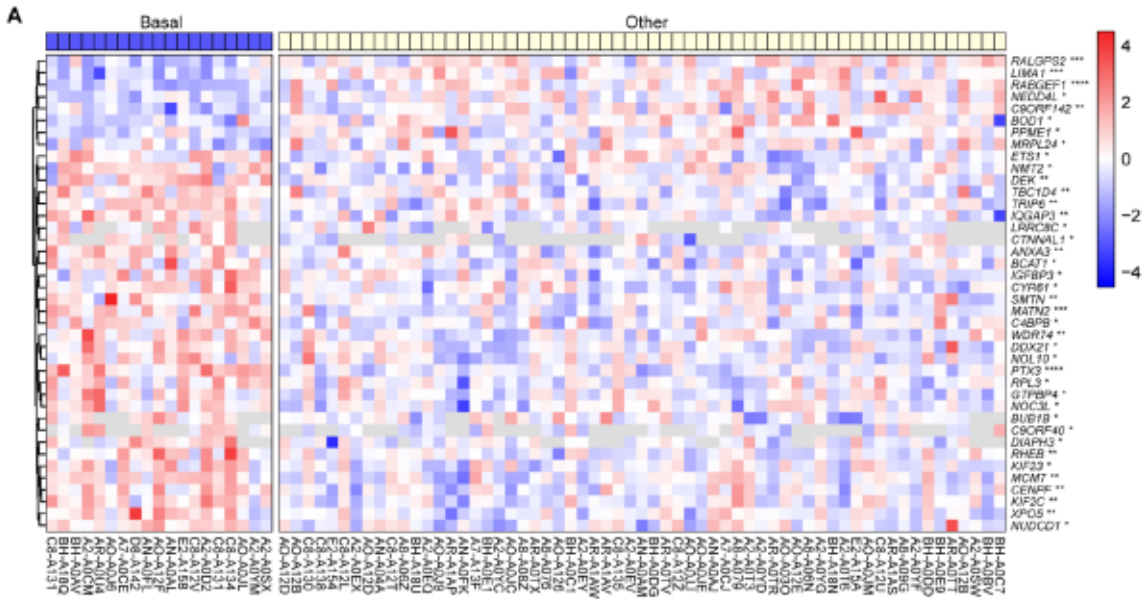

Figure 3.26: ***YAP transcriptional signature is increased in human basal breast cancer patients at the protein level.*** **A.** Heatmap of proteomics data from Mertins and colleagues 2016[135]. The provided CPTAC dataset was filtered for samples that passed the QC criteria. A two-sample moderated t-test was applied between samples that have been assigned to basal vs. all other subtypes combined. Selected significant proteins from Zanconato and collegues (2016) with an adjusted p-value (from Benjamini-Hochberg correction) < 0.05 from the lists are displayed. The heatmap uses median-MAD-normalised input data across all proteins and row-scaling across all samples. Hierarchical clustering (by Euclidian distance) was applied to rows while missing values are indicated by grey color. Significance as indicated: *adj. p-value < 0.05, **adj. p-value < 0.01, ***adj. p-value < 0.001, ****adj. p-value < 0.0001.

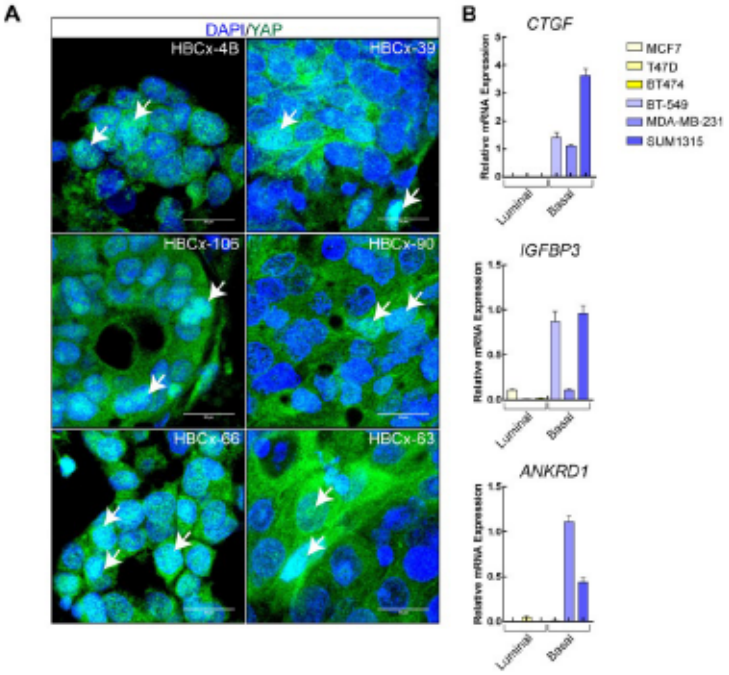

Figure 3.27: ***YAP is expressed and active in human basal-like breast cancer.*** **A.** Confocal microscopy of YAP in six PDX tumour samples from basal breast cancer patients. Arrows indicate nuclear YAP, scale bar 20μm. **B.** qPCR analysis of YAP target gene expression in luminal (yellow) and basal (blue) breast cancer cell lines.

3. 8. 2. YAP predicts the survival of human breast cancer patients in a subtype dependent manner

To assess if YAP and β-catenin could be used as predictive markers for patient outcome, I used the Kaplan-Meier plotter programme (http://kmplot.com)[192] to investigate disease-free survival (DFS) of breast cancer patients with high expression of *YAP* and *CTNNB1* (β-catenin) in ER+, PR+ (luminal) vs. triple negative breast cancer patients. *CTNNB1* expression proved not to be a predictive marker of DFS in ER+, PR+ patients. However, in triple-negative breast cancers, high *CTNNB1* expression strongly correlated with a decrease in DFS (Figure 3.28A, B, upper panel). Surprisingly, in ER+, PR+ breast cancers high *YAP* expression was correlated with an increase in DFS, suggesting *YAP* may act as a tumour suppressor in this context. In contrary to this, high *YAP* expression in triple-negative basal breast cancers correlated with a significant decrease in DFS (Figure 3.28A, B lower panel). Following this trend, high expression of the YAP target genes *CTGF, CYR61* and *IGFBP3* correlated with a decrease in DFS in patients with triple negative breast cancer (Figure 3.28C). Overall, these data show that YAP is highly expressed in basal breast cancers, compared to luminal breast cancer, and can predict patient survival in a subtype dependent manner.

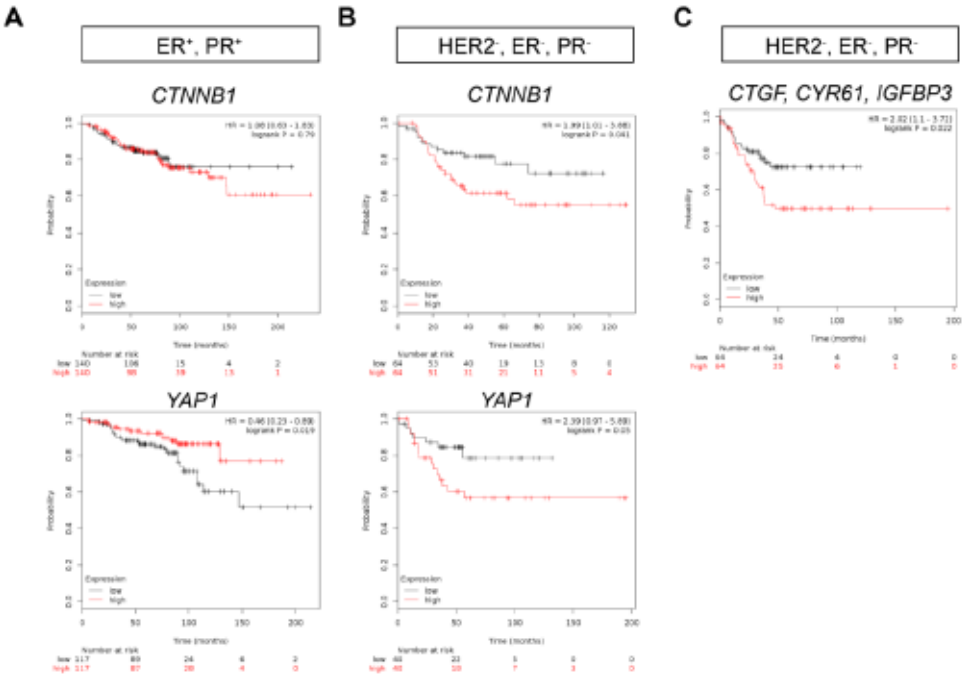

Figure 3.28: ***YAP predicts patient survival in a subtype-dependent manner.*** **A.** Kaplan-Meier plots showing survival of ER$^+$, PR$^+$ luminal breast cancer patients with either high or low expression of *CTNNB1* and *YAP1*. **B.** Kaplan-Meier plots showing survival of HER2$^-$, ER$^-$, PR$^-$ basal breast cancer patients with either high or low expression of *CTNNB1* and *YAP1*. **C.** Kaplan-Meier plots showing survival of HER2$^-$, ER$^-$, PR$^-$ breast cancer patients with either high or low expression of the YAP target genes *CTGF, CYR61 and IGFBP3*.

4. DISCUSSION

The relevance of YAP in breast has been disputed; it has been described as both an oncogene and a tumour suppressor gene in this context[153–155,193]. Here, I have identified the HIPPO transducer YAP as an oncogenic regulator in Wnt-Met-driven basal mammary gland tumorigenesis. Cancer stem cells (CSCs) are the major contributors of tumour initiation, metastasis, therapy resistance and minimal residual disease. I set out to identify CSC regulating pathways that could be used as potential anti-CSC therapies. In doing so, I found that YAP is highly expressed in the CSCs of Wnt-Met mice and promotes their expansion, in part through the regulation of β-catenin activity. I show that Met signalling controls the nuclear translocation and activation of YAP and β-catenin (Figure 4.1, left). Upon translocation, YAP and β-catenin interact and bind to enhancer regions of Wnt target genes leading to gene transcription. In the absence of YAP, Met signalling can no longer induce the nuclear translocation of β-catenin, sequestering it in the cytoplasm and preventing the transcription of Wnt target genes (Figure 4.1, right). Thus, YAP is a key bottleneck required for the oncogenic activity of Met and β-catenin in basal breast cancer.

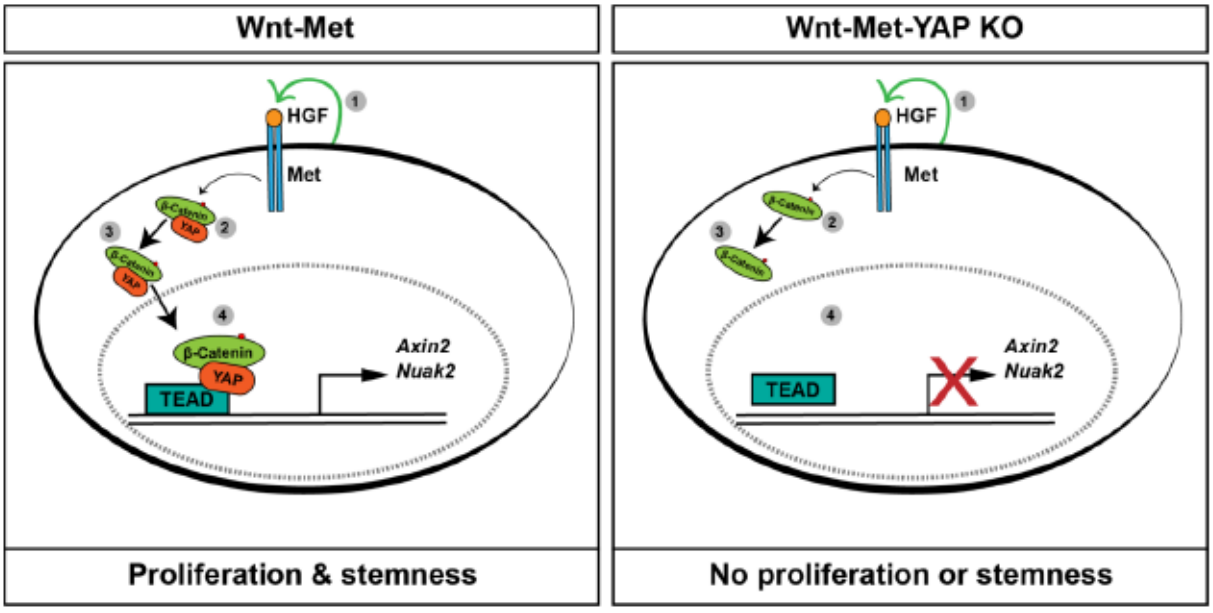

Figure 4.1: ***Schematic model for HGF-Met regulation of β-catenin and YAP activity.*** Left, (1) Extracellular HGF binds the Met receptor leading to hetero-dimerization and intracellular tyrosine phosphorylation. (2) β-catenin and YAP are activated and translocated to the nucleus, (3) where they interact and bind the transcriptional co-activator TEAD, leading to the transcription of target genes. Right, (1) HGF binds the Met receptor resulting in hetero-dimerization and tyrosine phosphorylation. (2) In the absence of YAP, β-catenin is sequestered in the cytoplasm and (3) can no longer induce the transcription of genes such as Axin2.

4.1. RTK regulation of YAP activity

YAP activation is dependent on the upstream kinases of the Hippo pathway, Lats1/2 and Mst1/2. In the absence of these signals, the Hippo pathway is inactive, resulting in the translocation of YAP into the nucleus, where it binds its transcriptional activator TEAD 1-4 and elicits gene transcription. However, an increasing number of alternative mechanisms leading to the activation of YAP have been described, such as Glucocorticoid, EGFR and Wnt signalling and caspase-3[142,143,176,194]. The vascular endothelial growth factor receptor (VEGFR) has been described as a new regulator of the HIPPO pathway. Activation of the receptor was found to inhibit the upstream kinases MST and LATS via PI3K/MAPK signalling leading to the activation of YAP/TAZ[195]. Based on this, I hypothesized that HGF-Met signalling, which has been reported to be associated with poor patient outcome in basal breast cancer might regulate YAP activity in Wnt-Met tumours[136,196]. Utilizing genetic models, proteomic and phospho-proteomic and human cell lines approaches, I showed that YAP and β-catenin nuclear localisation and activity are regulated by the receptor tyrosine kinase RTK Met. In addition, we identified two phosphorylation sites S-46 and T-48 that may aid YAP nuclear localisation and activation. The confirmation that these sites are crucial for YAP activation upon HGF stimulation will need further investigation by site-directed mutagenesis and analysis of the resulting YAP activity. Although these data support Met regulation of YAP activity, the exact signalling module remains unknown. One would first have to generate a signalling network based on the phosphoproteomic data in Wnt and Wnt-Met mammary glands to identify a potential downstream signalling cascade responsible for YAP activation. Following this, one could use various inhibitors of these pathways to identify essential components of the cascade.

Our analyses also revealed that YAP is required for HGF-Met-induced acquisition of basal characteristics. HGF-Met signalling has been shown convert luminal mammary gland cells into cells with basal characteristics including the induction of epithelial-mesenchymal transition (EMT)[179,196]. I have shown that Wnt-Met tumours generate basal mammary gland tumours, which are positive for the basal markers cytokeratin 14 and P63[33,34]. Upon YAP ablation, Wnt-Met activity no longer produce cells with basal characteristics; these cells remain in a luminal state with strong expression of the luminal marker cytokeratin 8 and no expression of the basal marker P63. Overall, I identified YAP as a regulator of trans-differentiation in the mammary gland. This suggests that not only in this model, but also other models of basal breast cancers that originate from luminal cells[156], YAP may play a major role in this trans-differentiation process. It would be

informative to conduct gene expression and YAP chip-seq analyses of YAP at different stages of this luminal-basal transition to identify what downstream regulators are responsible for this switch. In the future, inhibiting YAP in this context may actually induce basal tumour cells into a more targetable luminal state. Overall, our data show that i) the RTK Met is responsible for the activation of YAP and β-catenin, ultimately demonstrating why the cooperation of HGF-Met and Wnt-β-catenin signalling generates strongly aggressive basal mammary gland tumours in mice and that ii) the HGF-Met induction of basal-like characteristics is YAP dependent.

4.2. YAP is required for Wnt-Met tumour initiation and maintenance

Deregulation of Hippo signalling has been described in numerous human cancers. Sporadic and hereditary mutations in NF2 (Merlin), the upstream regulator of MST1/2 have been shown to promote the development of brain tumours[197,198]. However, mutations in the Hippo pathway components are uncommon in most cancers; nevertheless the pathway has been found to be dysregulated in the majority of cancers resulting in the overexpression of YAP[199–201]. This is likely attributed to the multitude of pathways that can feed into and regulate the Hippo pathway, such as GPCR, mechano-transduction and Wnt signalling[142,150,202]. Epigenetics adds another potential level of regulation. The Hippo components have also been found to be epigenetically silenced in cancer[203,204]. Although not often mutated, the functional importance of YAP cannot be ignored. In the case of non-small cell lung carcinoma, pharmacological targeting of the mutated EGFR receptor induces a YAP-driven senescence programme ultimately leading to resistance generation. Only a combination of EGFR and YAP inhibition effectively eradicates tumour cells, preventing resistance generation[205]. This is a perfect example of how important targeting non-mutated but dysregulated pathways is in cancer to prevent resistance generation and metastasis.

In support of the oncogenic role of YAP, studies have found that patients with elevated YAP/TAZ gene expression signatures strongly correlate with the enrichment of stem cell gene signatures, metastasis and poor patient outcome[162,206,207]. In contrast, a number of studies have found no evidence for oncogenic YAP activity in breast cancer, some even identifying YAP as a tumour suppressor gene in breast cancer[208–211]. Works that have implicated YAP as an oncogenic driver in breast cancer have based their findings on human breast cancer cell lines and the non-natural *MMTV-PyMT* mouse

model of mammary gland cancer[153,176,193,212]. Although these studies have led to important findings, the use of cell lines and an artificial breast cancer model does not accurately recapitulate tumours *in vivo*. To address this pitfall, I used a genetic mouse model of Wnt-Met-driven mammary gland cancer to investigate transcriptional regulators responsible for tumour initiation and maintenance in basal breast cancer[33]. I found that YAP was activated in Wnt-Met tumours, providing *in vivo* evidence for the activation of YAP in basal mammary gland tumours. Conditional knock-out and pharmacological inhibition of YAP in Wnt-Met mice significantly increased tumour latency highlighting the critical role of YAP in basal breast tumour initiation. Although tumour formation was delayed upon YAP ablation, tumours did eventually develop in YAP knockout mice. However, the tumour cells in these tumours were positive for YAP protein expression further supporting that YAP is required for Wnt-Met-driven tumorigenesis. These tumours have likely escaped recombination due to mosaic expression of cre-recombinase. This 'escape' is a common phenomenon in conditional knock-out mice, which we have previously observed in a number of genetic studies[124,213]. I found that recombination escape could be overcome by FACS of YFP^{+} cells and growing them as stem cell-enriched spheres, which led to an inhibition in expansion of Wnt-Met-YAP^{KO} spheres compared to controls.

YAP is not only required for tumour initiation but also maintenance. Culture of Wnt-Met stem cell-enriched spheres treated with the YAP inhibitors VP and SIM impaired both growth and proliferation. Overall, these data demonstrate that YAP is essential for both tumour initiation and tumour maintenance of Wnt-Met-driven mammary gland tumours.

4.3. YAP regulates cancer stem cells in basal breast cancer

Cancer stem cells (CSCs) are responsible for metastasis and tumour reoccurrence[214]. During normal organ development and cancer the HIPPO-YAP pathway controls differentiation and cell fate. In embryonic stem (ES) cell differentiation, YAP has been shown to be inactivated, in contrast YAP activity was found to increase during induced pluripotent stem cell (iPSC) generation, consistent with the idea that YAP is an important molecule in maintaining stemness[167].

Wnt-Met activation generates $CD24^{hi}$ $CD49f^{hi}$ cancer-propagating cells[33]. In the present study, I initially found that YAP is active/nuclear in the CK14-positive basal cell compartment of Wnt-Met tumours. In the mammary gland, both multipotent stem cells

and CSCs reside within the basal population[18,33], I hypothesized that YAP activity was located within CSCs. I isolated the CD24^{hi} CD49f^{hi} CSCs of Wnt-Met tumours and confirmed an upregulation of YAP target genes. Considering the role of YAP in tumorigenesis, organ repair and regeneration, it is not surprising that YAP activity is heightened in the CSCs of Wnt-Met tumours[194,215]. However, I needed to confirm that YAP functionally controls the cancer stem cell properties of these cells. To test this, I required a robust but easily manipulated system. I developed an *ex-vivo* culture system that enriches for CSCs, loosely based on previous methods[171,216]. These stem cell-enriched culture conditions readily expanded CD24^{hi} CD49f^{hi} CSCs and exhibited high YAP activity proving as an effective method to study the function of YAP in the CSCs of Wnt-Met tumours. Using these cultures, I showed by both pharmacological and genetic means that YAP is essential for the expansion of CSCs in Wnt-Met tumours. Furthermore, siRNA knock-down of YAP in human mammosphere cultures significantly reduced mammosphere-forming ability. Building on this I found that genetic ablation of YAP in Wnt-Met tumours lead to a reduction in the percentage of CD24^{hi} CD49f^{hi} cells. Overall, these data show that YAP is essential for the generation of basal breast CSCs and may be a rational target for the development of anti-CSC therapy.

4.4. Complex co-operation of YAP and Wnt

Wnt and Hippo signalling are generally tightly intertwined. For example, in the liver of mice co-activation of β-catenin and YAP have been shown to lead to the rapid generation of hepatocellular carcinoma[217]. In contrast, inhibition of β-catenin or YAP leads to a decrease in cell proliferation, suggesting that in these cells the two pathways cooperate to drive tumorigenesis. YAP/TAZ have been shown to be essential for the development of both liver, colon and pancreatic tumours[218–220]. Azolin et al.[142] describe a mechanism whereby the absence of Wnt signals result in YAP/TAZ sequestration in the cytoplasm by the β-catenin destruction complex comprised of APC, Axin and GSK3. They argue that knock-out of YAP/TAZ in embryonic stem cells leads to the activation of β-catenin activity and therefore compensates for loss of Wnt signalling. In contrast to these data, I found that genetic knock-out of YAP controls β-catenin activity at two levels: i) in the nucleus through co-binding the regulatory regions of β-catenin target genes such as Axin2, and ii) by regulating β-catenin nuclear translocation, showing that basal breast cancers require YAP for nuclear β-catenin activity. It is likely that this master regulatory control by YAP is context- and tissue-dependent.

It is clear that the interaction between YAP and β-catenin is more complex than meets the eye. I sought to further tweeze out these pathways by treating stem cell-enriched spheres with the β-catenin-CBP interaction inhibitor, ICG-001[180]. I found that ICG-001 treatment reduces cell viability and the self-renewal of stem cell-enriched spheres. Gene expression analysis revealed that ICG-001 treatment induces a senescence-like transcription programme marked by a decrease in the expression of cell cycle genes and an increase in senescence-controlling genes, suggesting that ICG-001-treatment forces stem cell-enriched cells into a state of dormancy. These formant cells could eventually enter out of this state leading to relapse. Strikingly, I found that this senescent state correlated with a strong increase in YAP activity. From these data, I speculated that increased YAP activity was responsible for the survival of ICG-001-treated CSCs. I further found that dual inhibition of both YAP and β-catenin drastically decreased the self-renewal abilities of Wnt-Met CSCs, confirming that YAP activity could lead to ICG-001 resistance by enabling cells to enter into a YAP-driven senescence programme. A similar phenomenon has been described for EGFR-mutant non-small cell lung carcinoma. It was found that upon targeted treatment of these tumours, a small proportion of cells survive by entering into a senescence-driven dormancy state that is driven by the YAP/TEAD transcription programme. Furthermore, combined inhibition of EGFR and YAP activity reduced dormancy and cell survival by increasing EGFRi-directed apoptosis. These data highlight the role of YAP in resistance generation to targeted therapies. Targeting YAP in combination with other targeted therapies, e.g. Wnt-directed therapies may prevent resistance generation, minimal residual disease and tumour re-occurrence in breast cancer.

4.5. YAP in human basal-like breast cancer

YAP's relevance in breast cancer is currently under dispute. YAP was recently shown to be inactive and even downregulated in ductal carcinoma in situ (DCIS)[155]. In addition, breast cancer patients displaying high YAP activity appeared to have a higher overall positive prognosis, leading to the belief that YAP might act as a tumour suppressor in breast cancer[154,221]. In this scenario, keeping YAP activity under tight control is thought to help tumour cells escape immunosurveillance[222]. However, other oncogenic transcriptional systems are equally likely to stimulate a strong immune response in the host[223,224]. These studies did not investigate the functional role of YAP in a context-dependent manner such as in breast cancer or in tumour cell subtypes. Our study addresses these issues by using genetic, siRNA and pharmacological interference

with YAP in basal breast cancer to demonstrate its function specifically in CSCs. In basal breast cancer, I show that YAP's genetic ablation strongly delayed Wnt-Met-driven tumorigenesis. Segregation of luminal (ER+, PR+) breast cancer patients and basal, triple-negative patients revealed that YAP expression correlated with patient survival in opposing ways. High YAP activity was associated with prolonged survival in luminal breast cancer patients, but decreased survival in basal/triple-negative patients. Thus, YAP appears to function as an oncogene in some cancer subtypes and a tumour suppressor gene in others. Further studies will be required to understand what mechanisms are responsible for the context-dependent function of YAP and whether its inhibition in breast cancer has converse therapeutic benefits in basal and luminal breast cancers.

In conclusion, our data demonstrate that YAP is essential for the co-operation of Wnt and RTK Met signalling in initiating and maintaining basal mammary gland tumours. I demonstrate that Met signalling controls the de-differentiation of luminal to basal mammary gland cells through the downstream activation of YAP. Furthermore, I show that YAP is highly expressed in the CSCs of Wnt-Met mice and promotes their expansion, partly by regulating the activity of β-catenin. I confirmed elevated YAP activity in mammospheres of human basal breast cancer cell lines, in tumours from human patients with basal breast cancer, and in PDX models of basal breast cancer and contrasted these findings to the luminal stages. Our data highlight the importance of YAP as a crucial tumour initiator and CSC regulator in basal breast cancer and demonstrate that its activity has prognostic value when comparing basal with luminal breast cancers. This suggests that targeting YAP through specific new drugs is a potential therapeutic avenue for treating basal breast cancers in the future.

4.6. YAP as a rational drug target for basal breast cancer

Wnt-Met tumours exhibit basal characteristics, i.e. high levels of basal markers K5, K14 and smooth muscle actin; whereas luminal cell markers K8 and K18 were low[33]. Gene expression analysis showed that Wnt-Met mutant tumours grouped closely with BRCA1+/-; p53+/- basal (triple-negative) but not with luminal breast cancers[33,225]. In the former tumours, Met controls the differentiation state of Wnt-Met tumour cells, while Wnt-β-catenin controls the stem cell property of self-renewal[33]. I found that HGF-Met and Wnt-β-catenin signalling converge into YAP signalling, the master regulator of both differentiation and self-renewal processes. Based on these data, YAP is a clear rational

target for therapies against basal breast cancers that frequently show hyper-activation of both RTK and Wnt-β-catenin signalling[107,136].

Unfortunately, currently available inhibitors against YAP activity are non-specific with a number of off-target effects resulting in toxicity[226]. Based on the remarkable oncogenic role of YAP, both academic and pharmaceutical research groups are racing to find specific inhibitors of its transcription activity. Due to the complexity of YAP regulation by upstream signals, the most promising target for therapeutic drugs are inhibitors of YAP/TEAD interaction. Auto-palmitoylation is essential for TEAD stability and transcription activity[227,228]. Recently, MYF-01-37 and CP-1, two inhibitors of TEAD auto-palmitoylation were identified and found to effectively block TEAD-dependent transcription both *in vitro* and *in vivo*[205,229]. These inhibitors require further testing regarding their specificity and toxicity, however they are currently the most promising small molecule inhibitors.

5. OUTLOOK

Yes-associated protein (YAP) is the downstream effector of the Hippo pathway, often found dysregulated in many cancers. Yet, the function and regulation of YAP in most deadly basal breast cancers, for which no rational therapies exists, remained unclear until now. To address this question, I utilized a mouse model of basal breast cancer driven by activation of both Wnt-β-catenin and receptor tyrosine kinase signalling. In this model, Wnt-β-catenin controls the self-renewal of cells, while RTK signalling regulates their differentiation. Using this model, proteomic analysis identified an upregulation of the YAP signature in response to RTK-Met signalling. I show that genetic, siRNA and pharmacological inhibition of YAP in Wnt-RTK-driven mammary gland tumours delays tumour initiation and the differentiation status. Importantly, I find high expression of YAP in tumour-initiating (cancer stem) cells *in vivo* and *ex vivo* that is essential for cancer stem cell expansion. Mechanistically, I show that this phenotype is due to the requirement of YAP for efficient Wnt-β-catenin transcription activity. In the absence of YAP, Wnt-β-catenin is no longer able to promote the self-renewing property of cancer stem cells. I confirmed elevated YAP activity in mammospheres of human basal breast cancer cell lines, in tumours from human patients with basal breast cancer, and in PDX models of basal breast cancer, and I contrasted these findings to luminal tumours. Of further clinical relevance, using proteomic data we confirm the upregulation of the YAP signature in basal breast cancer patients, compared to all other breast cancer subtypes, and identified opposing survival rates of basal and luminal breast cancer patients with high YAP expression. These data substantiate the clinical relevance of our findings from the mouse model.

Our data highlight the importance of YAP as a crucial tumour initiator and cancer stem cell regulator in basal breast cancer and demonstrates that its activity has prognostic value, when comparing basal with luminal breast cancers. This suggests that targeting YAP through specific new drugs, which researchers in academia and industry are presently developing, is a potential therapeutic avenue for treating basal breast cancers in the future.

6. Materials and Methods

6. 1. Mouse Strains

All animal experiments were conducted in accordance with European, National and MDC regulations. Wnt-Met mice were previously described (24). Yap1tm1.1Dupa/J flox mice were purchased from Jackson Laboratories (Stock No: 027929). Animal experiments were approved by the ethical board Landesamt für Gesundheit und Soziales (LaGeSo), Berlin. Mice were induced via pregnancy between 8-12 weeks old. Tumours were harvested between 1 and 2 weeks post-partum and reached a maximum size of $1cm^3$.

For genotyping, ear biopsies were digested in lysis buffer (100mM Tris pH 8.0 – 8.5, 10mM EDTA pH 8.0, 0.2% SDS and 200mM NaCl) with 1:30 10mg/ml Proteinase K (Roche, Cat. #03 115 879 001). Lysates were then diluted 1:20 in nuclease-free water and PCR was carried out using Taq DNA polymerase (Invitrogen). The following primers were used for genotyping:

Table 6.1: List of Genotyping primers

Target	Sequence
WapiCre F'	5' GAA AAG CAC CAG GAG AAG TCA C 3'
WapiCre R'	5' GAC ACA GCA TTG GAG TCA GAA G 3'
Wap-HGF F'	5' GAC ATG CTG CAG CAA CAG G 3'
Wap-HGF R'	5' CAT CCC AGA CAC TCA GAC AG 3'
β-cat^{GOF} F'	5' AGA ATC ACG GTG ACC TGG GTT AAA 3'
β-cat^{GOF} R'	5' CAT TCA TAA AGG ACT TGG GAG GTG T 3'
R26-stop-EYFP 1	5' GGC GAC TTC CAG TTC AAC ATC 3'
R26-stop-EYFP 2	5' AAA GTC GCT CTG AGT TGT TAT 3'
R26-stop-EYFP 3	5' GCG AAG AGT TTG TCC TCA ACC 3'
YAP^{flox} 1	5' CCATTTGTCCTCATCTCTTACTAAC 3'
YAP^{flox} 2	5' GATTGGGCACTGTCAATTAATGGGCTT 3'
YAP^{flox} 3	5' CAGTCTGTAACAACCAGTCAGGGAT AC 3'

6. 2. Isolation of Mammary Cells

Tumours were minced and digested in DMEM/F12 HAM (Invitrogen) supplemented with 5% FBS (Invitrogen), 5µg/ml insulin (Sigma-Aldrich), 0.5µg/ml hydrocortisone

(SigmaAldrich), 10ng/ml EGF (Sigma-Aldrich) (digestion medium) containing 300 U/ml Collagenase type III (Worthington), 100U/ml Hyaluronidase (Worthington) and 20µg/ml Liberase TM (Sigma) at 37°C for 1.5 hours shaking. Resulting organoids were resuspended in 0.25% trypsin-EDTA (Invitrogen) at 37°C for 1 minute and further dissociated in digestion medium containing 2 mg/ml Dispase (Invitrogen) and 0.1 mg/ml DNase I (Worthington) at 37°C for 45 minutes shaking. Samples were filtered with 40 µm cell strainers (BD Biosciences) and incubated with 0.8% NH_4Cl solution on ice for 3 minutes (RBC lysis). Lysis was stopped by washing in 30ml DPBS w/o Ca^{2+}, Mg^{2+} (Gibco, Cat. #14190169). Resulting pellet was used for downstream applications outlined below.

6. 3. Organotypic Stem cell-enriched 3D Cultures

Single cells from digested mammary glands were resuspended and plated on Collagen I coated plates (50µg/ml) in stem cell-enriching medium MEBM (Lonza Cat. #CC-3151), supplemented with 2% B27 (Invitrogen, Cat. # 17504044), 20 ng/ml bFGF (Invitrogen, Cat. # 13256029), 20 ng/ml EGF (Sigma, Cat. #SRP3196-500µg), 4 µg/ml heparin (Sigma, Cat. # H3149), 5 µg/ml insulin (Sigma, Cat. #I0516-5ml), 0.5µg/ml hydrocortisone (Sigma, Cat. #H0888-1G) and 1X Gentamicin (Sigma, Cat. # G1397-100ML) for 16-18 hours. Cells were washed X2 with DPBS, washed with 0.25% trypsin-EDTA for 30 seconds and then incubated with 0.25% trypsin-EDTA at 37°C for 5-7 minutes until cells detached. Trypsin was inactivated with DMEM/F12 supplemented with 10% FBS, 1% HEPES and 1% Pen/Strep. Cells were then resuspended in stem cell-enriching medium and counted. Cells were seeded in 25µl droplets containing 50% reduced growth factor Matrigel at a density of 100 cells/µl. Plated were carefully flipped and Matrigel was let solidify at 37°C for 45 minutes-1 hour. 0.5ml of stem medium was added per well of 24-well plate containing a 25µl droplet. Medium was changed every second day. For secondary sphere formation, spheres were dissociated for 10 minutes in 0.25% trypsin-EDTA, cells were then filtered using 0.45µm filters. Single cell suspensions were then reseeded as described for primary cells.

6. 4. Fluorescence-activated cell sorting (FACS)

Single cell suspensions from dissociated tumours were resuspended at 10,000cells/µl and incubated with conjugated primary antibodies at 4°C for 15 minutes. Cells were then washed X3 in DPBS and finally incubated with 7AAD (5µl/10^6 cells) at room temperature for 5 minutes to stain dead/dying cells. Cells were sorted using the

FACSAria II or III (BD Biosciences) or analysed using LSRFortessa (BD Biosciences). Compensation for was carried out for every FACS experiment. Data were analysed using FLowJo Analysis Software.

Table 6.2: List of FACS reagents

Antigen	Manufacturer and Catalogue#	Dilution
PE Rat Anti-Human CD49f	BD Biosciences #555736	1:50
APC Rat Anti-Mouse CD24	BD Biosciences #562349	1:250
7-AAD Viability Dye	Biolegend #20404	5µl/10^6 cells
AbC Total Compensation Bead kit	Life Technologies A10497	N/A

6. 5. Histology and Immunostaining

Mammary glands were fixed overnight at 4°C in 4% formaldehyde (Roth). Glands were then dehydrated and embedded in paraffin. For staining, tissue sections were de-paraffinized, rehydrated and stained with Hematoxylin and Eosin, dehydrated and mounted. Images were acquired with a bright-field Zeiss microscope. For immunostaining, antigen-retrieval was conducted on paraffin-embedded sections by boiling sections in Tris-EDTA buffer (10mmol/L Tris, 1mmol/L EDTA, pH 9.0) for 20 minutes. Cryosections were incubated for 5 minutes at room temperature and then fixed with 4% methanol-free paraformaldehyde for 15minutes. Adherent cells were fixed with 4% methanol-free paraformaldehyde for 15 minutes. Stem cell-enriched spheres were collected, centrifuged and then fixed in 4% formaldehyde before being dehydrated and paraffin embedded. All samples were blocked with 10% horse serum for 1 hour at room temperature prior to being incubated overnight with primary antibodies at 4°C (See supplementary table for antibody list). For fluorescent staining samples were incubated with secondary antibodies and DAPI for 1 hour at room temperature before being mounted with Immu-mount (Thermo Scientific).

For Immunohistochemistry, after antigen retrieval slides were washed and incubated with 3% H2O2 for 15 minutes at room temperature, washed X3 5 minutes in PBS and incubated with primary antibodies overnight at 4°C. Horseradish Peroxidase

(HRP) secondary antibodies were diluted and incubated on slides for 1 hour at room temperature. Slides were then washed and developed using DAB chromogenic substrate (DAKO), dehydrated and mounted.

6. 6. RNA isolation, cDNA generation and RT-qPCR

RNA was extracted using TRIzol (Invitrogen). For 3D cultures, Trizol was added directly to Matrigel. For tissue, snap frozen glands were pulverized on dry ice and 1ml of Trizol was added per 30mg tissue powder. For cell lines, Trizol was added directly to plate. For mammospheres, spheres were collected, pelleted and Trizol was added. After 5 minutes at room temperature, 200µl of chloroform was added per 1ml of Trizol and shook vigorously by hand for 15 seconds. Samples were then centrifuged at 12,000G for 15 minutes. The upper phase was transferred to a fresh Eppendorf and 500µl of isopropanol was added, mixed and incubated at room temperature for 10 minutes. Samples were then centrifuged at 12,000G for 10 minutes. RNA pellet was washed twice with 1ml of 70% EtOH. All steps were carried out at 4°C unless otherwise stated. RNA was quantified using NanoDrop or Qubit. For quantitative reverse transcription PCR (RT-qPCR) cDNA was generated from 90-5000 ng of total RNA using MMLV reverse transcriptase (Promega). RT-qPCR was performed using Power Up SybR Green master mix (Thermo Scientific #A25741) in a CFX96-C1000T thermal cycler (BioRad) according to manufacturer's recommendations. See Table 5 and 6 for primer list. *GAPDH* or *RPLO* were used as housekeeping genes to which values were normalized to. Bio-Rad CX manager was used to calculate Cq and analysed data.

6.7. Protein extraction, Western Blot and co-IP

For western blot protein was extracted using RIPA buffer with added cOMPLETE™ Mini Protease Inhibitor cocktail (#11836153001) and phosphatase inhibitor cocktail 2 and 3 (Sigma). For 2D cell culture, cells were scraped into RIPA buffer (150mM NaCl, 1% Triton-X-100, 0.5% sodium deoxycholate, 0.1% SDS, 50mM Tris pH 8.0 and cOMPLETE™ Mini Protease Inhibitor cocktail (#11836153001) and phosphatase inhibitor cocktail 2 and 3 (Sigma)) for lysis. Lysis was carried out on ice for 20 minutes, samples were then centrifuged at full speed and supernatant was transferred to fresh tube and protein concentration was measured using BioRad Bradford reagent.

For co-IP, cells were lysed as above in co-IP buffer (150mM NaCl, 50mM Tris pH 7.5, 1% IGPAL-CA-630 (Sigma #I8896), 5% glycerol, 0.5% deoxycholate, 0.1% SDS with cOMPLETE™ Mini Protease Inhibitor cocktail (#11836153001) and phosphatase inhibitor

cocktail 2 and 3 (Sigma)). Equal amounts of protein were incubated with primary antibodies overnight at 4°C rotating. Immunocomplexes were then captured on Dynabeads Protein GInvitrogen Cat#10003D for 1 hour at 4°C rotating. Samples were washed and boiled in sample buffer and resolved on 10% SDS-PAGE gels or gradient gels (4-20% Bio-Rad) and electrotransferred to PDVF membrane. Membranes were blocked with 5% BSA in TBS-T for 1 hour and incubated with primary antibodies (see antibody list).

6.8. siRNA

siRNAs were purchased from Thermo Scientific (see supplementary table for list of specific siRNAs). 75pmol/well (6-well) of siRNA was transfected using Lipofectamine 2000 following manufacturer's instructions. Cells were harvested 48 hours post transfection.

Table 6.3: List of siRNAs

siRNA	Cat#
Ctrl	AM4611
YAP	107951
MET	103545

6.9. shRNA

PLKO.1 shRNA plasmids were a gift from Yaron Fuchs[230]. Lentiviral packaging plasmids, pMD2.G and psPAX2 were co-transfected along with shscramble and shYAP1 into HEK293 cells. Viruses were collected and concentrated 24-48 hours post-transfection. Concentrated viruses were used to transduce Wnt-Met primary mammary cells before being seeded as stem cell-enriched spheres

6.10. Cell Culture

Breast cancer cell lines were purchased from ATCC (MCF10A, MCF7, BT474, T47D, MDA-MB-231 and BT-549) and Asterand Bioscience (SUM1315 and SUM149). MCF10A were maintained in DMEM/F12 Glutamax, 5% horse serum, 20ng/ml EGF, 0.5mg/ml hydrocortisone, 100ng/ml cholera toxin, 10µg/ml insulin and 1% pen/strep.

MCF7, BT474 and T47D were maintained in DMEM, 10% FBS, 5µg/ml insulin and 1% pen/strep. MDA-MB-231 and BT-549 were maintained in DMEM, 10% FBS, 1% NEAAs and 1% pen/strep. SUM1315 were maintained in DMEM/F12 HAM-Glutamax, 1% Hepes, 5% FBS, 10ng/ml EGF, 5µg/ml insulin and 1% pen/strep. SUM149 were grown in DMEM/F12 HAM-Glutamax, 1% Hepes, 5% FBS, 1µg/ml hydrocortisone, 5µg/ml insulin and 1% pen/strep. For mammosphere assays, cells were seeded at 5,000cells/ml on poly-HEMA coated non-adherent 10cm plates in DMEMF12, FGF 10ng/ml, EGF 20ng/ml, ITS 1X, B27 1X. Spheres were grown for up to 10 days with medium supplemented every second day.

6.11. CellTitre-Glo assay

3D cultures were seeding into 96-well opaque-walled plates. Control and treated spheres with 100µl of medium per well were incubated at 30mins at room temperature. 100µl of CellTiter-Glo reagent was added to each well and incubated for 2 minutes shaking to induce cell lysis. Plate was then rested for 10 minutes at room temperature to stabilise the luminescent signal. Luminescence was recorded on luminometer.

6.12. *In vivo* inhibitor studies

For simvastatin treatments, Wnt-Met mice received 100mg/kg of simvastatin or control via oral gavage daily. Simvastatin was diluted in 2% DMSO, 30% PEG 300, 5% Tween80 and ddH2O. For verteporfin, mice were treated with 2.5mg/kg daily via subcutaneous injection. Verteporfin was diluted in DMSO and then brought to 2.5% DMSO in PBS. Tumour volumes and body weight were determined several times per week.

6.13. PDX Models

PDX models were established from triple-negative breast cancer patients with their informed consent as previously described[191]. The experimental protocol and animal housing were in accordance with institutional guidelines as proposed by the French Ethics Committee (Agreement N° B75-05-18)

6.14. Nanostring

PanCancer Pathways panel was purchased from Nanostring including additional custom geneset for selected YAP target genes. RNA for analysis was prepared as stated above. RNA quality was checked using a high sensitivity RNA tape on the TapeStation. 70ng of RNA was hybridized for 16hours at 65°C as per manufacturer's recommendations. Hybridized RNA was loaded onto and analyzed using nCounter SPRINT Profiler. Data were analysed using nSolver software.

6.15. ChIP-Atlas data analysis

ChIP-seq tracks for CTNNB1 (SRX833403), TEAD4 (SRX190301) and YAP1 (SRX2844314) in H1-hESC were downloaded from chip-atlas.org[188,231]. Functional annotation for genome regions was taken from ChromHMM[232]. Data were loaded into UCSC genome browser[233] to make the plots. Plots were generated by Clemens Messerschmidt of the Humboldt-Universität zu Berlin.

6.16. Proteomics and Phospho-proteomics

Proteomics/Phospho-proteimics and analysis was performed by Oliver Popp and Philipp Mertins of the MDC-Berlin. For proteomics and phospho-proteomics analysis, sample preparation was carried out essentially according to Mertins and collegues, 2018[234]. Briefly, samples were lysed in urea lysis buffer containing protease and phosphatase inhibitors. From each sample, 500 µg was subjected to reduction with DTT and alkylation with iodoacetamide before performing digestion with LysC and trypsin. After desalting, peptides were labelled with TMT6 reagents (Thermo) and fractionated by basic reversed-phase separation into 24 fractions. 1.5 µg per fraction was injected into LC-MS for global proteome analysis, while the remaining majority of the samples were pooled into 12 fractions and enriched for phosphopeptides using robot-assisted iron-based IMAC on an AssayMap Bravo system (Agilent).

Proteomics samples were measured on an Exploris 480 orbitrap mass spectrometer (Thermo) connected to an EASY-nLC system (Thermo). HPLC-separation occurred on an in-house prepared nano-LC column (0.074 mm × 250 mm, 1.9 µm Reprosil C18, Dr Maisch GmbH) using a flow rate of 250 nl/min on a 110 min gradient with an acetonitrile concentration ramp from 4.7% to 55.2% (v/v) in 0.1% (v/v) formic acid. MS acquisition was performed at a resolution of 60,000 in the scan range from 375 to 1,500 m/z. Data-dependent MS2 scans were carried out at a resolution of 45,000 or 30,000 with an

isolation window of 0.4 m/z and a maximum injection time of 86 ms (120 ms for phosphoproteomics) using the TopSpeed setting with a 1 sec cycle time. Dynamic exclusion was set to 20 s and the normalised collision energy was specified to 35.

For analysis, the MaxQuant software package version 1.6.10.43[235,236] was used. TMT6 reporter ion quantitation was turned on using a PIF setting of 0.5. Variable modifications included Met-oxidation, acetylated N-termini and deamidation of Asn and Gln for proteomics analysis. For phosphoproteomics analysis, deamidation was replaced by phosphorylation on Ser, Thr and Tyr. An FDR of 0.01 was applied for peptides, sites and proteins, and the Andromeda search was performed using a mouse Uniprot database (July 2018, including isoforms). Further analysis was done using R and the Protigy package (https://github.com/broadinstitute/protigy). Protein groups were filtered for proteins that have been identified by at least one unique peptide and that had valid TMT reporter ion intensities across all samples. The phosphoproteome was also filtered for sites containing valid values for all samples. For both analyses, two-sample moderated t-tests (limma package[237]) comparing the two groups were calculated using the log2-transformed and median-MAD normalised TMT6 corrected reporter ion intensities, followed by a Benjamini-Hochberg (BH) p-value correction. Heatmaps of selected significant proteins or phosphosites according to BH-adjusted p-value were generated using the pheatmap package[238] employing hierarchical clustering based on Euclidean distance. For annotation of gene lists derived from a human proteome, i.e. Zanconato and collegues (2016), genes were converted into mouse orthologs using biomaRt[239] and manual curation.

6.17. Kaplan-Meier and GOBO analysis

Relapse-free survival of breast cancer patients was analyzed using Kaplan-Meier Plotter online software (http://kmplot.com). Trichotomization was set to Q1 vs Q4. Expression analysis of YAP in breast cancer cell lines and human datasets was generated using GOBO online software (http://co.bmc.lu.se/gobo).

Table 6.4: List of primary antibodies

Antigen	Manufacturer and Catalogue #	Dilution	Application
Ki-67	RM-9106	1:100	IHC, IF
β-catenin	BD #610153	1:500	IHC, IF, WB
K8	GP-K8	1:200	IF
K14	Convance PRB-155P	1:100	IF

YAP	Cell Signalling #14074S	1:100, 1:1000*	IHC, IF, WB*
GFP	Abcam ab6673	1:200	IHC, IF
GAPDH	Cell Signaling #5174S	1:1000	WB
Active YAP	Abcam ab205270	1:100, 1:1000*	IHC, IF, WB*
β-catenin	Rabbit (made in house)	1:1000	IHC, IF, WB
P63	Abcam ab124762	1:50	IF
MET	Cell Signaling #8198	1:1000	WB
Active β-catenin	Cell Signaling #8814	1:1000	WB
TEAD4	Abcam ab58310	1:1000	WB

Table 6.5: List of RT-qPCR primers (Mouse)

Target	Sequence
Gapdh F	ATCCTGCACCACCAACTGCT
Gapdh R	GGGCCATCCACAGTCTTCTG
Procr F	ACGCAAAACATGAAAGGGAGC
Procr R	ATTAGCAACGCCGTCCACTT
Lgr5 F	CAGTGTTGTGCATTTGGGGG
Lgr5 R	CAAGGTCCCGCTCATCTTGA
Twist F	GGACAAGCTGAGCAAGATTCA
Twist R	CGGAGAAGGCGTAGCTGAG
Snai1 F	CACACGCTGCCTTGTGTCT
Snai1 R	GGTCAGCAAAAGCACGGTT
Zeb1 F	GCTGGCAAGACAACGTGAAAG
Zeb1 R	GCCTCAGGATAAATGACGGC
Yap1 F	TTCGGCAGGCAATACGGAAT
Yap1 R	TGCTCCAGTGTAGGCAACTG
Amotl2 F	CACCTCCGTTGCTGACTGTA
Amotl2 R	TGGTCTCAGAGCACCGCT
Ankrd1 F	AGGTCAAGAACTGTGCTGGG
Ankrd1 R	AAAATGCCTGCGAACAGCTC
Ctgf F	AGAACTGTGTACGGAGCGTG
Ctgf R	GTCCACCATCTTTGGCAGTG
Sdpr F	AGAAGTCTCGCAAGGTCAGC

Sdpr R	AGGGATCTCACTTTCTTCCTGG
Cyr61 F	AGAGGCTTCCTGTCTTTGGC
Cyr61 R	CCAAGACGTGGTCTGAACGA
Axl F	AGGAGCCCAGGGGTGG
Axl R	TGTGTGTCCTTATGGGCTGC
Igfbp3 F	TCTAAGGGGGAGACAGAATACG
Igfbp3 R	CTCTGGGACTCAGCACATTGA
Csf2 F	TCGTCTCTAACGAGTTCTCC
Csf2 R	CTGTCTATGAAATCCGCATAGG
Cd44 F	CCTTGGCCACCACTCCTAATA
Cd44 R	GCCATCCGTTCTGAAACCAC
Cd29 F	TGCAGGTGTCGTGTTTGTGAATGC
Cd29 R	ACAAGTTGGCCCTTGAAACTTGGG
Cd49f F	TTCATTGATGTGACTGCTGCTGCC
Cd49f R	AAAAGCAAGCATCAAGATCCCAGCG
Sox10 F	CAAGCTCTGGAGGTTGCTGA
Sox10 R	CCGGATGGTCCTTTTTGTGC
Cd24 F	TACCCACGCAGATTTACTGCAACC
Cd24 R	TGTAGAAGAGAGAGAGAGAGAGCC
Axin2 F	AACTGAAACTGGAGCTGGAAAGCC
Axin2 R	TTTGTGGGTCCTCTTCATAGCTGC
Birc5 F	GCTTTAAGGAATTGGAAGGCTGGG
Birc5 R	TTGTTCTTGGCTCTCTGTCTGTCC
Ccnd1 F	CAGCCCCAACAACTTCCTCT
Ccnd1 R	CAGGGCCTTGACCGGG
Wap F	GTATCATCTGCCAAACCAACGAGG
Wap R	TTCATGTTGCCAGAACACTCACGG
Hgf F	ACCCTGGTGTTTCACAAGCAATCC
Hgf R	TCTTTCTGGCAAGAACTTGTGCCG
Id2 F	AAATCCTGCAGCACGTCATC
Id2 R	CATTCGACATAAGCTCAGAAGGG
Mmp7 F	TAGGCGGAGATGCTCACTTTGACAAG
Mmp7 R	TTCTGAATGCCTGCAATGTCGTCC
Krt8 F	TGCGGAATGAATGGGGTGAG
Krt8 R	GAACCAGGCGGAGATCCCTT

Dnp63 F	AGAGAGAGAGAGGCACCTGA
Dnp63 R	AGGTCCGTGTACTGTGGCTC

Table 6.6: List of RT-qPCR primers (Human)

Target	Sequence
RPLO F	CGGATTACACCTTCCCACTTG
RPLO R	CCGACTCTTCCTTGGCTTCA
ANKRD1 F	CACTTCTAGCCCACCCTGTGA
ANKRD1 R	CCACAGGTTCCATAATGATTT
CYR61 F	AGCCTCGCATCCTATACAACC
CYR61 R	TTCTTTCACAAGGCGGCACTC
CTGF F	CAGCATGGACGTTCGTCTG
CTGF R	AACCACGGTTTGGTCCTTGG
IGFBP3 F	AGAGCACAGATACCCAGAACT
IGFBP3 R	GGTGATTCAGTGTGTCTTCCATT
CCND1 F	CCGTCCATGCGGAAGATC
CCND1 R	ATGGCCAGCGGGAAGAC
CLDN1 F	GTGCGATATTTCTTCTTGCAGG
CLDN1 R	TTCGTACCTGGCATTGACTGG
MYC F	GGCCCCCAAGGTAGTTATCC
MYC R	TTTCCGCAACAAGTCCTCTTC

7. REFERENCES

1. Li, M. L. *et al.* Influence of a reconstituted basement membrane and its components on casein gene expression and secretion in mouse mammary epithelial cells. *Proc. Natl. Acad. Sci. U. S. A.* **84**, 136–140 (1987).

2. Lee, E. Y. H., Parry, G. & Bissell, M. J. Modulation of secreted proteins of mouse mammary epithelial cells by the collagenous substrata. *J. Cell Biol.* **98**, 146–155 (1984).

3. Nishimori, K. *et al.* Oxytocin is required for nursing but is not essential for parturition or reproductive behavior. *Proc. Natl. Acad. Sci. U. S. A.* **93**, 11699–11704 (1996).

4. Young, W. S. *et al.* Deficiency in Mouse Oxytocin Prevents Milk Ejection , but not Fertility or Parturition. *J. ofNeuroendocrinology* **8**, 847–853 (1996).

5. Crowley, W. R. & Armstrong, W. E. Neurochemical regulation of oxytocin secretion in lactation*. *Endocr. Rev.* **13**, 33–65 (1992).

6. Sternlicht, M. D., Kouros-Mehr, H., Lu, P. & Werb, Z. Hormonal and local control of mammary branching morphogenesis. *Differentiation* **74**, 365–381 (2006).

7. Mikaelian, I. *et al.* Expression of terminal differentiation proteins defines stages of mouse mammary gland development. *Vet. Pathol.* **43**, 36–49 (2006).

8. Wetzels, R. H. W. *et al.* Basal cell-specific and hyperproliferation-related keratins in human breast cancer. *Am. J. Pathol.* **138**, 751–763 (1991).

9. Haaksma, C. J., Schwartz, R. J. & Tomasek, J. J. Myoepithelial cell contraction and milk ejection are impaired in mammary glands of mice lacking smooth muscle alpha-actin. *Biol. Reprod.* **85**, 13–21 (2011).

10. Carroll, D. K. *et al.* p63 regulates an adhesion programme and cell survival in epithelial cells. *Nat. Cell Biol.* **8**, 551–561 (2006).

11. Deome, K. B., Faulkin, L. J., Bern, H. A. & Blair, P. B. Development of Mammary Tumors from Hyperplastic Alveolar Nodules Transplanted into Gland-free Mammary Fat Pads of Female C3H Mice. *Cancer Res.* **19**, 515 (1959).

12. Daniel, C. W., Deome, K. B., Young, J. T., Blair, P. B. & Faulkin, L. J. The in vivo life span of normal and preneoplastic mouse mammary glands: a serial

transplantation study. *J. Mammary Gland Biol. Neoplasia* **14**, 355–362 (1968).

13. Hoshino, K. & Gardner, W. U. Transplantability and life span of mammary gland during serial transplantation in mice [30]. *Nature* **213**, 193–194 (1967).

14. Smith, G. H. Experimental mammary epithelial morphogenesis in an in vivo model: Evidence for distinct cellular progenitors of the ductal and lobular phenotype. *Breast Cancer Res. Treat.* **39**, 21–31 (1996).

15. Shackleton, M. *et al.* Generation of a functional mammary gland from a single stem cell. *Nature* **439**, 84–88 (2006).

16. Stingl, J. *et al.* Purification and unique properties of mammary epithelial stem cells. *Nature* **439**, 993–997 (2006).

17. Visvader, J. E. & Stingl, J. Mammary stem cells and the differentiation hierarchy : current status and perspectives. *Genes Dev.* **28**, 1143–1158 (2014).

18. Wang, D. *et al.* Identification of multipotent mammary stem cells by protein C receptor expression. *Nature* **517**, 81–4 (2015).

19. Bach, K. *et al.* Differentiation dynamics of mammary epithelial cells revealed by single-cell RNA sequencing. *Nat. Commun.* **8**, (2017).

20. Robinson, G. W., Karpf, A. B. & Kratochwil, K. Regulation of mammary gland development by tissue interaction. *J. Mammary Gland Biol. Neoplasia* **4**, 9–19 (1999).

21. Fendrick, J. L., Raafat, A. M. & Haslam, S. Z. Mammary Gland Growth and Development from the Postnatal Period to Postmenopause: Ovarian Steroid Receptor Ontogeny and Regulation in the Mouse. *J. Mammary Gland Biol. Neoplasia* **3**, 7–22 (1998).

22. Hovey, R. C., McFadden, T. B. & Akers, R. M. Regulation of mammary gland growth and morphogenesis by the mammary fat pad: a species comparison. *J. Mammary Gland Biol. Neoplasia* **4**, 53–68 (1999).

23. Oakes, S. R., Hilton, H. N. & Ormandy, C. J. Key stages in mammary gland development: The alveolar switch: Coordinating the proliferative cues and cell fate decisions that drive the formation of lobuloalveoli from ductal epithelium. *Breast Cancer Res.* **8**, (2006).

24. Anderson, S. M., Rudolph, M. C., McManaman, J. L. & Neville, M. C. Key stages in mammary gland development. Secretory activation in the mammary gland: It's not just about milk protein synthesis! *Breast Cancer Research* vol. 9 1–14 (2007).

25. Zwick, R. K. *et al.* Adipocyte hypertrophy and lipid dynamics underlie mammary gland remodeling after lactation. *Nat. Commun.* **9**, 1–17 (2018).

26. Djonov, V. & Andres, A. Vascular Remodelling During the Normal and Malignant Life Cycle of the Mammary Gland. **189**, 182–189 (2001).

27. Jena, M. K., Jaswal, S., Kumar, S. & Mohanty, A. K. Molecular mechanism of mammary gland involution: An update. *Dev. Biol.* **445**, 145–155 (2019).

28. Burdon, T., Sankaran, L., Wall, R. J., Spencer, M. & Hennighausen, L. Expression of a whey acidic protein transgene during mammary development: Evidence for different mechanisms of regulation during pregnancy and lactation. *J. Biol. Chem.* **266**, 6909–6914 (1991).

29. Hennighausen, L. *et al.* Whey acidic protein extrinsically expressed from the mouse mammary tumor virus long terminal repeat results in hyperplasia of the coagulation gland epithelium and impaired mammary development. *Cell Growth Differ.* **5**, 607–613 (1994).

30. Sinn, E. *et al.* Coexpression of MMTV/v-Ha-ras and MMTV/c-myc genes in transgenic mice: synergistic action of oncogenes in vivo. *Cell* **49**, 465–475 (1987).

31. Muller, W. J., Sinn, E., Pattengale, P. K., Wallace, R. & Leder, P. Single-step induction of mammary adenocarcinoma in transgenic mice bearing the activated c-neu oncogene. *Cell* **54**, 105–115 (1988).

32. Rose-Hellekant, T. A. & Sandgren, E. P. Transforming growth factor alpha- and c-myc-induced mammary carcinogenesis in transgenic mice. *Oncogene* **19**, 1092–1096 (2000).

33. Holland, J. *et al.* Combined Wnt/β-Catenin, Met, and CXCL12/CXCR4 Signals Characterize Basal Breast Cancer and Predict Disease Outcome. *Cell Rep.* **5**, 1214–1227 (2013).

34. Valenti, G. *et al.* Cancer stem cells regulate cancer-associated fibroblasts via activation of Hedgehog signaling in mammary gland tumors. *Cancer Res.* (2017).

35. Bray, F. *et al.* Global cancer statistics 2018: GLOBOCAN estimates of incidence

and mortality worldwide for 36 cancers in 185 countries. *CA. Cancer J. Clin.* **68**, 394–424 (2018).

36. Silverstein, M. J. & Lagios, M. D. Ductal carcinoma in situ of the breast. *Breast Cancer A New Era Manag.* 269–311 (2014) doi:10.1007/978-1-4614-8063-1_15.

37. Mego, M., Mani, S. A. & Cristofanilli, M. Molecular mechanisms of metastasis in breast cancer-clinical applications. *Nat. Rev. Clin. Oncol.* **7**, 693–701 (2010).

38. Wang, Y. *et al.* Clonal evolution in breast cancer revealed by single nucleus genome sequencing. *Nature* **512**, 155–160 (2014).

39. Torres, L. *et al.* Intratumor genomic heterogeneity in breast cancer with clonal divergence between primary carcinomas and lymph node metastases. *Breast Cancer Res. Treat.* **102**, 143–155 (2007).

40. Navin, N. *et al.* Inferring tumor progression from genomic heterogeneity. *Genome Res.* **20**, 68–80 (2010).

41. Perou, C. M. *et al.* Molecular portraits of human breast tumours. *Nature* **406**, 747–752 (2000).

42. Howlader, N., Cronin, K. A., Kurian, A. W. & Andridge, R. Differences in breast cancer survival by molecular subtypes in the United States. *Cancer Epidemiol. Biomarkers Prev.* **27**, 619–626 (2018).

43. Gao, J. J. & Swain, S. M. Luminal A Breast Cancer and Molecular Assays: A Review. *Oncologist* **23**, 556–565 (2018).

44. Tran, B. & Bedard, P. L. Luminal-B breast cancer and novel therapeutic targets. *Breast Cancer Res.* **13**, (2011).

45. Wang, J. & Xu, B. Targeted therapeutic options and future perspectives for her2-positive breast cancer. *Signal Transduct. Target. Ther.* **4**, (2019).

46. Li, C. H., Karantza, V., Aktan, G. & Lala, M. Current treatment landscape for patients with locally recurrent inoperable or metastatic triple-negative breast cancer: A systematic literature review. *Breast Cancer Res.* **21**, 1–14 (2019).

47. Morel, A. P. *et al.* A stemness-related ZEB1-MSRB3 axis governs cellular pliancy and breast cancer genome stability. *Nat. Med.* **23**, 568–578 (2017).

48. Morel, A. P. *et al.* EMT inducers catalyze malignant transformation of mammary

epithelial cells and drive tumorigenesis towards claudin-low tumors in transgenic mice. *PLoS Genet.* **8**, (2012).

49. Jones, R. L., Constantinidou, A. & Reis-Filho, J. S. Molecular Classification of Breast Cancer. *Surg. Pathol. Clin.* **5**, 701–717 (2012).

50. Drebin, J. A., Link, V. C., Stern, D. F., Weinberg, R. A. & Greene, M. I. Down-modulation of an oncogene protein product and reversion of the transformed phenotype by monoclonal antibodies. *Cell* **41**, 695–706 (1985).

51. Drebin, J. A., Link, V. C., Weinberg, R. A. & Greene, M. I. Inhibition of tumor growth by a monoclonal antibody reactive with an oncogene-encoded tumor antigen. *Proc. Natl. Acad. Sci. U. S. A.* **83**, 9129–9133 (1986).

52. Jordan, V. C. Tamoxifen: Catalyst for the change to targeted therapy. *Eur. J. Cancer* **44**, 30–38 (2008).

53. Dent, R. *et al.* Triple-negative breast cancer: Clinical features and patterns of recurrence. *Clin. Cancer Res.* **13**, 4429–4434 (2007).

54. Luck, A. A. *et al.* The Influence of Basal Phenotype on the Metastatic Pattern of Breast Cancer. *Clin. Oncol.* **20**, 40–45 (2008).

55. Charles M. Perou. Molecular Stratification of Triple-Negative Breast Cancers. *Oncologist* **15**, 744–749 (2010).

56. Koboldt, D. C. *et al.* Comprehensive molecular portraits of human breast tumours. *Nature* **490**, 61–70 (2012).

57. Cheang, M. C. U. *et al.* Basal-like breast cancer defined by five biomarkers has superior prognostic value than triple-negative phenotype. *Clin. Cancer Res.* **14**, 1368–1376 (2008).

58. Engel, C. *et al.* Prevalence of pathogenic BRCA1/2 germline mutations among 802 women with unilateral triple-negative breast cancer without family cancer history. *BMC Cancer* **18**, 4–9 (2018).

59. Mj, S. *et al.* Linkage of Early-Onset Familial Breast Cancer to Chromosome 17q21. *Science (80-.).* **250**, (1990).

60. Shah, S. P. *et al.* The clonal and mutational evolution spectrum of primary triple-negative breast cancers. *Nature* **486**, 395–399 (2012).

61. Khramtsov, A. I. *et al.* Wnt / B-Catenin Pathway Activation Is Enriched in Basal-Like Breast Cancers and Predicts Poor Outcome. *Am. J. Pathol.* **176**, 2911–2920 (2010).

62. Dey, N. *et al.* Wnt signaling in triple negative breast cancer is associated with metastasis. *BMC Cancer* **13**, (2013).

63. Qi, J. *et al.* New Wnt/β-catenin target genes promote experimental metastasis and migration of colorectal cancer cells through different signals. *Gut* **65**, 1690–1701 (2016).

64. Cohnheim, J. F. *Vorlesungen uber allgemeine Pathologie (Erster Band) 2d edn.* (1880).

65. Lapidot, T. *et al.* A cell initiating human acute myeloid leukaemia after transplantation into SCID mice. *Nature* **362**, 31–39 (1994).

66. Al-Hajj, M., Wicha, M. S., Benito-Hernandez, A., Morrison, S. J. & Clarke, M. F. Prospective identification of tumorigenic breast cancer cells. *Proc. Natl. Acad. Sci. U. S. A.* **100**, 3983–3988 (2003).

67. Badve, S. & Nakshatri, H. Breast-cancer stem cells-beyond semantics. *Lancet Oncol.* **13**, e43–e48 (2012).

68. Yap, T. A., Gerlinger, M., Futreal, P. A., Pusztai, L. & Swanton, C. Intratumor heterogeneity: Seeing the wood for the trees. *Sci. Transl. Med.* **4**, 1–5 (2012).

69. Shackleton, M., Quintana, E., Fearon, E. R. & Morrison, S. J. Heterogeneity in Cancer: Cancer Stem Cells versus Clonal Evolution. *Cell* **138**, 822–829 (2009).

70. Gupta, P. B. *et al.* Stochastic state transitions give rise to phenotypic equilibrium in populations of cancer cells. *Cell* **146**, 633–644 (2011).

71. Chaffer, C. L. *et al.* Normal and neoplastic nonstem cells can spontaneously convert to a stem-like state. *Proc. Natl. Acad. Sci. U. S. A.* **108**, 7950–7955 (2011).

72. Iliopoulos, D., Hirsch, H. A., Wang, G. & Struhl, K. Inducible formation of breast cancer stem cells and their dynamic equilibrium with non-stem cancer cells via IL6 secretion. *Proc. Natl. Acad. Sci. U. S. A.* **108**, 1397–1402 (2011).

73. Oakes, S. R., Gallego-Ortega, D. & Ormandy, C. J. The mammary cellular hierarchy and breast cancer. *Cell. Mol. Life Sci.* **71**, 4301–4324 (2014).

74. Dick, J. E. & Bonnet, D. Human Acute Myeloid Leukaemia is organised as a heirarchy that originates from a primitive haematopoetic cell. *Nat. Med.* **3**, 730–737 (1997).

75. Weigelt, B., Peterse, J. L. & Van't Veer, L. J. Breast cancer metastasis: Markers and models. *Nat. Rev. Cancer* **5**, 591–602 (2005).

76. Pallini, R. *et al.* Cancer stem cell analysis and clinical outcome in patients with glioblastoma multiforme. *Clin. Cancer Res.* **14**, 8205–8212 (2008).

77. Woo, T. *et al.* Prognostic value of CD133 expression in stage I lung adenocarcinomas. *Int. J. Clin. Exp. Pathol.* **4**, 118–123 (2011).

78. Fidler, I. J. Metastasis : Quantitative Analysis of Dis- tribution and Fate of Tumor Emboli Labeled. *J. Natl. Cancer Inst.* **45**, 773–782 (1970).

79. Lawson, D. A. *et al.* Single-cell analysis reveals a stem-cell program in human metastatic breast cancer cells. *Nature* **526**, 131–135 (2015).

80. Chang, J. C. Cancer stem cells: Role in tumor growth, recurrence, metastasis, and treatment resistance. *Med. (United States)* **95**, S20–S25 (2016).

81. Balic, M. *et al.* Most early disseminated cancer cells detected in bone marrow of breast cancer patients have a putative breast cancer stem cell phenotype. *Clin. Cancer Res.* **12**, 5615–5621 (2006).

82. Yu, F. *et al.* let-7 Regulates Self Renewal and Tumorigenicity of Breast Cancer Cells. *Cell* **131**, 1109–1123 (2007).

83. Ginestier, C. *et al.* ALDH1 Is a Marker of Normal and Malignant Human Mammary Stem Cells and a Predictor of Poor Clinical Outcome. *Cell Stem Cell* **1**, 555–567 (2007).

84. Nüsslein-Volhard, C. & Wieschaus, E. Mutations affecting segment number and polarity in Drosophila. *Nature* **287**, 795–801 (1980).

85. Nusse, R. & Varmus, H. E. Many tumors induced by the mouse mammary tumor virus contain a provirus integrated in the same region of the host genome. *Cell* **31**, 99–109 (1982).

86. R. Nusse,' A. Brown, 2 J. Papkoff, 3, P. Scambler, 4 G. Shackleford, A. McMahon, 6 & R. Moon, and H. V. . A New Nomenclature for int-1 and Related Genes: The

Writ Gene Family. *Cell* **64**, 1991 (1991).

87. Rijsewijk, F. *et al*. The Drosophila homology of the mouse mammary oncogene int-1 is identical to the segment polarity gene wingless. *Cell* **50**, 649–657 (1987).

88. Behrens, J., Mareel, M. M., Van Roy, F. M. & Birchmeier, W. Dissecting tumor cell invasion: epithelial cells acquire invasive properties after the loss of uvomorulin-mediated cell-cell adhesion. *J. Cell Biol.* **108**, 2435–2447 (1989).

89. Harris, T. J. C. & Tepass, U. Adherens junctions: From molecules to morphogenesis. *Nat. Rev. Mol. Cell Biol.* **11**, 502–514 (2010).

90. Oda, H., Akiyama-Oda, Y. & Zhang, S. Two classic cadherin-related molecules with no cadherin extracellular repeats in the cephalochordate amphioxus: Distinct adhesive specificities and possible involvement in the development of multicell-layered structures. *J. Cell Sci.* **117**, 2757–2767 (2004).

91. Ozawa, M. Regulation of cadherin activity. *Seikagaku*. **78**, 588–594 (2006).

92. Wallingford, J. B. & Habas, R. The developmental biology of Dishevelled: An enigmatic protein governing cell fate and cell polarity. *Development* **132**, 4421–4436 (2005).

93. He, X., Semenov, M., Tamai, K. & Zeng, X. LDL receptor-related proteins 5 and 6 in Wnt/β-catenin signaling: Arrows point the way. *Development* **131**, 1663–1677 (2004).

94. Wu, C. H. & Nusse, R. Ligand receptor interactions in the Wnt signaling pathway in Drosophila. *J. Biol. Chem.* **277**, 41762–41769 (2002).

95. Bilić, J. *et al*. Wnt induces LRP6 signalosomes and promotes dishevelled-dependent LRP6 phosphorylation. *Science (80-.).* **316**, 1619–1622 (2007).

96. MacDonald, B. T., Tamai, K. & He, X. Wnt/β-Catenin Signaling: Components, Mechanisms, and Diseases. *Dev. Cell* **17**, 9–26 (2009).

97. Behrens, J. *et al*. Functional interaction of β-catenin with the transcription factor LEF- 1. *Nature* **382**, 638–642 (1996).

98. van de Wetering, M. *et al*. Armadillo coactivates transcription driven by the product of the Drosophila segment polarity gene dTCF. *Cell* **88**, 789–799 (1997).

99. Städeli, R., Hoffmans, R. & Basler, K. Transcription under the Control of Nuclear

Arm/β-Catenin. *Curr. Biol.* **16**, 378–385 (2006).

100. Brembeck, F. H. *et al.* Essential role of BCL9-2 in the switch between beta-catenin's adhesive and transcriptional functions. *Genes Dev.* **18**, 2225–2230 (2004).

101. Pfefferle, A. D. *et al.* The MMTV-Wnt1 murine model produces two phenotypically distinct subtypes of mammary tumors with unique therapeutic responses to an EGFR inhibitor. *DMM Dis. Model. Mech.* **12**, (2019).

102. Korinek, V. *et al.* Constitutive transcriptional activation by a β-catenin-Tcf complex in APC(-/-) colon carcinoma. *Science (80-.).* **275**, 1784–1787 (1997).

103. Morin, P. J. *et al.* Activation of β-catenin-Tcf signaling in colon cancer by mutations in β-catenin or APC. *Science (80-.).* **275**, 1787–1790 (1997).

104. Fodde, R. *et al.* A targeted chain-termination mutation in the mouse Apc gene results in multiple intestinal tumors. *Proc. Natl. Acad. Sci. U. S. A.* **91**, 8969–8973 (1994).

105. Grigoryan, T., Wend, P., Klaus, A. & Birchmeier, W. Deciphering the function of canonical Wnt signals in development and disease: conditional loss- and gain-of-function mutations of beta-catenin in mice. *Genes Dev.* **22**, 2308–2341 (2008).

106. Stamos, J. L. & Weis, W. I. The β-catenin destruction complex. *Cold Spring Harb. Perspect. Biol.* **5**, 1–16 (2013).

107. Geyer, F. C. *et al.* B-Catenin pathway activation in breast cancer is associated with triple-negative phenotype but not with CTNNB1 mutation. *Mod. Pathol.* **24**, 209–231 (2011).

108. Cho, R. W. *et al.* Isolation and Molecular Characterization of Cancer Stem Cells in MMTV- Wnt-1 Murine Breast Tumors . *Stem Cells* **26**, 364–371 (2008).

109. Birchmeier, C., Birchmeier, W., Gherardi, E. & Vande Woude, G. F. Met, metastasis, motility and more. *Nat. Rev. Mol. Cell Biol.* **4**, 915–925 (2003).

110. Gherardi, E., Birchmeier, W., Birchmeier, C. & Woude, G. Vande. Targeting MET in cancer: Rationale and progress. *Nat. Rev. Cancer* **12**, 89–103 (2012).

111. Weidner, K. M. *et al.* Evidence for the identity of human scatter factor and human hepatocyte growth factor. *Proc. Natl. Acad. Sci. U. S. A.* **88**, 7001–7005 (1991).

112. Stoker, M., Gherardi, E., Perryman, M. & Gray, J. Scatter factor is a fibroblast-derived modulator of epithelial cell mobility. *Nature* **327**, 239–242 (1987).

113. Toshikazu Nakamura*, T. N., Mitchio Hagiyat, Tatsuya Sekit, M. S. & Atsushi Sugimurat, K. T. & S. S. Molecular cloning and expression of human hepatocyte growth factor. *Nature* **87**, 377–386 (1989).

114. Naldini, L. *et al.* Extracellular proteolytic cleavage by urokinase is required for activation of hepatocyte growth factor/scatter factor. *EMBO J.* **11**, 4825–4833 (1992).

115. Hartmann, G. *et al.* A functional domain in the heavy chain of scatter factor/hepatocyte growth factor binds the c-Met receptor and induces cell dissociation but not mitogenesis. *Proc. Natl. Acad. Sci. U. S. A.* **89**, 11574–11578 (1992).

116. Lokker, N. A. *et al.* Structure-function analysis of hepatocyte growth factor: identification of variants that lack mitogenic activity yet retain high affinity receptor binding. *EMBO J.* **11**, 2503–2510 (1992).

117. Rodrigues, G. A. & Park, M. Autophosphorylation modulates the kinase activity and oncogenic potential of the Met receptor tyrosine kinase. *Oncogene* **9**, 2019–2027 (1994).

118. Ponzetto, C. *et al.* A multifunctional docking site mediates signaling and transformation by the hepatocyte growth factor/scatter factor receptor family. *Cell* **77**, 261–271 (1994).

119. Boccaccio, C. *et al.* Induction of epithelial tubules by growth factor HGF depends on the STAT pathway. *Nature* **391**, 285–288 (1998).

120. Syed, Z. A. *et al.* HGF/c-met/Stat3 signaling during skin tumor cell invasion: indications for a positive feedback loop. *BMC Cancer* **11**, 180 (2011).

121. Orian-Rousseau, V. *et al.* Hepatocyte growth factor-induced Ras activation requires ERM proteins linked to both CD44v6 and F-actin. *Mol. Biol. Cell* **18**, 76–83 (2007).

122. Uehara, Y. *et al.* Placental defect and embryonic lethality in mice lacking hepatocyte growth factor/scatter factor. *Nature* **373**, 702–705 (1995).

123. Bladt, F., Rlethmacher, D., Aguzzl, A. & Blrchmelert, C. Essential role for the c-met

receptor in the migration of myogenic precursor cells into the limb bud. **376**, 768–771 (1995).

124. Chmielowiec, J. *et al.* c-Met is essential for wound healing in the skin. *J. Cell Biol.* **177**, 151–162 (2007).

125. Andermarcher, E., Surani, M. A. & Gherardi, E. Co-expression of the HGF/SF and c-met genes during early mouse embryogenesis precedes reciprocal expression in adjacent tissues during organogenesis. *Dev. Genet.* **18**, 254–266 (1996).

126. Matsumoto, K., Funakoshi, H., Takahashi, H. & Sakai, K. HGF-Met pathway in regeneration and drug discovery. *Biomedicines* **2**, 275–300 (2014).

127. Huh, C.-G. *et al.* Hepatocyte growth factor/c-met signaling pathway is required for efficient liver regeneration and repair. *Proc. Natl. Acad. Sci.* **101**, 4477–4482 (2004).

128. Rong, S. & Vande Woude, G. F. Autocrine mechanism for met proto-oncogene tumorigenicity. *Cold Spring Harb. Symp. Quant. Biol.* **59**, 629–636 (1994).

129. Weidner, K. M., Behrens, J., Vandekerckhove, J. & Birchmeier, W. Scatter factor: molecular characteristics and effect on the invasiveness of epithelial cells. *J. Cell Biol.* **111**, 2097–2108 (1990).

130. Zeng, Q., McCauley, L. K. & Wang, C. Y. Hepatocyte growth factor inhibits anoikis by induction of activator protein 1-dependent cyclooxygenase-2: Implication in head and neck squamous cell carcinoma progression. *J. Biol. Chem.* **277**, 50137–50142 (2002).

131. Ding, S., Merkulova-Rainon, T., Han, Z. C. & Tobelem, G. HGF receptor up-regulation contributes to the angiogenic phenotype of human endothelial cells and promotes angiogenesis in vitro. *Blood* **101**, 4816–4822 (2003).

132. Rosen, E. M. & Goldberg, I. D. Regulation of angiogenesis by scatter factor. *EXS* **79**, 193–208 (1997).

133. Rong, S., Segal, S., Anver, M., Resau, J. H. & Vande Woude, G. F. Invasiveness and metastasis of NIH 3T3 cells induced by Met-hepatocyte growth factor/scatter factor autocrine stimulation. *Proc. Natl. Acad. Sci. U. S. A.* **91**, 4731–4735 (1994).

134. Raghav, K. P. *et al.* cMET and phospho-cMET protein levels in breast cancers and survival outcomes. *Clin. Cancer Res.* **18**, 2269–2277 (2012).

135. Sierra, J. R. & Tsao, M.-S. c-MET as a potential therapeutic target and biomarker in cancer. *Ther. Adv. Med. Oncol.* **3**, S21-35 (2011).

136. Garcia, S. *et al.* Poor prognosis in breast carcinomas correlates with increased expression of targetable CD146 and c-Met and with proteomic basal-like phenotype. *Hum. Pathol.* **38**, 830–841 (2007).

137. Qin, H. *et al.* YAP Induces Human Naive Pluripotency. *Cell Rep.* **14**, 2301–2312 (2016).

138. Rosado-Olivieri, E. A., Anderson, K., Kenty, J. H. & Melton, D. A. YAP inhibition enhances the differentiation of functional stem cell-derived insulin-producing β cells. *Nat. Commun.* **10**, 1–11 (2019).

139. Meng, Z., Moroishi, T. & Guan, K. L. Mechanisms of Hippo pathway regulation. *Genes Dev.* **30**, 1–17 (2016).

140. Zanconato, F., Cordenonsi, M. & Piccolo, S. YAP/TAZ at the Roots of Cancer. *Cancer Cell* **29**, 783–803 (2016).

141. Aragona, M. *et al.* A mechanical checkpoint controls multicellular growth through YAP/TAZ regulation by actin-processing factors. *Cell* **154**, 1047–1059 (2013).

142. Azzolin, L. *et al.* YAP / TAZ Incorporation in the b -Catenin Destruction Complex Orchestrates the Wnt Response. *Cell* **158**, 157–170 (2014).

143. Yu, F.-X. *et al.* Regulation of the Hippo-YAP pathway by G-protein-coupled receptor signaling. *Cell* **150**, 780–791 (2012).

144. Sorrentino, G. *et al.* Metabolic control of YAP and TAZ by the mevalonate pathway. *Nat. Cell Biol.* **16**, 357–366 (2014).

145. Vici, P. *et al.* The Hippo transducer TAZ as a biomarker of pathological complete response in HER2-positive breast cancer patients treated with trastuzumab-based neoadjuvant therapy. *Oncotarget* **5**, 9619–9625 (2014).

146. Xia, H. *et al.* EGFR-PI3K-PDK1 pathway regulates YAP signaling in hepatocellular carcinoma: The mechanism and its implications in targeted therapy article. *Cell Death Dis.* **9**, (2018).

147. Kechagia, J. Z., Ivaska, J. & Roca-Cusachs, P. Integrins as biomechanical sensors of the microenvironment. *Nat. Rev. Mol. Cell Biol.* **20**, 457–473 (2019).

148. Humphrey, J. D., Dufresne, E. R. & Schwartz, M. A. Mechanotransduction and extracellular matrix homeostasis. *Nat. Rev. Mol. Cell Biol.* **15**, 802–812 (2014).

149. Dupont, S. *et al.* Role of YAP/TAZ in mechanotransduction. *Nature* **474**, 179–184 (2011).

150. Park, H. W. *et al.* Alternative Wnt Signaling Activates YAP/TAZ. *Cell* **162**, 780–794 (2015).

151. Kim, M. K., Jang, J. W. & Bae, S. C. DNA binding partners of YAP/TAZ. *BMB Rep.* **51**, 126–133 (2018).

152. Fu, V., Plouffe, S. W. & Guan, K. L. The Hippo pathway in organ development, homeostasis, and regeneration. *Curr. Opin. Cell Biol.* **49**, 99–107 (2017).

153. Chang, S. S. *et al.* Aurora A kinase activates YAP signaling in triple-negative breast cancer. *Oncogene* **36**, 1265–1275 (2017).

154. Elster, D. *et al.* TRPS1 shapes YAP/TEAD-dependent transcription in breast cancer cells. *Nat. Commun.* **9**, (2018).

155. Lee, J. Y. *et al.* YAP-independent mechanotransduction drives breast cancer progression. *Nat. Commun.* 1–9 (2019) doi:10.1038/s41467-019-09755-0.

156. Molyneux, G. *et al.* Article BRCA1 Basal-like Breast Cancers Originate from Luminal Epithelial Progenitors and Not from Basal Stem Cells. *Stem Cell* **7**, 403–417 (2010).

157. Wagner, K. U. *et al.* Cre-mediated gene deletion in the mammary gland. *Nucleic Acids Res.* **25**, 4323–4330 (1997).

158. Harada, N. *et al.* Intestinal polyposis in mice with a dominant stable mutation of the β-catenin gene. *EMBO J.* **18**, 5931–5942 (1999).

159. Gallego, M. I., Bierie, B. & Hennighausen, L. Targeted expression of HGF/SF in mouse mammary epithelium leads to metastatic adenosquamous carcinomas through the activation of multiple signal transduction pathways. *Oncogene* **22**, 8498–8508 (2003).

160. Srinivas, S. *et al.* Cre reporter strains produced by targeted insertion of EYFP and ECFP into the ROSA26 locus. *BMC Dev. Biol.* **1**, 1–8 (2001).

161. Dall, G. V *et al.* SCA-1 Labels a Subset of Estrogen-Responsive Bipotential

Repopulating Cells within the CD24+ CD49fhi Mammary Stem Cell-Enriched Compar tment. *Stem Cell Reports* **8**, 417–431 (2017).

162. Zanconato, F. *et al.* Genome-wide association between YAP/TAZ/TEAD and AP-1 at enhancers drives oncogenic growth. *Nat. Cell Biol.* **17**, 1218–1227 (2015).

163. Barker, N. *et al.* Identification of stem cells in small intestine and colon by marker gene Lgr5. *Nature* **449**, 1003–1007 (2007).

164. Muramatsu, T. *et al.* YAP is a candidate oncogene for esophageal squamous cell carcinoma. *Carcinogenesis* **32**, 389–398 (2011).

165. Herbst, A. *et al.* Comprehensive analysis of β-catenin target genes in colorectal carcinoma cell lines with deregulated Wnt/β-catenin signaling. *BMC Genomics* **15**, (2014).

166. Zanconato, F., Cordenonsi, M. & Piccolo, S. YAP/TAZ at the Roots of Cancer. *Cancer Cell* vol. 29 783–803 (2016).

167. Lian, I. *et al.* The role of YAP transcription coactivator in regulating stem cell self-renewal and differentiation. *Genes Dev.* **24**, 1106–1118 (2010).

168. Zhao, B. *et al.* Cell detachment activates the Hippo pathway via cytoskeleton reorganization to induce anoikis. *Genes Dev.* **26**, 54–68 (2012).

169. Koren, E. & Fuchs, Y. The bad seed: Cancer stem cells in tumor development and resistance. *Drug Resist. Updat.* **28**, 1–12 (2016).

170. Nassar, D. & Blanpain, C. Cancer Stem Cells: Basic Concepts and Therapeutic Implications. *Annu. Rev. Pathol. Mech. Dis.* **11**, 47–76 (2016).

171. Jechlinger, M. Organotypic culture of untransformed and tumorigenic primary mammary epithelial cells. *Cold Spring Harb. Protoc.* **2015**, 457–461 (2015).

172. Dontu, G. *et al.* In vitro propagation and transcriptional profiling of human mammary stem/progenitor cells. *Genes Dev.* **17**, 1253–1270 (2003).

173. Liu-chittenden, Y. *et al.* Genetic and pharmacological disruption of the TEAD–YAP complex suppresses the oncogenic activity of YAP. *Genes Dev.* 1300–1305 (2012) doi:10.1101/gad.192856.112.

174. Hannah, R. C ELL T ITER -G LO ™ L UMINESCENT C ELL V IABILITY A SSAY : A S ENSITIVE AND R APID M ETHOD FOR D ETERMINING C ELL. 1–4 (2015).

175. Foster, B. M., Zaidi, D., Young, T. R., Mobley, M. E. & Kerr, B. A. CD117/c-kit in cancer stem cell-mediated progression and therapeutic resistance. *Biomedicines* **6**, 1–19 (2018).

176. Sorrentino, G. *et al.* Glucocorticoid receptor signalling activates YAP in breast cancer. *Nat. Commun.* **8**, 1–14 (2017).

177. Liao, M. J. *et al.* Enrichment of a population of mammary gland cells that form mammospheres and have in vivo repopulating activity. *Cancer Res.* **67**, 8131–8138 (2007).

178. Zhang, N. *et al.* Article The Merlin / NF2 Tumor Suppressor Functions through the YAP Oncoprotein to Regulate Tissue Homeostasis in Mammals. *Dev. Cell* **19**, 27–38 (2010).

179. Di-Cicco, A. *et al.* Paracrine met signaling triggers epithelial–mesenchymal transition in mammary luminal progenitors, affecting their fate. *Elife* **4**, 1–25 (2015).

180. Emami, K. H. *et al.* A small molecule inhibitor of β-catenin/cyclic AMP response element-binding protein transcription. *Proc. Natl. Acad. Sci. U. S. A.* **101**, 12682–12687 (2004).

181. Frescas, D. & Pagano, M. Deregulated proteolysis by the F-box proteins SKP2 and β-TrCP: Tipping the scales of cancer. *Nat. Rev. Cancer* **8**, 438–449 (2008).

182. Yam, C. H., Fung, T. K. & Poon, R. Y. C. Cyclin A in cell cycle control and cancer. *Cell. Mol. Life Sci.* **59**, 1317–1326 (2002).

183. M. Gudas, J. *et al.* Cyclin E2, a Novel G1 Cyclin That Binds Cdk2 and Is Aberrantly Expressed in Human Cancers. *Mol. Cell. Biol.* **19**, 612–622 (1999).

184. Beckerman, R. & Prives, C. Transcriptional regulation by p53. *Cold Spring Harb. Perspect. Biol.* **2**, a000935 (2010).

185. Kuilman, T., Michaloglou, C., Mooi, W. J. & Peeper, D. S. The essence of senescence. *Genes Dev.* **24**, 2463–2479 (2010).

186. Geiss, G. K. *et al.* Direct multiplexed measurement of gene expression with color-coded probe pairs. *Nat. Biotechnol.* **26**, 317–325 (2008).

187. Rosenbluh, J. *et al.* b -Catenin-Driven Cancers Require a YAP1 Transcriptional Complex for Survival and Tumorigenesis. *Cell* **151**, 1457–1473 (2012).

188. Oki, S. *et al.* Ch IP-Atlas: a data-mining suite powered by full integration of public ChIP-seq data. *EMBO Rep.* **19**, 1–10 (2018).

189. Yuan, W. C. *et al.* NUAK2 is a critical YAP target in liver cancer. *Nat. Commun.* **9**, 4834 (2018).

190. Mertins, P. *et al.* Proteogenomics connects somatic mutations to signalling in breast cancer. *Nature* **534**, 55–62 (2016).

191. Coussy, F. *et al.* A large collection of integrated genomically characterized patient-derived xenografts highlighting the heterogeneity of triple-negative breast cancer. *Int. J. Cancer* **1912**, 1902–1912 (2019).

192. Gyorffy, B. *et al.* An online survival analysis tool to rapidly assess the effect of 22,277 genes on breast cancer prognosis using microarray data of 1,809 patients. *Breast Cancer Res. Treat.* **123**, 725–731 (2010).

193. Chen, Q. *et al.* A temporal requirement for Hippo signaling in mammary gland differentiation, growth, and tumorigenesis. *Genes Dev.* **28**, 432–437 (2014).

194. Yosefzon, Y. *et al.* Caspase-3 Regulates YAP-Dependent Cell Proliferation and Organ Size. *Mol. Cell* **70**, 573-587.e4 (2018).

195. Azad, T. *et al.* A LATS biosensor screen identifies VEGFR as a regulator of the Hippo pathway in angiogenesis. *Nat. Commun.* **9**, (2018).

196. Ponzo, M. G. *et al.* Met induces mammary tumors with diverse histologies and is associated with poor outcome and human basal breast cancer. *Proc. Natl. Acad. Sci. U. S. A.* **106**, 12903–12908 (2009).

197. Gutmann, D. H. Functional analysis of neurofibromatosis 2 (NF2) missense mutations. *Hum. Mol. Genet.* **10**, 1519–1529 (2001).

198. Pan, D. The hippo signaling pathway in development and cancer. *Developmental Cell* vol. 19 491–505 (2010).

199. Zhang, X. *et al.* The Hippo pathway transcriptional co-activator, YAP, is an ovarian cancer oncogene. *Oncogene* **30**, 2810–2822 (2011).

200. Song, M., Cheong, J.-H., Kim, H., Noh, S. H. & Kim, H. Nuclear expression of Yes-associated protein 1 correlates with poor prognosis in intestinal type gastric cancer. *Anticancer Res.* **32**, 3827–3834 (2012).

201. Steinhardt, A. A. *et al.* Expression of Yes-associated protein in common solid tumors. *Hum. Pathol.* **39**, 1582–1589 (2008).

202. Chang, L. *et al.* The SWI/SNF complex is a mechanoregulated inhibitor of YAP and TAZ. *Nature* vol. 563 265–269 (2018).

203. Hill, V. K. *et al.* Frequent epigenetic inactivation of KIBRA, an upstream member of the salvador/warts/ hippo (SWH) tumor suppressor network, is associated with specific genetic event in B-cell acute lymphocytic leukemia. *Epigenetics* **6**, 326–332 (2011).

204. Xu, M. Z. *et al.* Yes-associated protein is an independent prognostic marker in hepatocellular carcinoma. *Cancer* **115**, 4576–4585 (2009).

205. Kurppa, K. J. *et al.* Treatment-Induced Tumor Dormancy through YAP-Mediated Transcriptional Reprogramming of the Apoptotic Pathway. *Cancer Cell* **37**, 104-122.e12 (2020).

206. Cordenonsi, M. *et al.* The hippo transducer TAZ confers cancer stem cell-related traits on breast cancer cells. *Cell* **147**, 759–772 (2011).

207. Di Agostino, S. *et al.* YAP enhances the pro-proliferative transcriptional activity of mutant p53 proteins . *EMBO Rep.* **17**, 188–201 (2016).

208. Kim, S. K., Jung, W. H. & Koo, J. S. Yes-associated protein (YAP) is differentially expressed in tumor and stroma according to the molecular subtype of breast cancer. *Int. J. Clin. Exp. Pathol.* **7**, 3224–3234 (2014).

209. Sheen-Chen, S. M. *et al.* Yes-associated protein is not an independent prognostic marker in breast cancer. *Anticancer Res.* **32**, 3321–3326 (2012).

210. Wang, X., Su, L. & Ou, Q. Yes-associated protein promotes tumour development in luminal epithelial derived breast cancer. *Eur. J. Cancer* **48**, 1227–1234 (2012).

211. Yuan, M. *et al.* Yes-associated protein (YAP) functions as a tumor suppressor in breast. *Cell Death Differ.* **15**, 1752–1759 (2008).

212. Kim, T. *et al.* A basal-like breast cancer-specific role for SRF–IL6 in YAP-induced cancer stemness. *Nat. Commun.* **6**, 10186 (2015).

213. Lan, L. *et al.* Shp 2 signaling suppresses senescence in PyMT -induced mammary gland cancer in mice. **34**, 1493–1508 (2015).

214. Shibue, T. & Robert A. Weinberg. EMT CSCs drug resistance. *Nat Rev Clin Oncol* **14**, 611–629 (2017).

215. Barry, E. R. *et al.* Restriction of intestinal stem cell expansion and the regenerative response by YAP. *Nature* **493**, 106–110 (2013).

216. Jechlinger, M., Podsypanina, K. & Varmus, H. Regulation of transgenes in three-dimensional cultures of primary mouse mammary cells demonstrates oncogene dependence and identifies cells that survive deinduction. *Genes Dev.* **23**, 1677–1688 (2009).

217. Tao, J. *et al.* Activation of β-catenin and Yap1 in human hepatoblastoma and induction of hepatocarcinogenesis in mice. *Gastroenterology* **147**, 690–701 (2014).

218. Rosenbluh, J. *et al.* β-Catenin-driven cancers require a YAP1 transcriptional complex for survival and tumorigenesis. *Cell* **151**, 1457–1473 (2012).

219. Bisso, A. *et al.* Cooperation between MYC and β-catenin in liver tumorigenesis requires Yap/Taz. *Hepatology* (2020) doi:10.1002/hep.31120.

220. Gruber, R. *et al.* YAP1 and TAZ Control Pancreatic Cancer Initiation in Mice by Direct Up-regulation of JAK–STAT3 Signaling. *Gastroenterology* **151**, 526–539 (2016).

221. von Eyss, B. *et al.* A MYC-Driven Change in Mitochondrial Dynamics Limits YAP/TAZ Function in Mammary Epithelial Cells and Breast Cancer. *Cancer Cell* **28**, 743–757 (2015).

222. Moroishi, T. *et al.* The Hippo Pathway Kinases LATS1/2 Suppress Cancer Immunity. *Cell* **167**, 1525-1539.e17 (2016).

223. Raulet, D. H. & Guerra, N. Oncogenic stress sensed by the immune system: Role of natural killer cell receptors. *Nat. Rev. Immunol.* **9**, 568–580 (2009).

224. Nepal, R. M. *et al.* AID and RAG1 do not contribute to lymphomagenesis in Eμ c-myc transgenic mice. *Oncogene* **27**, 4752–4756 (2008).

225. Herschkowitz, J. I. *et al.* Identification of conserved gene expression features between murine mammary carcinoma models and human breast tumors. *Genome Biol.* **8**, R76 (2007).

226. Konstantinou, E. K. *et al.* Verteporfin-induced formation of protein cross-linked

oligomers and high molecular weight complexes is mediated by light and leads to cell toxicity. *Sci. Rep.* **7**, 1–11 (2017).

227. Chan, P. *et al.* Autopalmitoylation of TEAD proteins regulates transcriptional output of the Hippo pathway. *Nat. Chem. Biol.* **12**, 282–289 (2016).

228. Noland, C. L. *et al.* Palmitoylation of TEAD Transcription Factors Is Required for Their Stability and Function in Hippo Pathway Signaling. *Structure* **24**, 179–186 (2016).

229. Li, Q. *et al.* Lats1/2 Sustain Intestinal Stem Cells and Wnt Activation through TEAD-Dependent and Independent Transcription. *Cell Stem Cell* 675–692 (2020) doi:10.1016/j.stem.2020.03.002.

230. Yosefzon, Y. *et al.* Caspase-3 Regulates YAP-Dependent Cell Article Caspase-3 Regulates YAP-Dependent Cell Proliferation and Organ Size. *Mol. Cell* **70**, 573-587.e4 (2018).

231. Ernst, J. *et al.* Mapping and analysis of chromatin state dynamics in nine human cell types. *Nature* **473**, 43–49 (2011).

232. Ernst, J. & Kellis, M. ChromHMM: Automating chromatin-state discovery and characterization. *Nat. Methods* **9**, 215–216 (2012).

233. Kent, W. J. *et al.* The Human Genome Browser at UCSC. *Genome Res.* **12**, 996–1006 (2002).

234. Mertins, P. *et al.* Reproducible workflow for multiplexed deep-scale proteome and phosphoproteome analysis of tumor tissues by liquid chromatography-mass spectrometry. *Nat. Protoc.* **13**, 1632–1661 (2018).

235. Cox, J. *et al.* Andromeda: A peptide search engine integrated into the MaxQuant environment. *J. Proteome Res.* **10**, 1794–1805 (2011).

236. Cox, J. & Mann, M. MaxQuant enables high peptide identification rates, individualized p.p.b.-range mass accuracies and proteome-wide protein quantification. *Nat. Biotechnol.* **26**, 1367–1372 (2008).

237. Ritchie, M. E. *et al.* Limma powers differential expression analyses for RNA-sequencing and microarray studies. *Nucleic Acids Res.* **43**, e47 (2015).

238. Kolde, R. pheatmap: Pretty Heatmaps. R package version 1.0.12. *https://CRAN.R-*

project.org/package=pheatmap (2019).

239. Durinck, S. *et al.* BioMart and Bioconductor: A powerful link between biological databases and microarray data analysis. *Bioinformatics* **21**, 3439–3440 (2005).

240. Hennighausen, L. & Robinson, G. W. Information networks in the mammary gland. *Nat. Rev. Mol. Cell Biol.* **6**, 715–725 (2005).

8. SUPPLEMENTARY DATA

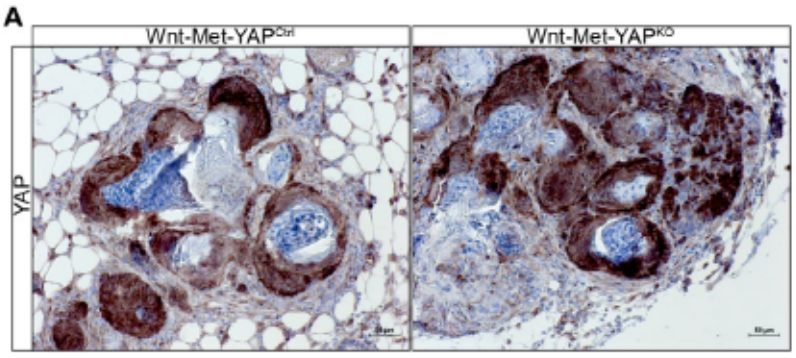

Supplementary Figure 8.1: ***YAP re-expression in YAP ablated tumours.*** **A.** Immunohistochemistry staining for YAP expression in Wnt-Met-YAP^{Ctrl} and Wnt-Met-YAP^{KO} tumours, scale bar = 50µm.

9. ACKNOWLEDGEMENTS

Firstly, I would like to express my deepest gratitude to Walter Birchmeier for welcoming me into his laboratory, giving me his guidance and for passing on his immense scientific wisdom and 'tricks of the trade'. Thanks to him, I believe I am now a better scientist.

Thank you to Prof. Thomas Sommer, my university supervisor, and the members of my annual PhD thesis committee, Michela DiVirgilio and Philipp Mertins. These meetings were fruitful and the constructive criticism I received, helped me direct the progression of this project.

I would like to thank all the members of my thesis examination committee for agreeing to be take the time to engage in my project and examine my knowledge.

I would like to give special thanks to Regina Vogel, who helped me get started in the lab and shared her skilful techniques with me. Most of all, I would like to thank her for always being present when needed and for taking care of the majority of mice. Without her I would have been lost.

Thank you to my joyful labmates Marion Müller, Daniel Bauer, Kamil Lisek and Adam Myszczyszyn for all the fun and laughter we have had over the past few years. They make work not feel like a work.

I have to thank my family, especially my Mother, Margaret, for believing in me and supporting me in throughout my career and my life in general. Without her, I would not have even dreamed to have accomplished this. Thank you to my Grandparents, who always put a roof over my head when needed and always make me smile. I also would like to thank my siblings, especially my sister, Erinn, who always listens to me complaining and stressing over work and life. A call from any of these amazing humans always cheers me up.

Last but not least, I would like to thank my amazing boyfriend, Antonino Asaro, who supported me both scientifically and emotionally through these stressful but exciting few years. With his countless amazing meals and ridiculous sense of humour he made even the most stressful of days seem brighter.

10. Selbstständigkeitserklärung

Erklärung

Hiermit erkläre ich, die vorliegende Dissertation selbstständig und nur unter Verwendung der angegebenen Hilfen und Hilfsmittel angefertigt zu haben. Ich habe mich anderwärts nicht um einen Doktorgrad beworben und besitze keinen entsprechenden Doktorgrad. Ich erkläre, dass ich die Dissertation oder Teile davon nicht bereits bei einer anderen wissenschaftlichen Einrichtung eingereicht habe und dass sie dort weder angenommen noch abgelehnt wurde. Ich erkläre die Kenntnisnahme der dem Verfahren zugrundeliegenden Promotionsordnung der Lebenswissenschaftlichen Fakultät der Humboldt-Universität zu Berlin vom 05. März 2015. Weiterhin erkläre ich, dass keine Zusammenarbeit mit gewerblichen Promotionsberaterinnen/ Promotionsberatern stattgefunden hat und dass die Grundsätze der Humboldt-Universität zu Berlin zur Sicherung guter wissenschaftlicher Praxis eingehalten wurden.

Declaration

I hereby declare that I completed the doctoral thesis independently based on the stated resources and aids. I have not applied for a doctoral degree elsewhere and do not have a corresponding doctoral degree. I have not submitted the doctoral thesis, or parts of it, to another academic institution and the thesis has not been accepted or rejected. I declare that I have acknowledged the Doctoral Degree Regulations which underlie the procedure of the Faculty of Life Sciences of Humboldt-Universität zu Berlin, as amended on 5th March 2015. Furthermore, I declare that no collaboration with commercial doctoral degree supervisors took place, and that the principles of Humboldt-Universität zu Berlin for ensuring good academic practice were abided by.

Berlin, _____

_____

Hazel Margaret Quinn